Bidirectional Neuron-glia Interactions in Isolated Rat Dorsal Root Ganglion Cells

NG, Kai Yu

A Thesis Submitted in Partial Fulfillment of the Requirements for the Degree of

Doctor of Philosophy

in

Pharmacology

The Chinese University of Hong Kong

February 2011

ProQuest LLC.
789 East Eisenhower Parkway
P.O. Box 1346
Ann Arbor, MI 48106 - 1346

Thesis/Assessment Committee

Professor RUDD John Anthony (Chair)
Professor WISE Helen (Thesis Supervisor)
Prof CHEUNG Wing Tai (Committee Member)
Professor SHUM Daisy Kwok-Yan (External Examiner)

Abstract

Dorsal root ganglia (DRG) cell preparations are commonly used to study the properties of sensory neurons in relation to nociception. A typical DRG cell preparation contains both neurons and glial cells, and in addition to a conventional supportive role of glial cells, an increasing volume of literature has reported interactions between neurons and accompanying glial cells. A typical mixed DRG cell preparation can be separated into a neuron-enriched cell fraction and a preparation of purified glial cells. Using these purified cell fractions, we can study the relative contributions and interactions between neurons and glial cells in regulating neurite outgrowth and adenylyl cyclase-dependent cell signalling activity *in vitro*.

From our previous studies, pretreating DRG cell cultures with pertussis toxin (PTx) caused neurite retraction over a period of 2 h following the initial stimulus of removal from incubator. The purpose of the current study was to investigate whether this PTx-dependent response was specific to any one of the three subpopulations of DRG neurons. Interestingly, no neurite retraction response was observed in enriched DRG cultures, including cultures enriched with isolectin B_4 (IB4)-positive neurons or IB4-negative neurons. Addition of glial cells or conditioned medium from glial cells to IB4-negative cultures was necessary to restore the PTx-dependent neurite retraction response, which was then only observed in large diameter proprioceptive neurons. To conclude, glial cells constitutively release factor/s that stimulate neurite retraction in larger diameter neurons, and is counterbalanced by neuroprotective $G_{i/o}$ protein signalling pathway.

In a parallel study, we proved that hyperalgesic agents such as prostaglandin E_2 (PGE_2) and the prostacyclin (PGI_2) mimetic (cicaprost) stimulate cAMP production

in DRG cell culture via EP_4 and IP receptors, respectively. These prostanoids were presumed to act only on the neurons in typical mixed cell cultures, but since we had acquired purified glial cell preparation, we tested for involvement of glial cells in measurement of agonist-stimulated cAMP production. Interestingly, a purified glial cell cultures also produced EP_4 and IP-dependent responses. The expression of EP_4 and IP receptors by DRG glia was further confirmed by the detection of EP_4 and IP-like immunoreactivity and mRNA. Moreover, these agonist-stimulated responses were greatest in the glial cell preparation, and surprisingly weakest in the neuron-enriched cell cultures. Furthermore, the presence of neurons significantly inhibited both EP_4 and IP receptor-dependent signalling in glial cells, but was without effect on forskolin (agonist-independent) stimulation of adenylyl cyclase. In order to characterize this neuron-glia interaction, we tested the adenylyl cyclase activities in glial cell cultures which were treated with conditioned medium derived from neurons or were separated from physical contact with neurons plated on transwell membrane. These studies further suggest that the neuron-glia interactions were dependent on both soluble factors and cell-cell contact.

From our studies, we have provided evidence of bidirectional interactions between neurons and glial cells, with glial cells regulating neurite outgrowth and neurons regulating adenylyl cyclase activity in glial cells. These findings reveal the properties of glial cells in regulating neurite outgrowth and in producing prostanoid-stimulated responses. Moreover, our findings provide foundation to understand complex neuron-glia interactions *in vivo* which will eventually help to overcome obstacles in promoting neurite regeneration and in controlling pain.

論文摘要

背根神經節（DRG）細胞被普遍應用於與痛覺有關的感覺神經研究。典型的 DRG 細胞包括神經元和神經膠質細胞，現今除了關於神經膠質細胞作用的傳統研究外，越來越多的文獻著重探討神經元和相應的神經膠質細胞的相互作用。典型的 DRG 細胞混合物可以被分離爲“部分神經元富集細胞”和“純化的神經膠質細胞”。我們正利用這些分離純化的細胞，研究神經元及神經膠質細胞相互作用對於體外突起生長和腺苷酸環化酶依賴的細胞信號傳導活性的貢獻。

我們的早期研究發現，從恒溫箱分離之後，百日咳毒素(PTx)的預處理會促使 DRG 細胞突起回縮超過兩個小時。本論文目的在於探討 PTx 依賴性反應是否對 DRG 的三種神經元亞群具有專一性。特別的是，我們在培養的 DRG 細胞富集群（包括 isolectin B4 (IB4)陽性神經元或 IB4 陰性神經元）中並沒有觀察到突起回縮反應。之後，我們發覺在 IB4 陰性神經元中添加神經膠質細胞或者源於神經膠質細胞的條件培養基，是可恢復 PTx 依賴性突起回縮反應，並只在大直徑本體感覺神經中觀察到。總括而言，神經膠質細胞合成釋放令大直徑神經元突起回縮的因數，而同時，神經保護性 Gi/o 蛋白信號傳導通路亦會相對平衡這些因數。

在平行實驗中，我們證明了痛覺過敏劑，比如前列腺素 E2（PGE2）和前列環素（PGI2）類似物西卡前列素（cicaprost）分別通過 EP4 和 IP 受體刺激 DRG 細胞中環磷酸腺苷（cAMP）的產生。這些前列腺素被普遍認爲只作用於典型的混合細胞培養中的神經元，然而我們在測量 PGE2 及 cicaprost 所引起的 cAMP 產生時，對純化的神經膠質細胞的參與性也進行了分析。有趣的是，純化的神經膠質細胞同樣也產生了 EP4 和 IP 受體依賴性反應。並且，這些 PGE2 及 cicaprost 引起的反應在純化的神經膠質細胞中最強，而在神經元富集的細胞群裡最弱。同時，利用 EP4 和 IP 樣蛋白表達和基因表達實驗，我們進一步證實了 DRG 細胞中 EP4 和 IP 受體的表達。此外，神經元的存在明顯地抑制了神

經膠質細胞中 EP4 和 IP 受體依賴的信號傳導，卻對福斯高林（forskolin）所致的腺苷酸環化酶沒有影響作用。爲了研究神經元和神經膠質細胞相互作用的表徵，我們對神經膠質細胞中的腺苷酸環化酶活性進行了檢測，這些神經膠質細胞一部分是被源自神經元的條件培養基處理過，另一部分亦從微孔濾膜培養小室(transwell)膜中直接與其接觸的神經元中分離得到的。這一部分的實驗進一步暗示了神經元與神經膠質細胞的相互作用依賴於可溶性因數和細胞間的相互接觸。

通過研究，我們證實了神經元和神經膠質細胞之間的相互作用。神經膠質細胞能夠調控神經元的突起生長，而神經元能夠控制神經膠質細胞的腺苷酸環化酶活性。這些發現揭示了神經膠質細胞對調節突起生長和產生前列腺素激動反應的特性，此將爲研究體內複雜的神經元與神經膠質細胞相互作用打下基礎，並對促進軸突再生和控制疼痛的探索有所幫助。

Acknowledgements

I would like to express my gratitude to my supervisor, Prof. Helen Wise, for her guidance, patience and support throughout the four-year study. Moreover, I would like to thank all the members of the former Department of Pharmacology and the current School of Biomedical Sciences for their kindly assistance, especially to Kevin Chow, Barry Yeung, Frank Tung, Henry Lai and Yolanda Chu. All of them provided constant support and encouragement during the four years.

This work was supported by a grant from the Research Grants Council of the Hong Kong Special Administrative Region (CUHK4516/06M). Special thanks to ONO Pharmaceuticals (Japan) for the EP-specific ligands and Schering AG (Germany) for cicaprost

Publications based on work in this thesis

Articles

Ng KY, Wong YH and Wise H (2010)
The role of glial cells in influencing neurite extension by dorsal root ganglion cells.
Neuron Glia Biology **6**(1), 11-19

Ng KY, Wong YH and Wise H (2010)
Isolation and culture of dorsal root ganglia permits expression of prostaglandin E_2 (EP4) and prostacyclin (IP) receptors by both neurons and glial cells. Manuscript in preparation

Ng KY, Wong YH and Wise H (2010)
Dorsal root ganglion neurons inhibit prostanoid-stimulated adenylyl cyclase activity in associated glial cells. Manuscript in preparation

Poster presentation

Ng KY, Wong YH and Wise H (2007)
Contribution of IP and EP_4 receptors to adenylyl cyclase activity in subpopulations of rat dorsal root ganglion cells
The 10th Scientific Meeting of the Hong Kong Pharmacology Society

Ng KY, Wong YH and Wise H (2008)
Influence of glial cells on stress-induced neurite retraction in rat dorsal root ganglion cells
The 2008 Asia-Pacific Society for Neurochemistry Meeting, Shanghai, China

Ng KY, Wong YH and Wise H (2009)
Role of glial cells on influencing neurite extension by rat dorsal root ganglion neurons
The 27th Scientific Meeting of the Hong Kong Society of Neurosciences and The Annual Biennial Meeting of The Biophysical Society of Hong Kong

Ng KY, Wong YH and Wise H (2009)
Interactions between neuronal and glial cells in rat dorsal root ganglion cell cultures: effects on IP and EP4 receptor-dependent signalling.
The 9th World Congress on Inflammation, Tokyo Japan

Ng KY, Wong YH and Wise H (2009)
Prostanoid-stimulated cAMP production in rat dorsal root ganglia cells: role of glial cells
The 12th Scientific Meeting of the Hong Kong Pharmacology Society

Yeung B, Ng KY, Wong YH, Wise H (2010)
Neuron-glia interactions for G_s-coupled GPCRS in cultures of adult rat dorsal root ganglia cells
The 28th Scientific Meeting of The Hong Kong Society of Neurosciences and The Annual Biennial Meeting of The Biophysical Society of Hong Kong

Ng KY, Wong YH and Wise H (2010)
Pertussis toxin inhibits EP4 and IP receptor-mediated cAMP production in adult rat dorsal root ganglion cells
WorldPharma2010, 16th World Congress on Basic and Clinical Pharmacology, Copenhagen, Denmark

Oral presentation
Ng KY, Wong YH and Wise H (2007)
Contribution of IP and EP_4 receptors to adenylyl cyclase activity in subpopulations of rat dorsal root ganglion cells
The 10th Scientific Meeting of the Hong Kong Pharmacology Society

Abbreviations

AA	Arachidonic acid
AC	Adenylyl cyclase
AMCA	Aminomethylcoumarin Acetate
Arg I	Arginase I
ATP	Adenosine triphosphate
BDNF	Brain derived growth factor
cAMP	Cyclic adenosine monophosphate
CGRP	Calcitonin gene-related peptide
CNS	Central nervous system
COX	Cyclooxygenase
CREB	cAMP response element binding protein
CSPG	Chondroitin sulfate proteoglycan
Cx	Connexin
Cy3	Indocarbocyanine
DIV	Days *in vitro*
DRG	Dorsal root ganglion
EP	Prostaglandin E_2 receptor
Epo	Erythropoietin
EPAC	Exchange protein directly activated by cAMP
ERK	Extracellular signal-regulated kinase
FITC	Fluoroscein isothiocyanate
GalC	Galactocerebinoside
GAP-43	Growth-associated protein 43
GDNF	Glial cell line-derived neurotrophic factor
GFAP	Glial fibrillary acidic protein
GFR	GDNF family receptor
GLAST	Glutamate-aspartate transporter
GPCR	G-protein coupled receptor
GRK2	G-protein receptor coupled kinase 2
GS	Glutamine synthetase
GSK	Glycogen synthase kinase 3
IB4	Isolectin B_4
ICC	Immunocytochemistry
IGF-1	Insulin-like growth factor 1
IL-1β	Interleukin-1β
IL-6	Interleukin-6

IL-10	Interleukin-10
ILK	Integrin-linked kinase
IP	Prostacyclin/Prostaglandin I_2 receptor
LIF	Leukaemia inhibitory factor
LPA	Lysophosphatidate
LPS	Lipopolysaccharide
MACS	Magnetic-assisted cell sorting
MAG	Myelin associated glycoprotein
N-WASP	Neuronal Wiskott-Aldrich-syndrome protein
NF200	Neurofilament 200 kDa
NGF	Nerve growth factor
NgR	Nogo receptor
NT-3	Neurotrophin-3
NT-4	Neurotrophin-4
P2X	P2X purinoceptor
$p75^{NTR}$	p75 neurotrophin receptor
PAK	p21-activated kinase
PEG300	Polyethylene glycol 300
PGD_2	Prostaglandin D_2
PGE_2	Prostaglandin E_2
PGES	Prostaglandin E synthase
PGF_2	Prostaglandin F_2
PGI_2	Prostacyclin/Prostaglandin I_2
PI3K	Phosphatidylinositol 3-kinase
PKA	Protein kinase A
PLA_2	Phospholipase A_2
PNS	Peripheral nervous system
PPAR	Peroxisome proliferator-activated receptor
PPTA	Preprotachykinin-A
PTx	Pertussis toxin
sGC	Soluble guanylyl cyclase
SGC	Satellite glial cell
SK3	Small conductance calcium-activated K^+ channel
TMP	Thiamine monophosphatase
TNFα	Tumor necrosis factor α
TRP	Transient receptor potential cation channel
Trk	Tropomyosin-related kinase
TTX-R	Tetrodotoxin resistance

TXA_2	Thromboxane A_2

Contents

Chapter 1

General introduction

1.1 Adult rat dorsal root ganglion (DRG) cell preparation

1.1.1 Subtypes of sensory neurons

Sensory neurons receive various sensory stimulations from the periphery, such as the skin, bones, muscles, and visceral organs, and transmit sensory information to the central nervous system (CNS). Unlike other neurons, sensory neurons lack dendrites and possess only axonal processes. Therefore, sensory neurons are pseudounipolar neurons with an axon fibre innervating the periphery and projecting to laminae of the spinal cord (Milligan *et al.*, 2009). Fibres innervating regions of the body arise from cell bodies in dorsal root ganglia, and those innervating the head region arise from trigeminal ganglia (Julius *et al.*, 2001). DRG neurons are heterologous and specialized for different types of sensation. Therefore, DRG neurons are categorised into distinct groups according to different properties.

Firstly, DRG neurons can be divided into several subgroups according to the modalities: (i) proprioceptors that sense body position, (i) mechanoceptors that sense low threshold stimuli such as touch, pressure and vibration, (iii) nociceptors that sense pain-inducing high threshold stimuli, (iv) thermoceptors that sense innocuous cold and warm temperatures, and (v) pruriceptors that sense itching-inducing compounds (Basbaum *et al.*, 2009; Liu *et al.*, 2010; Marmigere *et al.*, 2007). While each major modality represents a heterogeneous population of neurons, nociceptors are polymodal and perceive a greater diversity of stimuli than other sensory systems (Julius *et al.*, 2001; Liu *et al.*, 2010). Therefore, polymodal nociceptors are equipped with a diverse repertoire of transduction devices, and a single receptor can be excited by different stimuli of including both chemical (e.g. capsaicin and acid) and

physical (e.g. heat) stimuli (Julius *et al.*, 2001). This property enables sensory neurons to integrate information and respond to complex changes in the physiological environment. There are two proposed theories in explaining how our body processes polymodal sensory signal: (1) a specific sensory circuit is responsible for processing each sensory modality all the way from skin to the brain, and (2) one somatic sensation (e.g. innocuous cold) can dominate and mask another sensation (e.g. pain) upon signal integration (Liu *et al.*, 2010).

In addition, DRG neurons are categorized into three main subpopulations based on their biochemical and histochemical properties (Bennett *et al.*, 1998; Gavazzi *et al.*, 1999; Julius *et al.*, 2001; Molliver *et al.*, 1997). Each subtype of DRG neuron is responsible for different perceptual modalities. Large diameter neurons express phosphorylated heavy-chain neurofilament (NF200) with myelinated axons, and express tyrosine kinase neurotrophin receptors (mainly Trk B and C, and some express TrkA) that can selectively bind brain-derived neurotrophic factor (BDNF), neurotrophin 3 (NT3) and nerve growth factor (NGF), respectively, and possess myelinated Aα/β fibres (Fang *et al.*, 2006; Julius *et al.*, 2001; Priestley *et al.*, 2002). These large diameter neurons are responsible of proprioception and mechanosensation (e.g. light touch). Large diameter low threshold mechanoreceptive neurons conveying mechanical sensations express TrkB and/or TrkC; while large proprioceptive neurons sense limb movement and position and express only TrkC (Marmigere *et al.*, 2007). On the other hand, small diameter neurons have unmyelinated or lightly myelinated axons and respond to noxious stimuli and mediate pain sensations (nociception) (Marmigere *et al.*, 2007; Priestley *et al.*, 2002). Small diameter neurons can be further separated into two different subpopulations: peptidergic neurons and non-peptidergic neurons. Peptidergic neurons express neuropeptides, such as substance P and calcitonin gene-related

peptide (CGRP) (Priestley *et al.*, 2002). Peptidergic neurons also express TrkA and respond to NGF, and possess lightly myelinated Aδ fibres (Fang *et al.*, 2006; Julius *et al.*, 2001; Snider *et al.*, 1998). In contrast, non-peptidergic neurons express Ret and GFRα co-receptors and respond to glial cell line-derived neurotrophic factor (GDNF). These small diameter neurons possess cell surface α-D-galatose groups of glycol-conjugates that bind to isolectin B_4 (IB4) from *Griffonia simplicifolia* (Kashiba *et al.*, 2001; Molliver *et al.*, 1997) and express the enzyme thiamine monophosphatase (TMP) (Bennett *et al.*, 1998). IB4-binding neurons also coexpress $P2X_3$ receptors (Vulchanova *et al.*, 1998); it is this population in the adult that 'does not express detectable levels of the low affinity neurotrophin receptor p75 nor any known Trk receptor (Bennett *et al.*, 1998). Therefore this population of neurons does not respond to neurotrophins such as NGF. Moreover, non-peptidergic neurons possess unmyelinated slow conducting C fibres, (Fang *et al.*, 2006) while most C-nociceptors responding to noxious heat are IB4-binding neurons (Gerke *et al.*, 2001) and this heat responsiveness may result from their expression of GFRα2 receptors (Bennett *et al.*, 1998; Stucky *et al.*, 2002) and/or TRPV1 (Guo *et al.*, 1999). IB4-binding neurons have high Nav1.9 expression (TTX-R Na^+ channel) but not Nav1.8 (Fang *et al.*, 2006).

All these distinctly expressed biochemical and histochemical markers are associated with general functional groups of sensory neurons. Immunocytochemistry studies on DRG neurons using the following markers provide information on the neuronal functions: (1) IB4 binding, (2) CGRP-IR (immunoreactivity), (3) TrkA-IR and (4) NF200-IR. Subpopulations of small diameter nociceptive neurons are identified by the binding of IB4 or CGRP/TrkA-IR. For example, IB4-positive (IB4+ve) neurons do not express CGRP and TrkA, and are GDNF-responsive (small diameter). IB4-negative (IB4-ve) peptidergic neurons express CGRP and TrkA, and

are NGF-responsive (Julius *et al.*, 2001). On the other hand, large diameter proprioceptive neurons are identified by heavy neurofilament-IR (NF200-IR). Some of the large diameter neurons are also TrkA positive. On the other hand, large diameter proprioceptive neurons are identified by heavy neurofilament-IR (NF200-IR). It is noted that some of the large diameter neurons are also TrkA positive (Priestley *et al.*, 2002). Generally, these subpopulations of neurons are considered to be separate entities that do not substantially overlap in mice DRG, however it is noted that CGRP-IR population partly overlap with IB4-binding population in rat DRG (Price *et al.*, 2007).

In addition, DRG neurons can be classified into three main groups based on anatomical properties. Large diameter neurons possess myelinated, rapid conducting Aβ fibres which innervate and detect innocuous stimuli (i.e. do not contribute to pain) applied on skin, muscle and joints. In contrast, small- and medium-diameter nociceptive neurons possess unmyelinated, slowly conducting C fibres and thinly myelinated, more rapidly conducting Aδ fibres, respectively (Julius *et al.*, 2001). Sensory neurons have stereotypical innervation and termination, and connect to different subsets of second order neurons in the spinal cord. On the central side, axons of DRG neurons penetrate into the dorsal horn of spinal cord and terminate at different laminae. Small diameter nociceptive afferent neurons terminate in laminae I and II. Peptidergic neurons terminate in lamina I and outer lamina II while IB4-binding neurons terminate in inner lamina II (Snider *et al.*, 1998; Vulchanova *et al.*, 1998). Large diameter mechanoreceptive afferent neurons terminate in laminae III and IV, while large diameter proprioceptive afferent neurons terminate at ventral spinal cord (Caspary *et al.*, 2003). It is suggested that the experience of different perceptions depends on where the sensory neurons terminate in the spinal cord (Marmigere *et al.*, 2007).

1.1.2 Different types of associated glial cells

In addition to neurons, DRG neurons are associated with non-neuronal cells such as Satellite glial cells (SGCs), Schwann cells and fibroblasts. Glial cells, including SGCs and Schwann cells, are not only passive players only providing structural support, but are also involved in every function of the nervous system in both normal and pathological states.

SGCs are laminar in shape and normally form a tight sheath surrounding the cell bodies of sensory neurons and connect to each other with gap junctions (Hanani, 2005; Pannese, 2002). The gaps between SGCs and their parent neurons are about 20 nm and the non-neuronal face of SGCs has a basement membrane (Ohara *et al.*, 2009). SGCs are suggested to be the PNS equivalent of CNS astrocytes, but the embryonic origin of SGCs (neural crest cells) is different from that of astrocytes (neural plate) (Ohara *et al.*, 2009). Although there are far fewer SGCs in DRG than other glial cells such as astrocytes or Schwann cells in spinal cord and brain, the unique location of SGCs in dorsal root ganglion suggested that SGCs influence nociceptive sensation (Jasmin *et al.*, 2010). For example, as there is no blood-brain barrier in the sensory ganglia, it is suggested that the SGC sheath may perform like a barrier to protect neurons from circulating substances. Studies using tracer proteins suggested that the SGC sheath does not completely block the passage of large molecules, but slows down the diffusion of most substances (Hanani, 2005). These findings suggested that SGCs can partially control the neuronal environment. Moreover, SGCs are very important in supporting neurons and act as insulation, ion sink and for neurotransmitter recycling (Ohara *et al.*, 2009). For example, SGCs are important to uptake and recycle paracrine release of glutamate within DRGs. SGCs express glutamate-aspartate transporters (GLAST) to uptake glutamate, and express glutamine synthetase (GS) to convert glutamate to glutamine (Jasmin *et al.*, 2010).

SGCs also express a unique type of ion channel which is an inwardly rectifying potassium channel called Kir4.1. During neuronal excitation, K^+ is released in the perineuronal space, and increases neuronal excitability. It is hypothesized that Kir4.1 is responsible for removing excessive K^+ in the perineuronal space in order to control neuronal resting potential and excitability of DRG neurons (Ohara *et al.*, 2009). In addition, SGCs are connected by gap junctions which allow passage of small molecules up to 1 kDa (Hanani, 2005). Gap junctions on SGCs consist of connexin 43 (Cx43) subunits. It is believed that gap junctions permit passage of K^+ ion (Vit *et al.*, 2006) and pain-related neuromediators, such as ATP, cAMP, Ca^{2+} and IP3, between SGCs (Ohara *et al.*, 2009). Therefore, gap junctions are important for buffering and signalling. As a result, SGCs control the extracellular environment and changes in expression of gap junctions results in changes in neuronal excitability (Ohara *et al.*, 2009). GS, GLAST, Kir4.1 (inward rectifying K^+ channel), Cx43 (connexin 43) and $P2Y_4$ are selective markers for SGCs (Hanani, 2005; Vit *et al.*, 2006). In addition, SGCs can communicate with DRG neurons. For example, SGCs contain guanylyl cyclase, which is activated by nitric oxide (NO) from DRG neurons to catalyze cGMP formation (Thippeswamy *et al.*, 2002). SGCs can talk to neurons by supplying them with arginine to produce more NO (Aoki *et al.*, 1991; Thippeswamy *et al.*, 2002). Besides maintaining the normal function of neurons, SGCs were reported to be involved in pathological states. An increase (nerve injury) (Ohara *et al.*, 2008) or a decrease (knockdown Cx43 in normal rats) (Dublin *et al.*, 2007) in Cx43 expression in SGCs leads to hyperalgesia. SGCs are activated and divide following peripheral nerve damage (Lu *et al.*, 1993). Moreover, activation of $P2X_7$ receptor on SGCs is associated with CFA-induced inflammatory pain and allodynia (Chen *et al.*, 2008). Study also showed that expression of glutamate transporters such as GLAST and GLT-1 on spinal glial cells are reduced after nerve

injury, and this is associated with neuropathic pain behaviour (Sung *et al.*, 2003), while reducing GLAST expression in SGCs in trigeminal ganglia lowers the threshold to mechanical stimulation of the face (Jasmin *et al.*, 2010). Therefore, it is believed that the expression level of GLAST may be reduced on SGCs during pathological conditions which lead to increased concentration of glutamate in the perineuronal environment and increased neuronal excitability. Interestingly, SGCs can act like immune cells such as macrophages. Activated SGCs release pro-nociceptive peptides, such as TNFα (Dubovy *et al.*, 2006) and IL-β (Takeda *et al.*, 2007), which is associated with chronic neuropathic pain and inflammatory pain, respectively. SGCs are in close proximity to both neurons and microvascular endothelium, and are suggested to stimulate endothelial cells to release chemoattractants to recruit macrophages to the DRG following nerve injury (Ohara *et al.*, 2009).

On the other hand, Schwann cells include myelin-expressing S100β-positive Schwann cells and glial acidic fibrillary protein (GFAP)-expressing Schwann cells which ensheath the neurons (Campana, 2007). Schwann cells insulate nerve fibres in myelinating and non-myelinating forms (Ohara *et al.*, 2009). Myelinating Schwann cells produce myelin and wrap around medium and large diameter axons that include Aδ and Aβ primary afferent fibres, respectively; while non-myelinating Schwann cells ensheath small diameter axons (C-fibres) (Campana, 2007). Signals from Schwann cells determine the radial sorting, axonal diameter, axonal conduction velocity, and development of nodes of Ranvier (Campana, 2007). Besides insulating nerve fibres in myelinating and non-myelinating forms, Schwann cells de-differentiate to take part in repair processes including phagocytosis following injury (Ohara *et al.*, 2009). Schwann cells are reported to be dynamic players in regulating axon regeneration by releasing neurotrophic factors like NGF, BDNF,

IGF-1 and Epo (Hoke *et al.*, 2006; Li *et al.*, 2005). Moreover, Schwann cells release pro-inflammatory cytokines, such as TNF-α, IL-1β and IL-6 (Campana *et al.*, 2006; Shamash *et al.*, 2002), which are responsible for Wallerian degeneration and neuropathic pain (Shamash *et al.*, 2002; Wagner *et al.*, 1996). Also Schwann cells promote inflammation indirectly by recruiting immune cells, such as macrophages, to the site of injury through secretion of chemoattractants (Campana, 2007).

1.2 Regulation of neurite outgrowth

Neurite outgrowth is a multifactorial and complex differentiation process which involves morphological changes of neuronal cells. During neurite outgrowth, various activated pathways target on the growth cone and acting on the cytoskeletal machinery. There are various extracellular factors that control neurite outgrowth including both promoting and inhibiting neurite outgrowth. Various neurotrophic factors, such as NGF, BDNF, NT-3 and NT-4, may act on different Trk receptors on the neuronal cells to promote neurite outgrowth on different subtypes of neurons (Arevalo *et al.*, 2006). Moreover, cytokine LIF promotes neurite elongation and regeneration (Cafferty *et al.*, 2001).

1.2.1 Neurotrophic factors

Neurotrophins are growth factors that can trigger neurite outgrowth by activating a large variety of signal intermediates. Neurotrophins are synthesized within the tissue when growth cones of neurons reach target cells during development. Each type of target cell releases a limited amount of a specific neurotrophic factor for neurons innervating that target to survive. The neurons apparently compete for the factor, and those that do not get enough die by programmed cell death. Neurotrophins mediate their effect through binding to two different receptors, Trk and $p75^{NTR}$ (p75 neurotrophin receptor).

Trk receptors include Trk A, B and C. NGF binds preferentially to TrkA, BDNF

and NT-4 bind preferentially to TrkB and NT-3 binds preferentially to TrkC (Arevalo *et al.*, 2006). Among these neurotrophins, NGF is the prototypical neurotrophin. NGF, BDNF, NT-3 and NT-4 were reported to enhance axonal regeneration and neurite outgrowth in DRG neurons (Lindsay, 1988). As the Trk receptors have intracellular catalytic domains, neurotrophins can activate various signalling pathway such as MAPK and PI3K/Akt pathways. For the MAPK pathway, NGF can stimulate p42/44 MAPK in two phases, a transient phase through Ras and a prolonged phase through Rap (Arevalo *et al.*, 2006). Similarly, in PC12 cells, NGF-induced differentiation and neuritogenesis involved both ERK and PI3K pathway (Korhonen *et al.*, 1999; Pang *et al.*, 1995). It is reported that the Akt-mediated GSK-3 phosphorylation is involved in NGF-stimulated axon growths. (Zhou *et al.*, 2004) In addition, it is also reported that integrin-linked kinase (ILK) is an important effector in NGF-mediated neurite outgrowth. They also reported that the NGF-induced phosphorylations of Akt, Tau kinase and GSK-3 for neurite outgrowth involve ILK (Mills *et al.*, 2003).

The $p75^{NTR}$ belongs to the tumor necrosis factor (TNF) receptor superfamily. Interestingly, all neurotrophin stated before can bind to $p75^{NTR}$ with the same affinity. The function of $p75^{NTR}$ is complex and contradictory, as if is involved in the neurite outgrowth and facilitating growth-cone collapse. Unlike typical Trk receptor, $p75^{NTR}$ lacks the catalytic activity in its cytoplasmic domain and needs to recruit other proteins to carry out its function. $p75^{NTR}$ interacts and regulates the Rho pathway on neurite outgrowth in two different ways. In vivo studies showed that axonal outgrowth was retarded in mice carrying a mutation in the $p75^{NTR}$ gene (Yamashita *et al.*, 1999). In contrast, neurotrophin binding to $p75^{NTR}$ largely suppressed this $p75^{NTR}$-dependent Rho activation and lead to neurite outgrowth. This result indicates the possibility that $p75^{NTR}$ might regulate axonal growth either positively or

negatively, depending on the proportion of unliganded to liganded $p75^{NTR}$ present in the local microenvironment. Moreover, $p75^{NTR}$ can form a complex with the Nogo receptor (NgR) and displace Rho-GDI from RhoA, resulting in its activation and consequent axonal growth inhibition (Yamashita *et al.*, 2003).

1.2.2 Conditioning injury and cAMP pathway

Numerous growth inhibitors are present in the adult CNS and are believed to inhibit the regeneration of adult axons (David *et al.*, 2003; Grados-Munro *et al.*, 2003). They include CSPG (Canning *et al.*, 1996; Castro *et al.*, 2006), MAG (Mingorance *et al.*, 2005), and Nogo-A (Chen *et al.*, 2000). MAG and Nogo-A act on NgR complexes and activate the Rho pathway and downstream neurite growth inhibitory mechanisms (Niederost *et al.*, 2002). CSPG and MAG are also present in adult PNS myelin and inhibit axon regeneration (Castro *et al.*, 2006; Shen *et al.*, 1998).

Unlike the CNS, PNS axons are capable of regenerating after injury. This phenomenon attracted researchers to investigate the molecular changes after peripheral lesion. Since DRG neurons have both peripheral and central processes that project into peripheral terminals and the spinal cord, therefore DRG neurons are an ideal model system for studies on signalling events for neurite regeneration. Peripheral axotomy, but not central axotomy, of DRG axons upregulates GAP-43 expression and enhance intrinsic neurite outgrowth ability (Schreyer *et al.*, 1993). Moreover, a preconditioning peripheral lesion 1 or 2 weeks prior to the dorsal column injury promotes neurite regeneration into the spinal cord above the lesion (Neumann *et al.*, 1999). Interestingly, the cAMP levels in DRG neurons increase two-fold in twenty-four hours after sciatic nerve injury, and these neurons can overcome inhibition by myelin (Qiu *et al.*, 2002). Administration of dibutyryl cAMP (dbcAMP), a non-hydrolyzable cAMP analogue, overcomes

inhibition by MAG and myelin for DRG neurons (Cai *et al.*, 1999; Neumann *et al.*, 1999; Qiu *et al.*, 2002). Endogenous neuronal levels of cAMP levels determine the neuronal responsiveness to various axon guidance factors (Bandtlow, 2003). For example, elevating the cAMP concentration in neurons blocks Nogo-A and MAG induced inhibition of neurite outgrowth by suppressing the RhoA signalling pathway (Bandtlow, 2003; Borisoff *et al.*, 2003). All these findings suggested that the inhibitory effect of the environment of CNS can be overcomed by peripheral conditioning lesion which is associated with elevated intracellular cAMP level (Hannila *et al.*, 2008).

cAMP is synthesized by adenylyl cyclase from ATP and degraded by phosphodiesterase to 5'-AMP. cAMP-dependent protein kinase (PKA) is the primary downstream target of cAMP. There are two phases for the downstream pathways of cAMP for regulating neurite outgrowth, initially PKA-dependent and subsequently PKA-independent pathways (Qiu *et al.*, 2002). The PKA-independent pathway is transcription dependent. CREB is activated by elevated levels of cAMP and mediates cAMP-induced transcription (Lonze *et al.*, 2002). Activated CREB is reported to be responsible to overcome growth inhibition by MAG and myelin (Gao *et al.*, 2004). CREB also contributes to the increased neurite outgrowth of sensory neurons by releasing activity-dependent neurotrophic factor when induced by vasoactive intestinal polypeptide (VIP) (White *et al.*, 2000). cAMP-regulated genes, such as Arg I and IL-6, are suggested to play a role to overcome inhibition by myelin (Hannila *et al.*, 2008). Besides conditioning lesion, priming neurons with neurotrophins, such as NGF and BDNF, also elevates cAMP levels by two folds, and these primed neurons can overcome MAG inhibition and have enhanced outgrowth ability (Cai *et al.*, 1999).

Epac, a guanine nucleotide exchange factor for the small G-protein Rap1, has

been identified to be a downstream effector of cAMP, independent of PKA (de Rooij *et al.*, 1998). In addition to PKA, a Epac-dependent pathway is also involved in cAMP-dependent axon guidance and neurite outgrowth (Murray *et al.*, 2008). cAMP mediates growth cone attraction or repulsion by distinctly activating Epac or PKA, respectively. It is suggested that there is a developmental switch in growth cone response of DRG neurons to gradients of cAMP-dependent guidance cues from attraction to repulsion, and this is the result of a switch from Epac- to PKA-mediated signalling pathways (Murray *et al.*, 2009).

Besides the cAMP pathway, extracellular signals can act on neuronal cells to activate other signalling intermediates and pathways, e.g. ERK, PI3K and small GTPases. These intermediates integrate to regulate neurite outgrowth. Signal intermediates can modulate neurite outgrowth by acting on the cytoskeleton of the growth cone. Actin polymerization or stabilizing microtubules can lead to neurite outgrowth while destabilizing the actin filament and microtubules leads to growth cone collapse and neurite retraction (da Silva *et al.*, 2002; Meyer *et al.*, 2002; Mitchison *et al.*, 1988). The neuronal cells receive both positive and negative extracellular stimuli resulting in stabilization or destabilization of the cytoskeleton of neurites (Tanaka *et al.*, 2004), and eventually producing morphological changes. cAMP was reported to activate ERK pathway to participate in neuritogenesis (Vossler *et al.*, 1997). Together, it shows these signalling molecules are essential to neurite outgrowth and their role may be varying in different conditions. These signalling pathways interact with each other under specific conditions and provide the basis of a fine tuning mechanism controlling neurite outgrowth. In fact, neurite outgrowth is governed by counteraction between the growth promoting signals and the growth inhibitory signals. Successful neurite outgrowth requires activation of the intrinsic growth ability on the neurons as well as avoiding the inhibitory

environment. When comparing to CNS, PNS neurons are more capable in regeneration after injury, so it is interesting to study the regulations of neurite outgrowth in DRG neurons which process axons that connect the periphery to the spinal cord.

1.2.3 $G_{i/o}$ protein

$G_{i/o}$ proteins are one of the most abundant proteins in neuronal growth cones suggesting an important role for $G_{i/o}$-proteins in regulating neurite outgrowth and growth-cone guidance (He *et al.*, 2006). However, while activation of $G_{i/o}$ protein-dependent pathways by cannabinoid CB1, dopamine D3 and serotonin-1B receptor agonists can stimulate neurite extension (He *et al.*, 2006; Lotto *et al.*, 1999; Reinoso *et al.*, 1996; Swarzenski *et al.*, 1996) and constitutively active Gao expressed in PC12 and N1E-115 cells can increase the number of neurites per cell (Strittmatter *et al.*, 1994), the activation of $G_{i/o}$-dependent pathways by mastoparan and GP55 caused growth-cone collapse and inhibition of neurite outgrowth, respectively (Clarke *et al.*, 1997; Igarashi *et al.*, 1993). Moreover, pretreatment of olfactory ensheathing cells (OECs) with Pertussis toxin (PTx), but not its B-oligomer, increases the number of regrowing neurites in subsequently cocultured adult retinal ganglion cells (RGCs) (Hayat *et al.*, 2003).

In addtion, the downstream signalling of $G_{i/o}$ can be carried by α or $\beta\gamma$ subunits. $G_{\beta\gamma}$ regulates PLC-β, K^+ channels, adenylyl cyclase, and PI3K, while $G\alpha_o$ acts on actin organization via small GTPases (He *et al.*, 2006). $G\alpha_o$ can activate Rap via promoting ubiquitination and proteasomal degradation of Rap1GAPII (Jordan *et al.*, 2005). Ral can be activated by Rap1 in Neuro2A cells (He *et al.*, 2006). Moreover Src is activated through Rap1 and Ral and converges with JNK signaling to activate STAT3 and regulate neurite outgrowth (He *et al.*, 2006). In addition, $G_{i/o}$ signalling may activate the MAPK cascade which was suggested to be involved in

neuritogenesis (Waetzig *et al.*, 2005). Although there is no solid conclusion on the signalling pathway of $G_{i/o}$-proteins, it is clear that $G_{i/o}$-proteins are involved in regulating neurite outgrowth.

1.3 Prostanoids and hyperalgesia

Basal levels of prostanoids are important for homeostatic functions in many tissues, particularly in the kidney, gastric mucosa and platelets (Samad *et al.*, 2002). Prostanoids are derived from arachidonic acids (AA) liberated from membrane phospholipids by PLA_2. Then COX catalyses the subsequent two reactions to convert AA to PGH_2. PGH_2 is an intermediate metabolite which can be metabolized by tissue specific isomerases into PG isoforms PGE_2, PGD_2, PGF_2 and PGI_2 or TXA_2 (Samad *et al.*, 2002)

During tissue damage and inflammation, an array of chemical mediators such as ATP, bradykinin, prostanoids, protons, cytokines and substance P are released (Tilley *et al.*, 2001). These proinflammatory signals alter transcriptional and post-translational processes and lead to an increase in prostaglandin synthetic enzyme levels and activities (Samad *et al.*, 2002). Prostanoids, like PGE_2 and PGI_2, can sensitize neurons to pain stimulation and are regarded as powerful hyperalgesic agents (Bley *et al.*, 2006; Kidd *et al.*, 2001; Samad *et al.*, 2002). An early observation from local injection of PGE_2 and PGI_2 suggested the hyperalgesic effects in rat paws or dog knee joints (Ferreira *et al.*, 1978). Since then, sensitizing effects of PGE_2 and PGI_2 are believed to be peripheral through prostanoid receptors located on the peripheral terminals of DRG neurons. However, behavioural studies showed that intrathecal injection of PGE_2 into spinal cord also caused pain sensitization (Ferreira *et al.*, 1996; Minami *et al.*, 1994) while intrathecal cicaprost injection causes mechanical hyperalgesia under inflammatory conditions (Doi *et al.*, 2002). These findings suggested that the pronociceptive effect of prostanoids can

also be central at the level of the spinal cord. According to the pivotal role of PGE_2 and PGI_2 in pain, the following sections will only focus on PGE_2 and PGI_2 synthesis and their signalling pathways.

1.3.1 Synthesis of Prostanoids

1.3.1.1 PLA_2

PLA, is responsible for diverse cellular processes including phospholipid digestion and metabolism, host defense, and signal transduction. Moreover, PLA_2 generates precursors for eicosanoid generation when the cleaved fatty acid is arachidonic acid or for platelet-activating factor formation when the sn-1 position of the phospholipid contains an alkyl ether linkage (Dennis, 1994). PLA_2s are a diverse enzyme superfamily with more than 13 different enzymatically active isoforms. There are calcium-dependent secretory ($sPLA_2$), calcium-dependent cytosolic ($cPLA_2$) and calcium-independent intracellular ($iPLA_2$) PLA_2s (Balsinde *et al.*, 1997). Although $iPLA_2$ is the predominant form of PLA_2 in rodent brain, it only serves a membrane remodeling and homeostasis function. $cPLA_2$ translocates to cellular membranes in response to increase in $[Ca^{2+}]_i$ and regulates the release of AA for prostanoid production. $sPLA_2$s that bind to glypican family of heparan sulphate proteoglycans have an enhanced ability to release AA to a pool that is coupled to COX-2. $sPLA_2$ appears to be internalized by sensory neurons and contributes to increased eicosanoid synthesis and inflammatory pain (Samad *et al.*, 2002)

1.3.1.2 COX

COXs are bifuntional enzymes that catalyse the conversion of AA to PGG_2 and then PGH_2, which is further metabolised into prostaglandin isoforms or thromboxane (Bingham *et al.*, 2006; Zeilhofer, 2007). There are two isoforms of COX, COX-1 and COX-2, which share a 60% sequence identity (Bingham *et al.*, 2006). COX-1 is expressed constitutively and produces prostanoids that fine-tune physiological

processes requiring instantaneous or continuous regulation. Studies suggest that COX-1 plays a role in acute nociception, since COX-1 is identified as a marker for small unmyelinated neurons in DRG (Chopra *et al.*, 2000). However, COX-1 can be induced by nerve injury (Samad *et al.*, 2002). In contrast to other tissues, COX-2 is also constitutively expressed in CNS spinal neurons and ventral horn motor neurons. However, neither dorsal horn sensory neurons nor glial cells constitutively express COX-2 (Maihofner *et al.*, 2000). Constitutive expression of COX-2 contributes to some of the efficacy as well as side effect profiles of COX-2 inhibitors. In the spinal cord, it may enable immediate prostanoid production in reaction to transmitter release (Bingham *et al.*, 2006; Samad *et al.*, 2002). Furthermore, the COX-2 expression level is strongly upregulated during inflammation (Maihofner *et al.*, 2000) by the products of tissue damage and inflammation such as proinflammatory cytokines (IL-1β, IL-6 and TNFα), LPS, calcium, phorbol esters and small peptide hormones) (Bingham *et al.*, 2006; Zeilhofer, 2007). Neurotransmitters and growth factors can also induce the expression of COX-2 (Samad *et al.*, 2002). Furthermore, COX activation can operate in a positive feedback loop. PGE_2, as a product of COX activation, acts on EP_3 and EP_4 receptors to increase COX-2 expression, via a p38/MAPK mechanism in human non-pigmented ciliary epithelial cells (Rosch *et al.*, 2005).

1.3.1.3 PG Synthase

There are more than 10 PGES that can convert prostanoid precursors into biologically active prostanoids. There are three different isoenzymes for the production of PGE_2, which show different temporal expression profiles and couple to different COX enzymes. mPGES is a membrane associated enzyme. mPGES-1 is inducible and couples to COX-2. mPGE-2 is constitutively expressed and shows no preferential coupling. The cytosolic form, cPGES, is inducible in brain and couples

to COX-1 (Zeilhofer, 2007). PGES can be induced by IL-1β, LPS or adjuvant administration. This observation suggested a regulatory role of PGES in inflammation, pain and fever. Moreover, cerebral vascular endothelial cells respond to circulating IL-1β and upregulate the expression of both COX-2 and PGES levels to produce PGE_2. PGE_2 can diffuse into brain parenchyma and contribute to the systemic responses to inflammation such as fever, fatigue and hypersensitivity to pain (Samad *et al.*, 2002). In contrast, only one terminal synthase is responsible for PGI_2 synthesis. PGIS is constitutively expressed and couples to COX-2 (Zeilhofer, 2007).

1.3.1.4 Prostanoid receptors

Prostanoids work as local mediators through their binding to specific GPCRs on plasma membranes. Besides signalling through cell surface GPCRs, PGI_2 also bind to nuclear PPARs (Hatae *et al.*, 2001), however, there is no evidence for an involvement of PPARs in pronociceptive effects of prostanoids in vivo (Zeilhofer, 2007). In the early days, there were no available specific antagonists for the physiological study of prostanoid receptors. Therefore, studies on physiological functions mostly relied on genetically modified mice. From receptor knockout mice studies, EP receptor subtypes knockout mice showed reduced colon polyp formation, fertilization, febrile response and bone resorption; while IP receptor knockout mice showed reduced inflammatory swelling and reduced acetic acid writhing (Kobayashi *et al.*, 2002). However, the absence of the respective enzyme or receptor already throughout development of these non-conditional mouse mutants may trigger the up-regulation of other receptors and enzymes compensating this loss. Therefore, inducible mutants are needed for further analysis (Zeilhofer, 2007). Besides, prostanoids have been injected locally at peripheral or central sites and either spontaneous nociceptive reactions or changes in sensitivity of thermal or mechanical

stimulation were monitored (Doi *et al.*, 2002; Ferreira *et al.*, 1996; Minami *et al.*, 1994). However, these studies did not considered the possibility that inflammation and neuropathy could potentially induce expressions of prostaglandin receptors which is not present in naïve animals. As a result, these studies may produce false negative results (Zeilhofer, 2007).

Among all prostanoids, PGE_2 and PGI_2 are well established hyperalgesic agents (Bley *et al.*, 1998; Kidd *et al.*, 2001; Samad *et al.*, 2002). As a result, EP receptors subtypes and IP receptors are suggested to be involved in hyperalgesia. PGE_2 stimulates four subtypes of prostanoid EP receptors: EP_1 receptor which couples to intracellular Ca^{2+} mobilization, EP_2 and EP_4 receptors which couple to Gs, and EP3 receptor which couples primarily to $G_{i/o}$ proteins (Narumiya *et al.*, 1999). In addition, EP_3 receptor splice variant subtypes, which have equal affinity for PGE_2, couple to different G-protein (A: G_i; B: G_s; C: $G_{s;}$; D: G_i, G_s, G_q) (Namba *et al.*, 1993; Narumiya *et al.*, 1999). Prostanoid EP_1, EP_2, EP_{3C}, EP_4 and IP receptor mRNA have been identified in isolated rat DRG cells (Southall *et al.*, 2001). Antisense oligonucleotides studies demonstrated that PGE_2-induced sensitization of sensory neurons was dependent on EP_{3C} and EP_4 receptors (Southall *et al.*, 2001). Moreover, there is no evidence for EP_{3C} and EP_4 receptors to work cooperatively (Wise, 2006). Study using synthetic agonists showed that EP_1 and IP receptors are involved in sensitization of TRPV1 response in mouse DRG neurons (Moriyama *et al.*, 2005).

EP_3 and EP_4 receptors are widely distributed, whereas EP_1 and EP_2 receptors distribution are restricted to the kidney, stomach, uterus and also neurons and non-neuronal cells in the nervous system (Sugimoto *et al.*, 2000) while IP receptors are abundantly expressed in DRG neurons and are upregulated in the spinal cord under inflammatory conditions (Doi *et al.*, 2002; Narumiya *et al.*, 1999). Moreover, using in situ hybridization techniques, EP_3, and to a lesser extent EP_1 and EP_4,

receptor mRNAs have been detected in mouse DRG neurons, and there are no reports regarding the localization of EP2 mRNA in sensory neurons (Oida *et al.*, 1995; Sugimoto *et al.*, 1994). In mouse DRG, approximately 40% of neurons were strongly labelled with IP receptor mRNA. The majority (>70%) of IP receptor-expressing neurons had a small diameter although both large and small neurons were also labelled. Almost 70% of cells showed colocalization with PPTA (substance P precursor) and IP receptor mRNA (Oida *et al.*, 1995). A high density of binding sites for [^{3}H]iloprost, a PGI_2 analog that binds with high affinity to IP, EP_1 and EP_3 receptors, was observed in rat DRG and the dorsal horn of the spinal cord. [^{3}H]iloprost binding site density decreased in the dorsal horn following dorsal rhizotomy and [^{3}H]iloprost binding sites accumulated proximal to ligation site following ligation of the vagus nerve (Matsumura *et al.*, 1995). These findings suggested that the IP receptor is expressed on the terminals of primary afferents and IP receptors are transported from cell bodies via axons to central and/or peripheral terminals of primary afferents (Matsumura *et al.*, 1995).

1.3.2 cAMP/PKA pathway and hyperalgesia

The cAMP-protein kinase A (PKA) pathway mediates peripheral hyperalgesic actions of inflammatory mediators (Aley *et al.*, 1999). cAMP is implicated in pain and nociceptor sensitization. Intradermal injection of membrane permeable cAMP analogs (8-bromo-cAMP) (Taiwo *et al.*, 1989) or the adenylyl cyclase activator forskolin (Taiwo *et al.*, 1991) produce hyperalgesia. cAMP analogues 8-bromo-cAMP and dibutryl cAMP sensitize nociceptor responses to capsaicin in primary cultures of adult rat DRG (Pitchford *et al.*, 1991). PGE_2-induced hyperalgesia was significantly attenuated by inhibiting adenylyl cyclase with 2′5′-dideoxyadenosine (DDA) (Khasar *et al.*, 1995) and the inactive cAMP analog (Rp-cAMP) (Taiwo *et al.*, 1991). PGE_2 produced a transient sensitization of

whole-cell currents elicited by the vanilloid capsaicin via cAMP/PKA pathway in cultured embryonic rat sensory neurons (Lopshire *et al.*, 1998). Hyperexcitability and spontaneous activity in DRG somata after either dissociation or CCD treatment require ongoing activation of cAMP-PKA (Zheng *et al.*, 2007). Interestingly, activation of endogenous μ-, δ-, κ-opioid receptors can reduce the concentration of cAMP in nociceptive neurons and is responsible for their antinociceptive effect (Aley *et al.*, 1997).

PKA, the downstream signalling partner of cAMP, is widely believed to be important for the hyperalgesic effect of cAMP pathway. Pharmacological inhibition of PKA attenuates inflammatory mediator-induced hyperalgesic responses (Aley *et al.*, 1999; Khasar *et al.*, 1995). From studies using neuronal-specific isoform of the type I regulatory subunit (RIβ) of PKA mutant mice, inflammatory mediator-induced hyperalgesic properties are attenuated (Malmberg *et al.*, 1997). Moreover, studies showed that PKA is required for bradykinin-induced peptide release (Oshita *et al.*, 2005), sensitization of ion channels such as tetrodotoxin-resistant sodium channel (TTX-R I_{Na}; NaV1.8) (Fitzgerald *et al.*, 1999) and TRPV1 channel (Bhave *et al.*, 2002). In addition, cAMP can couple to the PKC pathway via Epac (de Rooij *et al.*, 1998). Epac plays a critical role in P2X3 sensitization by activation of *de novo* PKC-dependent signalling of PGE_2 after intraplantar injection with CFA (Wang *et al.*, 2007). Epac mediates epinephrine-induced hyperalgesia via PI-PLC, PLD and PKC (Hucho *et al.*, 2005). These findings imply that activation of cAMP production and its downstream signalling events is important for sensitizing neurons and for hyperalgesic responses.

1.4 Pain processing

The ability to detect noxious stimuli as a painful alert is essential to protect one from potential injury or tissue damaging events, since sensation of pain is intrinsically

unpleasant and associated with hurting and soreness (Woolf, 2004). Pain can be divided into four types: 1) nociceptive pain which is the perception of noxious peripheral stimuli, such as heat, cold, intense mechanical force, and chemical irritants; 2) inflammatory pain which is triggered by inflammatory mediators released by immune cells and injured tissue; 3) neuropathic pain which is triggered by peripheral nerve damage; and 4) functional pain which is generated by abnormal central processing with normal peripheral tissue and nerves (Woolf, 2004).

Pain processing starts at peripheral terminals where cutaneous and deep somatic tissues are innervated by primary afferent neurons. Firstly, noxious stimuli are detected by peripheral nerve endings of subpopulations of primary afferent neurons called nociceptors (transduction); then sensory information is passed from peripheral terminals to the spinal cord (conduction); and sensory signals are synaptically transferred to neurons within specific laminae of the dorsal horn (transmission) (Kidd *et al.*, 2001). The neuronal cell bodies of these primary afferent neurons controls the identity and integrity of the neuron (Woolf *et al.*, 2007), and are located in the DRG for the body or the trigeminal ganglia (TRG) for the head and face (Basbaum *et al.*, 2009). The axons connect peripheral nerve endings to presynaptic elements in the spinal cord. These primary afferent neurons transduce stimuli to electrical signals by high-threshold transducer ion channels, such as transient receptor potential (TRP) channels (including TRPV1 and TRPA), acid-sensitive channels, serotonin 5-HT3 receptors, and purinergic P2X receptors that are activated by noxious, mechanical or chemical stimuli (Benarroch, 2010; Woolf *et al.*, 2007). This transducer potential depolarizes the peripheral terminals activating voltage-dependent sodium channels (particularly Nav1.7, Nav1.8, and Nav1.9) (Benarroch, 2010; Woolf *et al.*, 2007). Electrical signals are transmitted along the axon and reach the CNS where DRG neurons form synaptic connection

with second order neurons. At the presynaptic terminal, the electric impulse triggers calcium influx which leads to release of glutamate as well as multiple synaptic modulators and signalling molecules (e.g. substance P, CGRP and BDNF) and is subject to both excitatory and inhibitory influences (Woolf *et al.*, 2007). Although the nociceptors carry electrical signals in one direction, these pseudounipolar neurons work as a bidirectional machines. The majority of proteins are synthesized at the cell body and distributed to both peripheral and central terminals. This suggests that the nociceptor can send and receive messages from either end. For example, while neurotransmitters are released at central ends to transmit signals to second order neurons, neurotransmitters are also released at peripheral ends to generate neurogenic inflammation. Moreover, neuronal sensitivity can be regulated by endogenous molecules at both ends (Basbaum *et al.*, 2009).

Primary afferent nerves project to projection neurons within laminae I and V of the dorsal horn of the spinal cord. A subset of these projection neurons transmits information to the somatosensory cortex via the thalamus and provides information about the location and intensity of the stimuli. Other projection neurons terminate at cingulate and insular cortices via brainstem and amygdala. This subset of projection neurons is responsible for the affective component of pain experience. Along with these ascending pathways another subset of neurons project to the rostral ventral medulla and midbrain periaqueductal gray to engage descending regulatory feedback systems on transmission of pain messages at the level of the spinal cord (Basbaum *et al.*, 2009).

1.4.1 Inflammatory pain

Inflammatory pain is characterized by an increased sensitivity to mechanical or heat stimuli of the affected tissue. Pain hypersensitivity after an inflammatory stimulus largely depends on peripheral sensitization which is the modification of the

properties of primary afferent neurons to subsequent stimuli. During chronic inflammation, nociceptors are sensitized by inflammatory signals which are released from surrounding cells at the peripheral nerve terminal. Such factors include adenosine and its related mono- or polyphosphorylated compounds (AMP, ADP and ATP), bradykinin, glutamate, histamine, IL-1, IL-6, NGF, platelet-activating factor, PGE_2, protons, serotonin, substance P and TNF-α (Milligan *et al.*, 2009; Safieh-Garabedian *et al.*, 1995). For example, bradykinin is released during inflammation and sensitizes sensory neurons to other stimuli, while bradyzide (non-peptide bradykinin receptor antagonist) can reverse inflammatory hyperalgesia (Burgess *et al.*, 2000). Pro-inflammatory cytokines, such as TNFα, IL-1β and IL-6, are involved in the development of heat hyperalgesia (Opree *et al.*, 2000). Intraplantar injection of TNFα or IL-1β reduces mechanical nociceptive thresholds in a prostaglandins-dependent manner (Cunha *et al.*, 1992). In addition, cytokines and neurotrophins induce PGE_2 levels in peripheral tissues during inflammation, and PGE_2 can sensitize nociceptors to bradykinin and other mediators (Smith *et al.*, 2000; Stucky *et al.*, 1996), and lower the threshold for activating TTX-R sodium channels (England *et al.*, 1996).

During inflammation, immune cells are also recruited to tissue injury sites and release further mediators including cytokines and growth factors (Kidd *et al.*, 2001). These mediators can activate peripheral nociceptors directly and lead to spontaneous pain, or stimulate inflammatory cells to release additional pain-inducing agents. Moreover, these inflammatory mediators sensitize primary afferent neurons to subsequent stimuli (peripheral sensitization) via the change in sensitivity of receptor

molecules themselves, or modulation of voltage-gated ion channels (Kidd *et al.*, 2001).

1.4.2 Neuropathic pain

Neuropathic pain results from injury or disease causing dysfunction at any level of the somatosensory (primarily spinothalamic) system. The manifestations of neuropathic pain, including spontaneous pain, hyperalgesia, and thermal and mechanical allodynia, reflect excessive excitability of peripheral nociceptors (peripheral sensitization), central nociceptive neurons (central sensitization), or both (Benarroch, 2010). For central sensitization, repetitive firing of DRG neurons after nerve injury triggers release of l-glutamate, substance P (SP), ATP, BDNF, and the cysteine-cysteine chemokine ligand CCL2. These multiple signals lead to increased neurotransmitter release from primary afferents and increased excitability of dorsal horn projection neurons via changing the function of their neuronal NMDA receptor (Benarroch, 2010; Milligan *et al.*, 2009). These signalling events involve neuron-glia interaction between neurons, astrocytes and microglia.

Similar to the generation of inflammatory pain, pro-inflammatory cytokines are suggested to be involved in the generation and maintenance of neuropathic pain. Levels of pro-inflammatory cytokines increase in the lesioned nerve. Blockade of pro-inflammatory cytokine such as TNFα, or administration of anti-inflammatory cytokines can reduce neuropathic hyperalgesia in animal models (Sommer *et al.*, 2004). It has been shown that Schwann cells can produce TNF-α after injury, which is possibly involved in neuropathic pain (Sommer *et al.*, 2004). These findings suggested that pro-inflammatory cytokines are involved in neuropathic pain.

In contrast to inflammatory conditions, neuropathic pain studies using

peripheral nerve injury showed a decrease in SP, CGRP, VR1, and Nav1.8, and an increase in the brain III sodium channel (Nav1.3). Besides, μ opiate receptorexpression is also decreased in rat dorsal horn and leads to diminished opiate sensitivity for neuropathic pain. Moreover, peripheral nerve injury induces phenotypic shifts similar to inflammation, with expression of SP and BDNF in A-fibres that may enable these fibres to evoke central sensitization (Woolf *et al.*, 2000).

1.5 Interaction between neurons and glial cells

Increasing numbers of studies suggested that glial cells talk with neurons (Fields *et al.*, 2002), and these neuron-glia interactions are also involved in pain processing in CNS (Benarroch, 2010). In the PNS, neurotransmitters were supposed to be released at presynaptic terminal of sensory neurons in dorsal horn to communicate with other cells. However, it was found that neurotransmitters such as substance P can also be released from somata of DRG neurons (Huang *et al.*, 1996). This finding suggested that sensory neurons can communicate with SGCs that enwrap neuronal somata in the DRG. The following examples on neuron-glia interactions are focused on the PNS within the sensory ganglia.

Following peripheral nerve section in adult rats, nNOS is expressed in many small peptidergic DRG neurons that have been axotomized. At the same time, cGMP synthesis is increased in SGCs (Thippeswamy *et al.*, 2002). It is found that NO released from sensory neurons activates sGC in SGCs to increase cGMP synthesis (Thippeswamy *et al.*, 2005). Moreover, the increase in cGMP synthesis in Schwann cells induces NGF and NT3 synthesis and protects neonatal neurons in coculture system (Thippeswamy *et al.*, 2005)

Neuronal somatic ATP release triggers neuron–satellite glial cell

communication in dorsal root ganglia (Zhang *et al.*, 2007). Electrical stimulation triggers somata to release ATP which activates P2X7 receptors in SGCs. As a result, SGCs release TNFα which in turn potentiates the neuronal P2X3 receptor-mediated responses and increases the excitability of DRG neurons (Zhang *et al.*, 2007). Moreover, another purinergic receptor, P2Y4 receptor, has been shown to be exclusively expressed by SGCs in sensory ganglia (Vit *et al.*, 2006). Following nerve injury, ATP is released and activates P2Y4 receptors on SGCs to increase $[Ca^{2+}]_i$ (Weick *et al.*, 2003). Then, K^+ channels on SGCs are activated and alter extracellular $[K^+]$. As a result, excitability of nociceptive neurons is increased (Ohara *et al.*, 2009).

Neuron-glia interactions also involve glutamate. As described in previous sections, glutamate recycling activities of SGCs can control the concentration of glutamate in the perineuronal space, thus it is also important in regulating the activity and sensitivity of sensory neurons. Moreover, nerve injury is associated with an increase in Cx43 expression in SGCs. This upregulation of protein expression in SGCs affects neuronal activities and leads to neuropathic pain (Ohara *et al.*, 2009). Hanani's group has shown that neuropathic pain associated with an increase in Cx43 expression in SGCs can be reduced by injection of Cx43 double-strand RNA.

During normal transmission of nociceptive afferent signals in the dorsal horn there is no activation of astrocytes or microglia. These 'normal' astrocytes have an important homeostatic role by active reuptake of glutamate (Milligan *et al.*, 2009). At peripheral endings, inflammatory cells such as Schwann cells and invading macrophages produce a wide array of inflammatory mediators, including PGE_2, to generate neuropathic pain (Ma *et al.*, 2008). At central endings, central sensitization involves astrocytes and activated microglia which release pro-inflammatory factors, such as glutamate, ATP, TNFα, IL-1β, IL-6, NO and PGE_2 (Milligan *et al.*, 2009).

Moreover, this pro-inflammatory role, activated glia can also be neuroprotective, as they release anti-inflammatory cytokines such as IL-10 and IL-4 and express CB_1 and CB_2 receptors that have been shown to exert anti-inflammatory functions and to inhibit microglial toxicity. Besides, TNFα released from activated glia protects neurons from glutamate-induced toxicity. Activated astrocytes also reduce the spread of tissue degeneration after direct injury through the controlled removal of dying neurons and tissue debris (Milligan *et al.*, 2009).

Above examples have shown that neurons and their associated neighbours (e.g. SGCs and Schwann cells) communicate by soluble factors. Besides, the close proximity between axons and Schwann cells provide a great opportunity for them to communicate by cell-cell contact. For example, Nr-CAM expressed by Schwann cells can bind to neurofascin on axon to regulate sodium channel clustering at node of Ranvier (Lustig *et al.*, 2001). On the other hand, neurite membrane fraction has been shown to stimulate Schwann cell proliferation by elevating cAMP level in Schwann cells (Salzer *et al.*, 1980). These two examples suggested proteins interaction at the membrane level of neurons and glial cells can regulate each other's properties.

1.6 Aim of thesis

A typical DRG cell preparation contains both neurons and glial cells, and in addition to a conventional supportive role of glial cells, an increasing volume of literature has reported interactions between neurons and accompanying glial cells. From previous studies in our lab, we showed that neurite outgrowth of cultured DRG neurons is affected by PTx treatment, and adenylyl cyclase activities of DRG cells is stimulated by EP_4 and IP receptor agonists. Since we have developed a method to separate mixed DRG cells to generate neuron-enriched and purified glial cell fractions, we

are interested to study the contributions of neurons and glial cells in DRG cultures. Our studies cover two important aspects of neuronal properties after injury, which are neurite outgrowth and regeneration, and pain sensitization of neurons. The aim of this thesis is to identify, if any, bidirectional crosstalk between neurons and glial cells in neurite outgrowth and prostanoid-stimulated signalling pathways. Moreover, in contrast to those *in vivo* studies on neuropathic or inflammatory pain states, we can alter the cell composition in our cultures in order to study individual responses from neurons and glial cells and their interaction in a coculture system. Therefore, we aimed to make use of the advantage of our *in vitro* cultures of DRG cells to study any neuron-glial interactions in neurite outgrowth and prostanoid signalling pathways. Eventually, these studies will aim to provide a better understanding for the complex interactions between neurons and glial cells, and will provide a basis for understanding their complex interactions *in vivo*.

Chapter 2

Materials, media, buffers and solutions

2.1 Materials

[8-^{3}H]adenine (specific activity 29.0 Ci/mmol, stored at 4 °C; Amersham)

5′-fluoro-2′-deoxy-uridine (FdU; Sigma)

Acetone (Lab Scan)

Adenosine 5'-triphosphate (ATP; Sigma)

Alumina column (Aluminium oxide, Type WN-3, Neutral; Sigma)

Biotinylated conjugated Isolectin B_4 (biotinylated IB4; Sigma) was prepared as 1 mg/ml in 0.9% NaCl, aliquoted and stored at 4°C

Bovine serum albumin (BSA; Sigma)

cAMP Biotrak Enzymeimmunoassay (EIA) System (GE Healthcare)

CAY10441 (RO1138452; Cayman Chemical) was prepared as a 10mM stock in DMSO and stored at -20°C.

CELLECTION Binder kit (Invitrogen) included Streptavidin-coated Dynabeads (magnetic beads) and releasing buffer (DNase)

Chloroform (Sigma)

Cicaprost was a gift from Schering which was prepared as a 1 mM stock in ultra-pure water and stored at -20°C.

Collagenase B (Roche Applied Science) was prepared as 1.25% stock in Ham's F14 medium and stored at 4°C

Coverslips (25 mm; Menzel Glaser)

Cytosine-β-D-Arabinofuranoside (Ara-C; Sigma) was prepared as 10 mM stock in Ham's F14 medium, aliqouted and stored at 4°C

Diethypyrocarbonate (DEPC; Sigma)

Deoxynucleoside triphosphates (dNTPs; Invitrogen)

Deoxyribonuclease I, Amplification Grade (Invitrogen)

Deoxyribonuclease I (DNase I; Sigma)

Dimethyl sulphoxide (DMSO; Sigma)

Dimethyl-dichlorosilane (Sigma)

Dorminal (20% pentobarbital solution; Alfasan) was diluted with ddH_2O prior to use to concentration of 5%

Dowex column (AG 50W X4 resin, 200 – 400 mesh hydrogen form; Bio Rad)

Dynal Magnetic Separator (Invitrogen)

Ethanol (Absolute; Merck)

FastStart High Fidelity PCR System, dNTPack (Roche)

Forskolin (Sigma) was prepared as 10 mM stock in DMSO and stored at -20 °C

Glass slide (Marienfeld Laboratory Glassware)

Glucose (Sigma)

L-glutamine (Gibco) was prepared as a 200 mM solution with Ham's F14 medium, filter sterilized, aliquoted and stored at -20 °C

Glycerol (Sigma)

HEPES (Sigma)

Hoechst 33342 (Invitrogen) is prepared as 10 mg/ml stock in ddH_2O, aliquoted and stored at -20 °C

Hydrochloric acid (HCl, 12.1 M; Merck)

IBMX (3-isobutyl-1-methyl-xanthine; Sigma) was prepared as 100 mM stock in DMSO and stored at -20 °C

Imidazole Hydrochloride (Sigma)

Isopropanol (BDH)

Laminin (Sigma) is prepared as 0.25 mg/ml in sterile PBS, aliquoted and stored at

-20 °C

Methanol (Lab Scan)

Normal Donkey serum (Jackson Immunoresearch)

OptiPhase 'Hi-safe'3 (Perkin Elmer)

Paraformaldehyde (Sigma)

Penicillin/Streptomycin (10000 units/ml and 10000 μg/ml; Gibco)

Pertussis toxin (PTx; List Biological Lab)

Pertussis toxin B-oligomer (PTx B-oligomer; List Biological Lab)

Polyethylene Glycol (PEG; Sigma)

Poly-DL-ornithine (Sigma)

Prostaglandin E_2 (PGE_2; Sigma) was prepared as 10 mM stock in absolute ethanol and stored at -20 °C

Soybean trypsin inhibitor (Sigma)

SuperScript™ III First Strand Synthesis SuperMix (Sigma)

Toluene

Trichloroacetic acid (TCA; Sigma) was prepared as 10 % stock solution (w/v) in ddH_2O

Triton X-100 (Sigma)

TRIzol Reagent (Invitrogen)

Trypan blue was prepared as 0.4% stock with PBS and store at R.T.

Trypsin (Roche Applied Science) was prepared as a 2.5% (w/v) stock in sterile PBS and stored at -20 °C

Trypsin inhibitor (Type I-S, From Soybean; Sigma)

Ultroser G (USG; Pall Life Science) as reconstituted with 20 ml sterile ddH_2O and stored at 4 °C

Uridine (Sigma)

Common laboratory reagents not listed (ACS grade) were purchase from Sigma. All disposable culture plates were purchased from Nunc.

2.2 Culture media, buffer and solutions

2.2.1 General culture buffers

Dulbecco's PBS buffer (PBS: Ca^{2+}/Mg^{2+} free) was prepared by dissolving NaCl (137 mM), Na_2HPO_4 (8.1 mM), KCl (2.68 mM) and KH_2PO_4 (1.47 mM) in 1 L ddH_2O. The solution was adjusted to pH 7.5 and made up to 1 L, filter sterilized and stored at 4 °C.

2.2.2 Culture medium

Ham's Nutrient Mixture F14 (F14 medium; SAFC Biosciences). One packet of F14 powder was reconstituted with 1 L ddH_2O, and supplemented with $NaHCO_3$ (1.176 g/L). The medium was adjusted to pH 7.2 with 1 M HCl and filter sterilized to give a final pH of 7.6. Penicillin (100 units/ml) and streptomycin (100 μg/ml) were added to the medium and stored at 4 °C.

Complete F14 medium (200 mL). 191 ml of F14 medium was supplemented with 8 ml of serum substitute Ultroser G (4%, v/v) and 1 ml of L-glutamine (2 mM) immediately prior to experiment and stored at 4 °C.

2.2.3 Assay buffers and solutions

2.2.3.1 Buffers and solutions for RT-PCR

DEPC-treated water (0.1%, v/v) was prepared by dissolving 0.2 ml of DEPC in 200 ml of ddH_2O with stirring overnight. The solution was then autoclaved before use.

50X TAE buffer was prepared by dissolving 121 g of Tris base in 421.4 ml of ddH_2O then mixing with 28.6 ml of acetic acid and 50 ml of 0.5M EDTA (pH 8.0). The buffer was approximately pH 7.8 and stored at R.T..

2.2.3.1 Buffers and solutions for Immunocytochemistry

Triton X-100 (0.3%, v/v) was prepared by adding 0.6 ml of Triton X-100 to 199.4 ml of PBS and stored at 4°C

Triton X-100 (0.01%, v/v) was prepared by adding 0.3 ml of Triton X-100 (0.3%) to 8.7 ml of PBS immediately prior to experiment.

Blocking buffer (3%, v/v) was prepared by adding 0.3 ml of normal donkey serum to 9.7 ml of PBS immediately prior to experiment.

Kryofix solution was prepared by dissolving 10 g of PEG into 79 ml of absolute ethanol and 74 ml of ddH_2O (ethanol:H_2O:PEG300 at a ratio of 7.9:7.4:1), and stored at 4°C

Acetone and methanol (1:1) was prepared by adding 10 ml of acetone to 10 ml of methanol and stored at 4 °C.

Paraformaldehyde (4%, w/v) was prepared by dissolving 0.48 g of paraformaldehyde in 8 ml of ddH_2O with 80 µl of 1M NaOH at 60 °C. Then, the solution was removed from heat and was supplemented with 4 ml of 3X PBS

3X Dulbecco's PBS (3X PBS: Ca^{2+}/Mg^{2+} free) was prepared by dissolving NaCl (411 mM), Na_2HPO_4 (24.3 mM), KCl (8.04 mM) and KH_2PO_4 (4.41 mM) in 1 L ddH_2O. The solution was adjusted to pH 7.5 and made up to 1 L, filter sterilized and stored at 4 °C.

Mounting medium (90% glycerol) was prepared by mixing 18 ml of glycerol to 2 ml of ddH_2O and stored at R.T.

2.2.3.2 Buffers and solutions for assay of [^{3}H]cAMP production

HEPES-buffered saline buffer (HBS) buffer was prepared by dissolving HEPES (15 mM), NaCl (140 mM), KCl (4.7 mM), $CaCl_2.2H_2O$ (2.2 mM), $MgCl_2.6H_2O$ (1.2 mM) and KH_2PO_4 (1.2 mM) in ddH_2O. The buffer was adjusted to pH 7.4 with 1M

NaOH, filter-sterilized and stored at 4°C.

Washing Buffer was prepared by dissolving glucose (3.3 mM) into HBS immediately prior to experiment.

Assay Buffer was prepared by adding IBMX (1 mM) into washing buffer immediately prior to experiment.

Imidazole solution (0.5 M) was prepared by dissolving 104.5 g of imidazole powder and 27 g of NaOH in ddH_2O. The solution was adjusted to pH 7.5 and made up to 2 L, and stored at room temperature.

Imidazole solution (0.1 M) was prepared by mixing 200 ml of 0.5 M Imidazole solution with 800 ml of ddH_2O.

Hydrochloric acid (4 M) was prepared by adding 330 ml of 12.1 M stock solution to 670 ml of ddH_2O and stored at R.T.

Hydrochloric acid (1 M) was prepared by adding 250 ml of 4 M HCl to 750 ml of ddH_2O and stored at R.T.

Stop solution (10% TCA with 2 mM ATP) was prepared by dissolving 22 mg of ATP in 20 ml of 10% TCA. The stop solution was prepared freshly and temporary stored at 4°C until use.

2.2.3.3 Buffers and solutions for cAMP Biotrak EIA System

Assay buffers, lysis reagents, standard solution, antiserum, cAMP Peroxidase conjugate and wash buffers were prepared according to manufacturer's instructions and stored at 4°C.

2.3 Reagents for immunocytochemistry studies

2.3.1 Primary antibodies

Antibody	Host	Types	Company	Dilution
TUJ-1	Mouse	Monoclonal IgG2a	Abcam	1:500
TUJ-1	Rabbit	Polyclonal IgG	Sigma	1:1000
GFAP (cy3 conjugated)	Mouse	Monoclonal IgG1	Sigma	1:500
CGRP	Rabbit	Polyclonal IgG	Sigma	1:2000
TrkA	Rabbit	Polyclonal IgG	Abcam	1:500
SMI32	Mouse	Monoclonal IgG1	Covance	1:100
IP receptor (N-term)	Rabbit	Polyclonal IgG	Cayman	1:500
EP_4 receptor (C-term)	Rabbit	Polyclonal IgG	Cayman	1:500
IB4	----	----	Sigma	1:100
CD11b (OX-42)	Mouse	Monoclonal IgG2a	Serotec	1:1000
GalC	Rabbit	Polyclonal IgG	Sigma	1:1000
GS	Mouse	Monoclonal IgG2a	Chemicon	1:1000
Thy1.1	Mouse	Monoclonal IgM	Sigma	1:1000
S100β	Mouse	Monoclonal IgG1	Sigma	1:1000

2.3.2 Secondary antibodies

Antibody	Company	Dilution
FITC anti-mouse IgG	Jackson Immunoresearch	1:500
Cy3 anti-rabbit IgG	Jackson Immunoresearch	1:500
Streptavidin AMCA	Vector Lab	1:100
FITC anti-mouse IgG subtype Fcγ subclass 2a specific	Jackson Immunoresearch	1:100
FITC anti-mouse IgM μ chain specific	Jackson Immunoresearch	1:100
FITC anti-rabbit IgG	Jackson Immunoresearch	1:200

Chapter 3

Methods

3.1 Preparation of DRG cell cultures

All experiments were performed under licence from the Government of the Hong Kong SAR and endorsed by the Animal Experimentation Ethics Committee of the Chinese University of Hong Kong. The dorsal root ganglia were removed from all levels of the spinal cord of male Sprague–Dawley rats (150–200 g) and cultures were prepared as described previously (Rowlands *et al.*, 2001). Firstly, rats were anaesthetized with pentobarbitone (175 mg/kg, i.p.). Whole spinal column was dissected out from rostral end of the hind legs to the base of skull. Excess tissue was removed with small scissors and rongeurs to expose the dorsal side of vertebra. Spinal cord was exposed by cutting a strip of bone from the dorsal roof of the vertebral column using Malleus Nippers. Using Vannas curved spring scissors and fine forceps, dorsal root ganglia were dissected into complete Ham's F14 medium, followed by incubation with 0.125% collagenase for 3 h, then 0.25% trypsin for 30 min in serum-free Ham's F14 medium. The dorsal root ganglia were resuspended in DNase I (90 μg/ml) and soybean trypsin inhibitor (100 μg/ml) and dispersed by trituration with a flame-polished salinized pipette. The cell suspension was centrifuged through a cushion of bovine serum albumin (15%) to eliminate much of the myelin and cellular debris. After that, the supernatant was aspirated and the cell pellet was resuspended in complete Ham's F14 medium. For neurite outgrowth studies, arabinoside C (10 μM) was used to inhibit glial cell proliferation. This mixed DRG cell preparation was plated onto glass coverslips precoated with poly-DL-ornithine (500 μg/ml) and laminin (5 μg/ml) either at 3000 neurons per well in six-well tissue culture plates for neurite outgrowth assay or at 5000 neurons per

well in 24-well tissue culture plates for cAMP assay. Mixed DRG cell preparations were assayed after 40 h in culture in an atmosphere of 5% CO_2 at 37°C.

3.1.1 Preparation of neuron-enriched and glial-cell enriched fractions

For neuron-enriched preparations, the mixed DRG cells were plated on poly-DL-ornithine-coated tissue culture dishes (DRG from two rats per 10-cm culture dish), according to Lindsay (1988). After overnight incubation, the loosely attached neuronal cells were gently removed from the more firmly attached glial cells by repetitive stream of F14 medium (4 ml) delivered by a flame-polished salinized pipette. Neuron-enriched cultures were plated either at 3000 neurons per well in six-well tissue culture plates for neurite assay or at 5000 neurons per well in 24-well tissue culture plates for cAMP assay, as described for the mixed DRG cell preparation, and assayed after another 24 h in culture so that cell age (2 days *in vitro*, i.e. 2 DIV) is equivalent to those in the mixed DRG cell cultures on the day of assay.

The remaining glial cells were harvested using 1 ml of trypsin (0.05% in PBS) for 1 min. Harvested glial cells were plated at 6000 cells per well onto poly-DL-ornithine/laminin-coated glass coverslips in six-well tissue culture plates to prepare conditioned medium, or cocultured (3000 cells per well) with purified neuronal cell cultures. For cAMP study, glial cells were plated at 10000 cells/well and were assayed after 1 day in culture so that cell age (2 DIV) and cell numbers are equivalent to those in the mixed DRG cell cultures on the day of assay.

3.1.2 Preparation of different ratios of neurons and glial cells

Neurons from neuron-enriched fractions were plated at defined numbers onto poly-DL-ornithine/laminin-coated 24-well tissue culture plates and glial cells were added as required. Adenylyl cyclase activity was measured after 1 day in culture (i.e., 2 DIV). Glial cells continue to proliferate in culture, therefore the glial cell numbers cited in the figures represent estimated numbers on the day of assay.

3.1.2 Preparation of IB4-positive and IB4-negative fractions

Subpopulations of DRG neurons were selected using magnetic bead-assisted cell sorting (Tucker *et al.*, 2005a). Briefly, streptavidin-coated Dynal beads (100 µl per 2 rats) were incubated with biotinylated IB4 (40 µg) for 1 h in R.T. immediately prior to use. Washed beads were incubated with the neuron-enriched cell preparation at 4°C for 30 min and then IB4-positive cells were captured with a Dynal magnetic separator. These cells were washed and then incubated with 1 ml of releasing buffer (DNase I solution; 200–300 U) for 10 min to release the selected IB4-positive cells from the beads. For the neurite outgrowth assay, both IB4-positive and IB4-negative cells were plated at 3000 neurons per well onto poly-DL-ornithine/laminin-coated glass coverslips in six-well tissue culture plates. For cAMP assay, both IB4-positive and IB4-negative cells were plated at 5000 neurons/well onto poly-DL-ornithine/laminin-coated 24-well tissue culture plates. Cells were assayed after 1 day (IB4-negative) or 2 days (IB4-positive), to allow time to establish neurite outgrowth comparable with neurons in the mixed cell preparation.

3.2 Determination of neurite extension/retraction

Culture medium was replaced with 1 ml of complete F14 medium without AraC, and cells were incubated with PTx or PTx-B oligomer (100 ng/ml) for 16 h before assay. Neurite-bearing neurons were defined as neurons with a neurite longer than the diameter of the cell body (Franklin *et al.*, 2009; Wise, 2006). As indicated in Fig. 5.1G, at one hour before stress induction (marked as time = -1 h, basal), phase-contrast images of cells were captured over a period of 10 min per dish, using a stereoscopic microscope TMS-F with digital sight camera system TDS-L1 (Nikon). After approximately 50 min, cells were removed from the incubator for 20 min as the stress stimulus, then neurite-bearing cells were counted at time 0 h. The proportion of neurite-bearing neurons at subsequent time points (time 1, 2, 4 and 6 h)

was also determined. The data were then normalized against the proportion of neurite-bearing neurons in each well at the start of the experiment (i.e. time = -1 h). Photos were analyzed using Scion Image (Scion Corporation, Frederick, MD, USA) and Infraview (Austria). Six photos per well were chosen randomly, and the proportion of neurite-bearing neurons was calculated by counting a minimum of 100 neurons/well. The number of large diameter neurons (diameter > 30 μm) and small diameter neurons (diameter < 30 μm) (Wewetzer *et al.*, 1999), was also determined from these images.

3.2.1 Adding back glial cells to purified DRG cell cultures

Purified glial cells were added to IB4-positive and IB4-negative cells to mimic the quantity of glial cells in mixed DRG cell cultures. Therefore, 3000 neurons and 3000 glial cells were plated onto poly-DL-ornithine/laminin-coated glass coverslips in six-well tissue culture plates, and cultured for a further 40 h before assay.

3.2.2 Conditioned medium treatment

Purified glial cells were seeded onto poly-DL-ornithine/laminin-coated six-well tissue culture plates at 6000 glial cells per well and incubated for 16 h in Ham's F14 medium. On the day of neurite assay, glial cells were left at room temperature for 20 min to mimic the stress response of the mixed DRG cell cultures. Medium was collected from both stressed and non-stressed glial cells. Medium from the IB4-positive and IB4-negative neuron cultures was aspirated and replaced with 1 ml of glial cell conditioned medium at time 0 h. The proportion of neurite-bearing neurons was determined from -1 to 2 h as described above.

3.3 Determination of [^{3}H]cAMP production in DRG cells

3.3.1 Principle of assay

The adenylyl cyclase activity was determined by loading DRG cells with

[^{3}H]adenine which gets converted to [^{3}H]ATP inside the cells. When adenylyl cyclase is stimulated, the [^{3}H]ATP will be converted to [^{3}H]cAMP (Wise, 2006). Breakdown of [^{3}H]cAMP was prevented by incubating cells with IBMX (a phosphodiesterase inhibitor). Xanthines such as IBMX have non-specific effects on the release from intracellular Ca^{2+} store (Chapman *et al.*, 1974) and blockade of the adenosine receptor (Daly *et al.*, 1987; Schultz *et al.*, 1973). It is believed that these interfering effects do not affect prostanoid receptor signalling on cAMP production. [^{3}H]cAMP were separated from other radioactive-labelled materials, including [^{3}H]ATP, using Dowex-Alumina column chromatography. The [^{3}H]cAMP production in the presence of IBMX reflects the activity of AC (Barber *et al.*, 1980; Wise, 2006).

3.3.2 Loading DRG cells with [^{3}H]adenine

As indicated in Fig. 6.12, in order to determine the total cAMP production in DRG cell cultures, DRG cells were plated on 24-well plates, washed with 1 ml of F14 medium and incubated in 0.5 ml of complete F14 medium containing [^{3}H]adenine (2 μCi/ml; 1 μCi/well) for 16 h. For distinguishing the contributions of neurons and glial cells, neuron-enriched fraction and purified glial cell preparations were loaded with a higher concentration of [^{3}H]adenine (20 μCi/ml; 10 μCi/well) before being harvested for subsequent coculture with unlabelled neurons or glial cells in 0.5 ml of complete F14 medium for 16 h.

3.3.3 Column preparation

Dowex AG50W-X4 resin columns were washed with 10 ml of distilled water before use. The columns were reusable and washed with 4 ml of 1 M HCl followed by 10 ml of distilled water three times after use. The alumina columns were washed with 8 ml of 0.1 M imidazole solution before use. The columns were reusable and washed with 8 ml of 0.1 M imidazole solution (4 times) after use.

3.3.4 Measurement of [^{3}H]cAMP production in DRG cells

Unless otherwise specified, DRG cells were incubated overnight with [^{3}H]adenine (2 μCi/ml; 1 μCi/well), with or without PTx or PTx B-oligomer (100 ng/ml) as required. Cells were washed twice with 1 ml of washing buffer and incubated in 0.5 ml assay buffer (HBS containing 1 mM IBMX). Then, the cells were incubated ± antagonists for 15 min prior to addition of agonist for a further 30 min at 37 °C in assay buffer. Treatment was stopped by addition of 0.5 ml of ice-cold stop solution (10% TCA with 2 mM). Then, the samples were left on ice for at least 1 h for the extraction of [^{3}H]cAMP and other radioactive-labelled materials. This method measures both intracellular and extracellular [^{3}H]cAMP production.

[^{3}H]cAMP was isolated from other [^{3}H]adenine nucleotides ([^{3}H]AXP; i.e. cAMP, ADP and ATP) using column chromatography. Firstly, the Dowex columns were placed over scintillation vials. Then TCA extracts (1 ml) were loaded on to the columns followed by 3 ml of distilled water to elute the [^{3}H]AXP into the scintillation vials. The eluate was mixed thoroughly with 7 ml of scintillant (OptiPhase 'Hi-safe' 3).

The Dowex columns were then placed over the alumina columns. The remaining [^{3}H]cAMP fraction was eluted with 10 ml of distilled water. When water had completely run through both set of columns, the Alumina columns were already loaded with [^{3}H]cAMP fraction. Then, the alumina columns were placed over another set of scintillation vials and [^{3}H]cAMP was eluted by 6 ml of 0.1 M imidazole solution. At last, the eluate was mixed thoroughly with 10 ml of scintillant (OptiPhase 'Hi-safe' 3).

In parallel to test samples, blank samples (a mixture of 0.5 ml assay buffer and 0.5 ml stop solution) were also run through the columns for the determination of the background count of the columns, and this value was subtracted from all the test

values. The radioactivity of samples was measured by liquid scintillation counting (Packard LS2900TR).

3.3.5 Data analysis

The production of [^{3}H]cAMP from cellular [^{3}H]ATP was estimated as the ratio of radiolabelled cAMP to total AXP, and is expressed as [cAMP]/[total AXP] x 100 (i.e. % conversion) (Salomon, 1991). All assays were performed in duplicate.

3.4 Quantitative measurement of basal cAMP production by ELISA

3.4.1 Principle of assay

The cAMP Biotrak competitive enzyme immunoassay system was used to quantify the absolute amount of cAMP present in cultures. Cells were lysed by dodecyltrimethylammonium bromide (0.25 %) and the lysates (supernatant) were transferred to a anti-rabbit IgG-coated microplate. Then the lysates were incubated with antiserum (rabbit anti-cAMP) and cAMP-peroxidase which can convert the substrate (TMB) into blue colour. This assay is based on competition between unlabelled cAMP (cAMP from DRG cells) and a fixed quantity of peroxidise-labelled cAMP, for a limited number of binding sites on cAMP specific antibody. As a result, a low optical density (OD) corresponds to high concentration of cAMP and vice versa. The protocol we used is designed for measure both the intracellular and cell supernatant cAMP and provide quantitative information of cAMP which is not provide by the conventional [^{3}H]cAMP assay.

3.4.2 Sample preparation

On the assay day (2 DIV), DRG cells were washed twice with 1 ml HBS and incubated, in duplicate, for 30 min at 37°C in 0.5 ml of HBS containing IBMX (1 mM). The reaction was stopped by addition of 50 µl of lysis reagent 1A containing dodecyltrimethylammonium bromide, at a final concentration of 0.25%. The

supernatant was collected after the cells were lysed at R.T. for 10 min. The samples were diluted 75 times by mixing 10 µl of supernatant with 740 µl of lysis reagent 1B.

3.4.3 Measurement of cAMP production in DRG cells

Working standards and diluted samples (100 µl) were loaded onto the anti-rabbit IgG-coated microplate in duplicate and incubated with 100 µl of antiserum (rabbit anti-cAMP) at 4°C for 2 h. Non-specific binding wells were set up by adding 100 µl of lysis reagent 1B and 100 µl of lysis reagent 2B and incubated at 4°C for 2 h without antiserum, while blank wells were left empty. Then, all wells were incubated with 50 µl cAMP-peroxidase conjugate at 4°C for 1 h. After that, all wells were aspirated and washed 4 times with 400 µl of wash buffer followed by incubating with 150 µl enzyme substrate at R.T. for 1 h. To halt the reaction, 100 µl of 1.0 M sulphuric acid was added to all wells and the OD was determined in a plate reader at 450 nm within 30 min.

3.4.3 Data analysis

The production of cAMP was calculated from the OD reading from the samples. Standard and sample OD was obtained by subtracting each OD reading by blank OD. The percentage bound (%B/B_o) for each standard and sample was calculated as (standard or sample OD – NSB OD)/(zero standard OD – NSB OD) x 100. The standard curve was generated by plotting the %B/B_o as a function of the log cAMP concentration. The actual fmol/well value of sample was determined from the standard curve and multiplied by the dilution factor (75 X).

3.5 Determination of EP and IP receptor mRNA expression in DRG cells by RT-PCR analysis

3.5.1 RNA isolation

Mixed DRG cell cultures (5000 neurons/well & 10,000 glial cells/well), neuron-enriched cell cultures (5000 neurons/well) and glial cell cultures (10000 glial cells/well) were cultured in 0.5 ml of complete F14 medium in 24-well plates. On 2 DIV (i.e. equivalent to the day for cAMP assay), total RNAs were extracted from cells using TRIzol reagent. Firstly, cells were washed with 1 ml of PBS, harvested using 0.2 ml of trypsin solution (0.05% in PBS) for 1 min at 37°C. The trypsin activity was neutralized with 0.8 ml of complete F14 medium. The harvested cells from 12 wells were combined and then collected by centrifugation (200 x g; 10 min). The supernatant was aspirated and discarded. The collected cells were lysed in 1 ml of TRIzol reagent with vortex in a 1.5 ml microcentrifuge tube, and then left at R.T. for 5 min. In order to extract total RNA, 0.2 ml of chloroform was added per microcentrifuge tube, followed by vigorous shaking for 15 sec and incubation for 3 min at R.T.. RNA was then separated from DNA by centrifugation at 12,000 x g for 15 min at 4°C. After that, the top colourless aqueous phase containing RNA was transferred to another microcentrifuge tube. Isopropanol (0.5 ml) was added to precipitate RNA and the mixture was incubated for 10 min at R.T.. The RNA pellet was collected by centrifugation at 12,000 x g for 10 min at 4°C and was washed with 1 ml of 75% ethanol. After centrifugation at 7,500 x g for 5 min at 4°C, ethanol was removed, and the RNA pellet was air dried by leaving on an open bench for 3 min. The air dried pellet was dissolved in 20 µl of DEPC-treated water (0.1%). The concentration and purity of the RNA extract were determined by measuring its absorbance at 260 nm (A_{260}) and 280nm (A_{280}). The A_{260} reading of 1 corresponds to approximately 40 µg/ml total RNA. A good RNA purity was indicated by an

A_{260}/A_{280} ratio more than 1.5. RNA extracts were stored at -70°C.

3.5.2 cDNA synthesis by reverse transcription (RT)

In order to remove genomic DNA contamination, the RNA extracts were treated with DNase I. 2 μg of RNA extract was incubated with 1 μl of DNase I (amplification grade; 1 U/μl) in 1 μl of 10X DNase I reaction buffer. DEPC-treated water was added to give final volume of 10 μl and this final mixture was incubated in RNase-free 1.5 ml microcentrifuge tube for 15 min at R.T. After that, DNase I was inactivated by addition of 1 μl of 25 mM EDTA solution to the reaction mixture followed by heating for 10 min at 65°C. The RNA sample (10 μl) was then ready to use in reverse transcription and subsequent amplification.

RNA sample was reverse-transcripted to first-strand complementary DNA (cDNA) using SuperScript III First-strand cDNA Synthesis SuperMix. Firstly, in a 0.2-mL thin-walled PCR tube, 5 μl of DNase-treated RNA solution was mixed with 1 μl of 50 μM oligo $(dT)_{20}$ primer, 1 μl of annealing buffer and 1 μl of DEPC-treated water. This mixture was then heated for 5 min at 65°C in an auto-thermocycler (Stratagene) and was immediately placed on ice for 1 min. Primer extension was performed by adding 10 μl of 2 x first strand buffer and 2 μl of SuperScript III/RNaseOUT Mix, and followed by incubating for 50 min at 50°C. The reaction mixture was finally heated for 15 min at 72 °C to terminate cDNA synthesis. Negative control samples were generated in the absence of reverse transcriptase to ensure the samples were free from contaminating DNA and reagent contamination. These synthesized first-strand cDNAs were used as templates for subsequent PCR.

3.5.3 Semi-quantitative PCR

Relative expression of EP and IP receptor mRNAs was determined by PCR using the internal standard GAPDH mRNA level. PCR amplification was carried out using FastStart High Fidelity PCR System as per manufacturer's instructions. For each

PCR reaction, 2 μl of cDNA was mixed with 0.5 μl of 10 mM dNTPs, 4 μl of 1 μM forward primer, 4 μl of 1 μM reverse primer, 2.5 μl of 10X reaction buffer with 18 mM $MgCl_2$, 0.25 μl of 5 U/μl FastStart High Fidelity Enzyme Blend, and 11.75 μl DEPC water in a 0.2-mL thin-walled PCR tube. The total volume of each reaction mixture is 25 μl. The quantities of glial cells in glial cell cultures were set up to match the quantity of glial cells in mixed DRG cell cultures and to reflect the relative contribution by glial cells in mixed DRG cell cultures. From our studies, neuron-enriched cultures were estimated to have 200 glial cells out of 5000 neurons, which is 1 % of number of glial cells in our glial cell cultures. Therefore, in order to evaluate the relative contribution by contaminating glial cells in neuron-enriched cultures, 0.02 μl of cDNA from glial cultures was mixed with 1.98 μl of DEPC water as a starting template. The primers for EP_4, IP and GAPDH are listed in Table 1. PCR amplification was performed in an auto-thermocycler (Stratagene). The cycling conditions for EP_4 and IP receptors were as follows: initial denaturation for 2 min at 94°C, followed by 42 amplification cycles of 45 s at 94°C (denaturation), 45 s at 60°C (annealing), and 45 s at 72°C (extension), followed by final extension cycle of 10 min at 72°C. For GAPDH, initial denaturation cycle was followed by 36 amplification cycles of 45 s at 94°C (denaturation), 45 s at 53°C (annealing), and 45 s at 72°C (extension). The final extension was carried out at 72°C for 10 min. The PCR products were resolved using a 1.5% agarose gel containing 1 x GelRed™ and the DNA bands were visualized by UV illumination and were quantified using Quanity One (Bio-Rad). The relationship between the amount of PCR products and the number of amplification cycles (32 – 42 for EP_4 and IP, and 36 – 42 for GAPDH) was linear (data not shown).

3.6 Immunocytochemistry

3.6.1 Identification of various cell subtypes in DRG cell culture

Cells cultured on glass coverslips were preserved in kyrofix (Raye *et al.*, 2007) at 4°C until immunocytochemistry was performed. Following washing with PBS, then fixing in ice-cold acetone–methanol (1:1) for 30 min, cells were then permeabilized with 0.03% Triton X-100 and blocked with 3% donkey serum for 30 min. For identification of neurons, antibodies against neuron-specific class III β-tubulin (TUJ-1; 1:1000) were used. To identify neuronal subpopulations, we used biotinylated IB4 (1:250) and antibodies against CGRP (1:1000), TrkA (1:1000), and heavy neurofilament NF200 (SMI32; 1:250). Glial cells were identified with Cy3-conjugated anti-GFAP antibodies (1:100). Cells were incubated with the primary antibodies at 4°C for 16–20 h, followed by FITC- or Cy3-conjugated secondary antibodies (1:500) for 1 h at R.T.. For IB4 detection, AMCA-streptavidin (1:250) was used. For nucleus staining, samples were incubated with Hoechst 33342 (0.2 μg/ml) for 10 min. The coverslips were mounted with glycerol (90%) on glass slides and imaged using a Zeiss Axioskop II Plus microscope with AxioCam digital camera. Bright field or phase contrast images and fluorescent images were merged using SPOT software (Diagnostic Instruments Inc., Sterling Heights, MI, USA). The number of immunoreactive neurons was determined by counting a minimum of 100 neurons in each of three to four independent experiments.

3.6.2 Identification of EP and IP receptor localization in DRG cell cultures

DRG cells were cultured on glass coverslips and were fixed using paraformaldehyde (4% in PBS) for 15 min, permeabilized with Triton X-100 (0.01% in PBS) for 15 min, then blocked with donkey serum (3%) in PBS for 30 min. Primary antibodies used recognised EP_4 receptor (1:500) and IP receptor (1:500). Specificity of immunostaining was demonstrated by loss of signal after preincubating primary

antibodies with EP_4 or IP receptor antibody blocking peptides for 1 h, respectively, (Fig. 6.5Q). Neurons were identified with antibodies recognising neuron-specific class III β-tubulin (TUJ-1,1:500) and glial cells with antibodies recognising glial fibrillary acidic protein (Cy3-conjugated GFAP, 1:500). Cells were incubated with primary antibodies at 4 °C for 16 – 20 h, followed by FITC- and Cy3-conjugated secondary antibodies (1:500), as appropriate. Hoechst 33342 stain (0.2 μg/ml; 4 min) was used to identify cell nuclei. The coverslips were mounted with glycerol (90%) on glass slides and imaged using an Olympus FV1000-ZCD laser scanning confocal system fitted with an IX81 inverted microscope (Center Valley, PA, USA). Fluorescent images were merged using Adobe Photoshop CS3 (San Jose, CA, USA)

Table 1. Sequences of primers for PCR amplification of cDNA of DRG cell cultures

Gene (PCR cycles)	Primer sequence F: forword primer; R: reverse primer	Product size (bp)	References
EP4	5'- TTCCGCTCGTGGTGCGAGTGTTC-3' 5'- GAGGTGGTGTCTGCTTGGGTCAG-3'	423	(Southall *et al.*, 2001)
IP	5'- GCATCCTGGGTGCCCGACG-3' 5'- CAGGCTGGGGGGAACGCAT-3'	431	(Southall *et al.*, 2001)
GAPDH	5'- ACCACAGTCCATGCCATCAC-3' 5'- TCCACCACCCTGTTGCTGTA-3'	452	(Wu *et al.*, 2009)

Chapter 4

Characterization of DRG cell cultures

4.1 Introduction

Dissociated DRG cell cultures are regularly used for studying the cellular responses of sensory neurons *in vitro*. Unlike neurons from neonatal rats, neurons from adult DRG can survive independently of support from trophic factors (Lindsay, 1988). This property of adult DRG cell cultures provides advantages in studying neurite outgrowth and regeneration, because the additional effect of neurotrophic factors in the cultures can be eliminated. A typical dissociated DRG cell culture is heterogeneous and consists of at least three major populations of neurons (large diameter neurons, small diameter peptidergic neurons and small diameter non-peptidergic neurons) and two major populations of non-neuronal cells (SGCs and Schwann cells). Each of these subpopulations of DRG cells has different physiological functions. For example large diameter neurons are proprioceptive while small diameter neurons are nociceptive. In order to study cellular responses from different subpopulations of neurons, we aimed to separate subpopulations of DRG neurons. A subpopulation of small diameter neurons can be identified by their ability to bind to IB4, and can be isolated using MACS (Tucker *et al.*, 2005b). Briefly, DRG cells were isolated from adult rat and were enriched in neurons by the process of differential adhesion. After that, IB4-binding neurons were captured by magnetic beads linked with IB4, and isolated from other cells. As a result, we generated two fractions of neurons: (1) IB4-positive cells which bind to IB4, and (2) the remaining IB4-negative cells which do not bind to IB4.

The aim of this chapter is to characterize different kinds of cells present in DRG cell cultures, and to verify the effectiveness of MACS in separating or

enriching IB4-positive and IB4-negative cells. After that, we can make use of this technique to separate subpopulations of DRG cells for subsequent studies in later chapters.

4.2 Results and discussion

4.2.1 Characterization of DRG cell cultures

A typical mixed DRG cell preparation consisted of phase bright neurons surrounded by phase dark non-neuronal cells (Fig. 4.1A) which are likely to include glial cells (Schwann cells and SGCs) and fibroblasts. The identity of the DRG cells were confirmed by immunocytochemistry using antibodies against neuron-specific class III β-tubulin (TUJ-1) and antibodies against glial cell-specific intermediate filament (GFAP). TUJ-1-positive neurons are surrounded by GFAP-positive glial cells (Fig. 4.1B). Some GFAP-negative non-neuronal cells were present, which may be fibroblasts or non-myelinating Schwann cells (Campana, 2007). Furthermore, immunohistochemistry studies on DRG sections showed that TUJ-1-IR neurons were surrounded by a lot of TUJ-1-negative non-neuronal cells which were visualised by counter staining the cell nuclei using Hoechst 33342 (Fig. 4.2A). When we stained the DRG sections with anti-SK3 antibody, all those perineuronal cells were stained positive (Fig. 4.2B). This staining pattern reveals the histological structure of a DRG, where SK3-IR SGCs enwrap TUJ-1-IR neuronal cell bodies.

In order to better understand the composition of non-neuronal cells in DRG cell cultures, antibodies against specific markers of SGCs, Schwann cells, fibroblasts and microglia were used. Antibodies against Thy1.1 (Murwani *et al.*, 1998) and CD11b (OX-42) (Kingham *et al.*, 1999) were used to identify fibroblast and microglia, respectively. No Thy1.1-IR and CD11b-IR cells were found in our DRG cell cultures (Fig. 4.3 D,E), and this result indicates the absence of fibroblast and

microglia in our DRG cell cultures. The function of Thy1.1 antibody was checked by using fibroblasts as the positive control. Furthermore, there are several specific markers for distinguishing SGCs and Schwann cells *in vivo*. Antibodies against glial-specific glutamate transporter (GLAST) and glutamine synthetase (GS) (Hanani, 2005; Vit *et al.*, 2006; Vit *et al.*, 2008) were used to identify SGCs; while antibodies against GalC and S100β were used to identify Schwann cells (Iwanaga *et al.*, 1989; Ma *et al.*, 2002; Parrinello *et al.*, 2008). However, SGCs in culture lose their specific expression of GS (M. Hanani, personal communication), and antibodies against GS, S100β and GalC non-specifically bound to DRG neurons in culture (Fig 4.3 A-C). In addition, it was suggested that antibodies against small conductance calcium-activated K^+ channel (SK3) are better to differentiate SGCs even comparing with GS or GLAST (P.T. Ohara, personal communication). Although SGCs were specifically identified by anti-SK3 antibodies, recent findings from our lab showed that antibody against SK3 also lose their specificity in distinguishing glial cells in culture, and we are unable to distinguish SGCs from Schwann cells at this moment.

4.2.2 Verification of MACS

In my studies, the majority (~80%) of non-neuronal cell population in DRG cell cultures was GFAP positive on Day 2, so they were regarded as glial cells. In order to facilitate the separation of neuronal fractions, we first eliminate the glial cells present in DRG cell cultures. We made use of the differential abilities of neurons and glial cells in adhering to poly-DL-ornithine surface to separate neurons from glial cells. After 16 h incubation on a poly-DL-ornithine-coated surface, cultures enriched in neurons or glial cells was prepared by their differential adhesion on poly-DL-ornithine. As shown in the phase contrast microscopy images, the differential adhesion process decreased the proportion of contaminating glial cells

(phase dark cells; Fig. 4.4A–D). Fig. 4.4E showed that the differential adhesion process significantly increased the proportion of neurons in cell cultures from 15 ± 1 to 51 ± 5 % of total cell numbers ($p < 0.001$). The proportion of neurons in neuron-enriched cultures, IB4-negative and IB4-positive cell cultures were 51 ± 5, 47 ± 2 and 41 ± 5%, respectively, which were significantly higher than that of the mixed DRG cell culture (15 ± 1%, $p < 0.001$; Fig. 4.4E).

In mixed DRG cell preparations, 12 ± 3% neurons had cell body diameters larger than 30 μm, and this proportion was significantly decreased to 3 ± 1% in the IB4-positive cell preparation ($p < 0.05$; Fig. 4.4F). In the IB4-negative cell preparation, approximately 11 ± 2% of neurons were large diameter neurons, which was not significantly different from the mixed DRG cell preparation or the neuron-enriched preparation (12 ± 2%; Fig. 4.4F). Size distribution analysis further confirmed the elimination of large diameter neurons in the IB4-positive cell preparation and revealed the significant enrichment of neurons with cell body diameter of 21 – 24 μm (Fig. 4.5A-D; $p < 0.01$).

In order to verify the enrichment of target cell types in the cultures, the relative compositions of neuron subpopulations (i.e. CGRP, TrkA, IB4 and SMI32) were determined by immunocytochemistry. Fluorescence microscopic images shown in Fig. 4.6 indicated that the proportion of CGRP-IR neurons was significantly greater in the IB4-negative cell preparation (48 ± 5%) compared with both the mixed DRG cell preparation and IB4-positive cell preparation (24 ± 3 and 12 ± 2 respectively; $p < 0.01$; Fig. 4.6I), demonstrating the enrichment of neuropeptide-containing neurons in the IB4-negative cells. Similarly, more TrkA-IR neurons were observed in the IB4-negative cells (41 ± 1%) compared with both the mixed DRG cell preparation and IB4-positive cell preparation (29 ± 3% and 14 ± 1%; $p < 0.05$ and $p < 0.001$ respectively; Fig. 4.6J), demonstrating the enrichment of NGF-responding neurons

in the IB4-negative cells. Moreover, the proportion of cells binding IB4 increased significantly in IB4-positive cell preparation (56 ± 2%) from the mixed DRG cell preparation (35 ± 6 %, $p < 0.01$; Fig. 4.7M), demonstrating the enrichment of IB4-binding neurons in the IB4-positive cells.. The proportions of cells binding IB4 in neuron-enriched preparation and IB4-negative preparation (28 ± 2% and 30 ± 2% respectively; Fig. 4.7M) were similar to that in mixed DRG cell preparation. Lastly, the proportion of SMI32-positive cells decreased significantly in IB4-positive cell preparation (8 ± 1%) from mixed DRG cell preparation (34 ± 1% $p < 0.01$; Fig. 4.7N), demonstrating the depletion of large-diameter neurons in the IB4-possitive cells. The proportion of SMI32-positive cells in neuron-enriched preparation and IB4-negative preparation (31 ± 1% and 35 ± 6% respectively) were similar to that in mixed DRG cell preparation.

4.3 Conclusion

From above results, we concluded that our mixed DRG cell cultures consist of two major cell types which are neurons and glial cells. In our mixed DRG cell cultures, the proportions of the three major subpopulations of neurons were similar (~20 – 30%). However, the relative proportions of SGCs and Schwann cells in our DRG cell cultures remain to be elucidated. Moreover, MACS is able to enrich neuronal fractions. Our IB4-negative cell preparation represents IB4-depleted fraction. On the other hand, the IB4-positive cell preparation represents large-diameter neuron-depleted and IB4-enriched fraction. One thing to note for the cells isolated using MACS is that the proportion of large diameter neurons and SMI32-positive cells were not enriched in the IB4-negative cell fractions. The proportion of large diameter neurons and SMI32-positive cells were similar in mixed DRG preparations and IB4-negative fractions. This observation may due to only a relatively small population of IB4-positive cells were removed from IB4-negative

fractions. Thus, the overall proportion of large diameter neurons was not significantly affected. As a result, although we eliminated a portion of small diameter neurons by MACS in the IB4-negative fraction, the overall proportion of large diameter neurons to total neuronal population was not increased significantly. Therefore, the IB4-negative fraction was an IB4-positive cell-depleted fraction, but not large diameter neuron-enriched fraction. Moreover, we could not get highly purified (> 95%) fractions of subpopulations of DRG neurons, MACS is still a valuable tool to be used in studying the contributions of DRG subpopulations (IB4-positive or IB4-negative cells) in subsequent chapters. Moreover, since we also generated neuron-enriched cell fractions and purified glial cells prior to MACS, these two DRG cell fractions can be used to investigate the contribution of glial cells and to study any possible neuron-glia interactions.

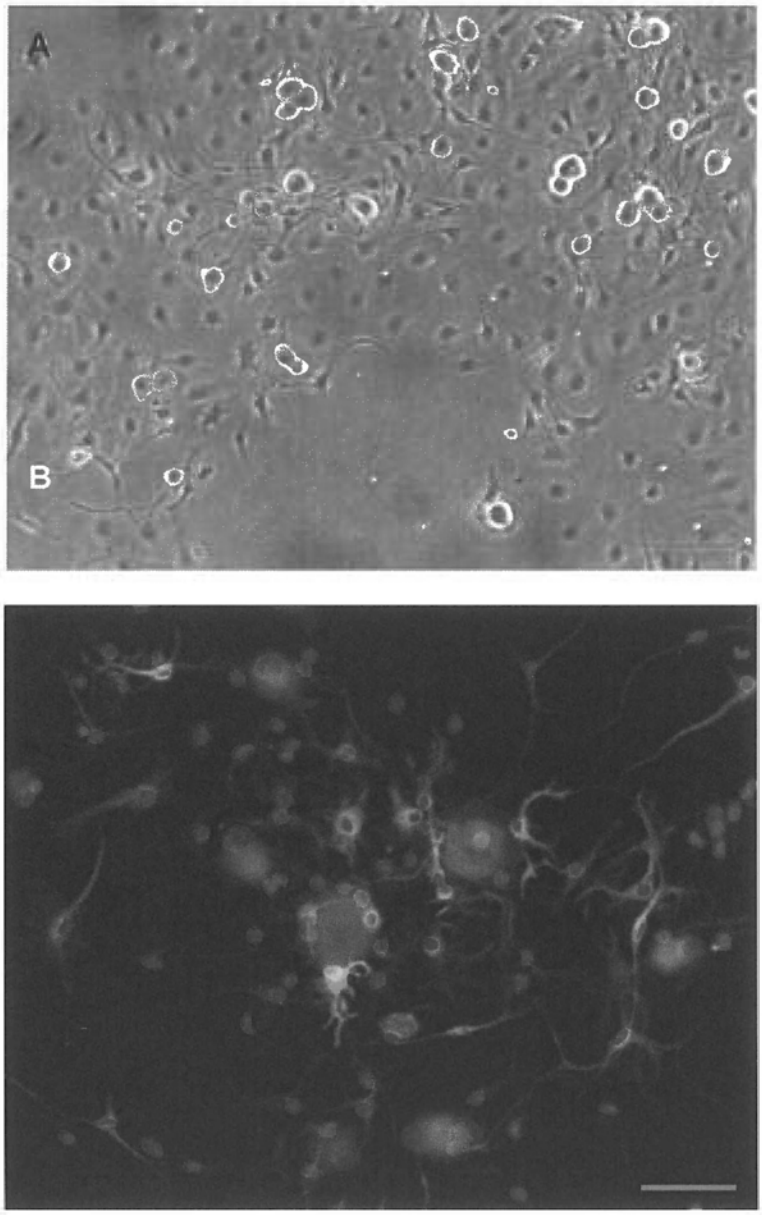

Fig. 4.1. Mixed cultures of DRG cells contain neurons and non-neuronal cells. (A) Representative phase contrast microscopic field of typical dissociated DRG cultures on assay (i.e. 2 DIV), with neurons (phase bright) and non-neuronal cells (phase dark). (B) Representative fluorescence microscopic field of typical dissociated DRG cultures on assay day. Neurons were visualized with anti-TUJ-1 antibodies (FITC secondary antibodies; green), glial cells with Cy3-conjugated anti-GFAP antibodies (red) and cell nuclei are stained blue with Hoechst 33342 stain. Scale bars are 100 μm (A) and 25 μm (B).

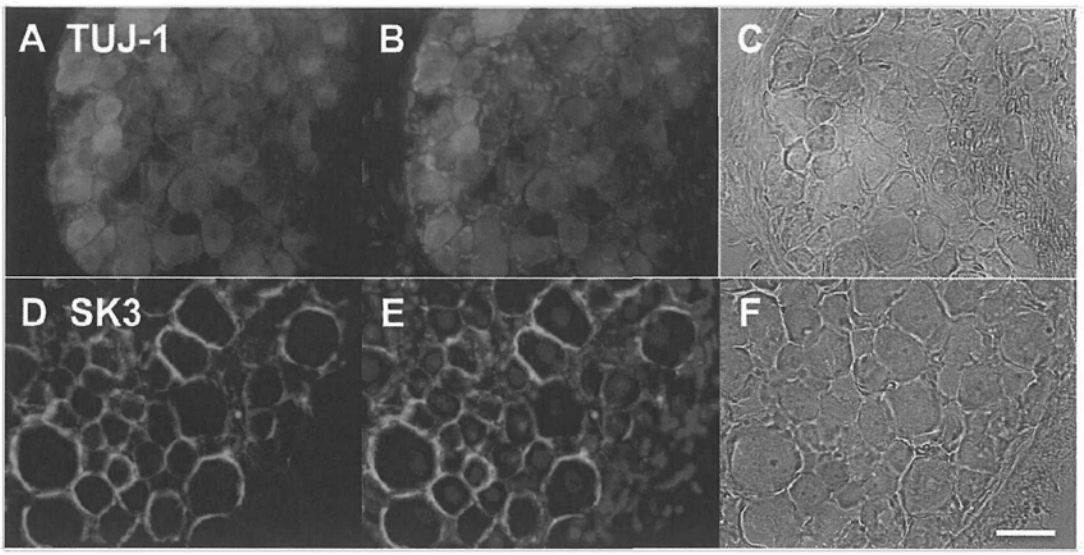

Fig. 4.2. Immunohistochemistry study on DRG sections reveal the distribution of DRG neurons and glial cells. Representative confocal microscopic images of DRG sections stained with anti-TUJ-1 antibodies (FITC secondary antibodies; green; A-C) or anti-SK3 antibodies (cy3 secondary antibodies; red; D-F). (B) Cell bodies of neurons (green) are surrounded by cell nuclei (blue dots) of non-neuronal cells (TUJ-1 negative cells). (E) These non-neuronal cells surrounding neuronal cell bodies are SK3-IR SGCs (red). Cell nuclei are stained blue with Hoechst 33342 stain (B, E). Scale bar is 25 μm.

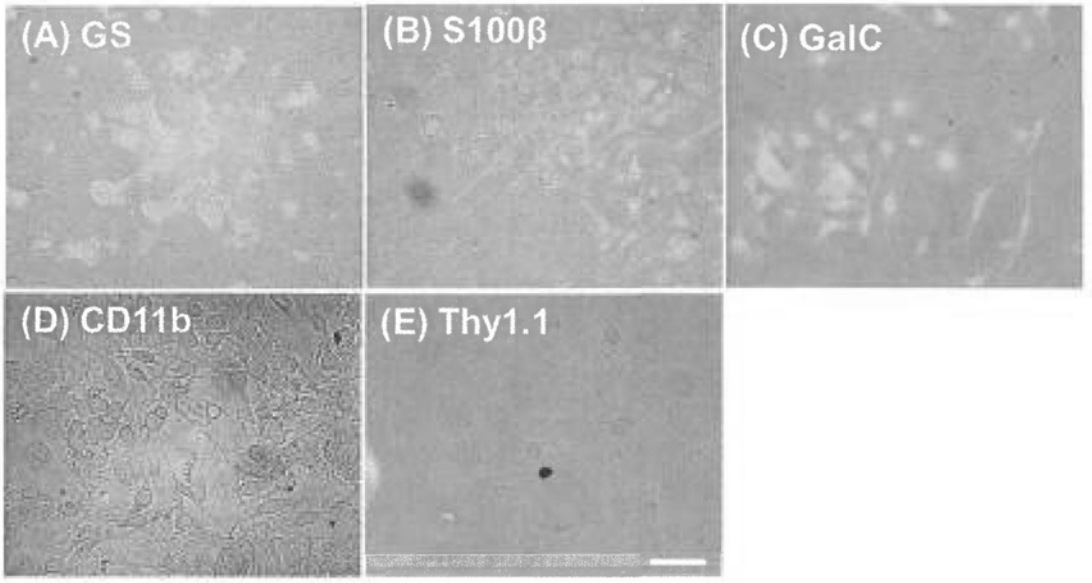

Fig. 4.3. Immunocytochemistry study on DRG cell cultures. Representative phase contrast and fluorescence microscopic images of DRG cell cultures stained with anti-GS antibodies (FITC secondary antibodies; green; A), anti-S100β antibodies (FITC secondary antibodies; green; B), anti-GalC antibodies (cy3 secondary antibodies; red; C), anti-CD11b antibodies (cy3 secondary antibodies; red; D) or anti-Thy1.1 antibodies (FITC secondary antibodies; green; E). Scale bar is 50 μm.

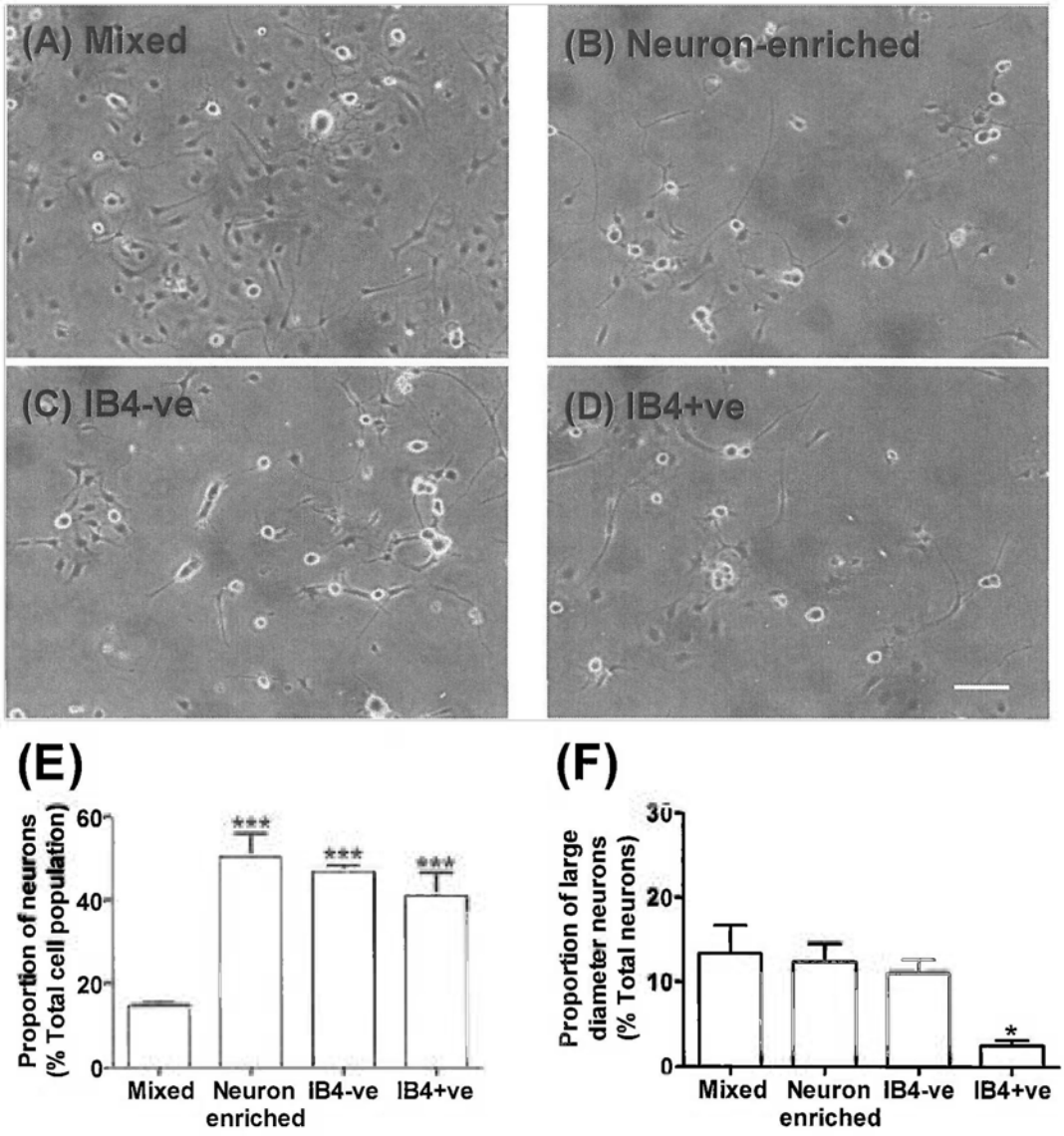

Fig. 4.4. Differential adhesion increased neuronal purity and MACS eliminated large diameter neurons from IB4-positive cell fraction. Phase contrast images of (A) mixed DRG cell cultures, (B) neuron-enriched cultures, (C) IB4-negative and (D) IB4-positive cell cultures. Scale bar is 100 μm. Note the reduction of phase dark glial cells in purified cultures (B – D) and the absence of large diameter neurons in IB4-positive cell cultures (D). Quantification of neuronal cell purity (E) and proportion of large diameter neurons (F) of each DRG culture on day 2, from six independent experiments.* $p < 0.05$, *** $p < 0.001$ compared with mixed DRG cell cultures using one-way ANOVA with Bonferroni's *post hoc* tests.

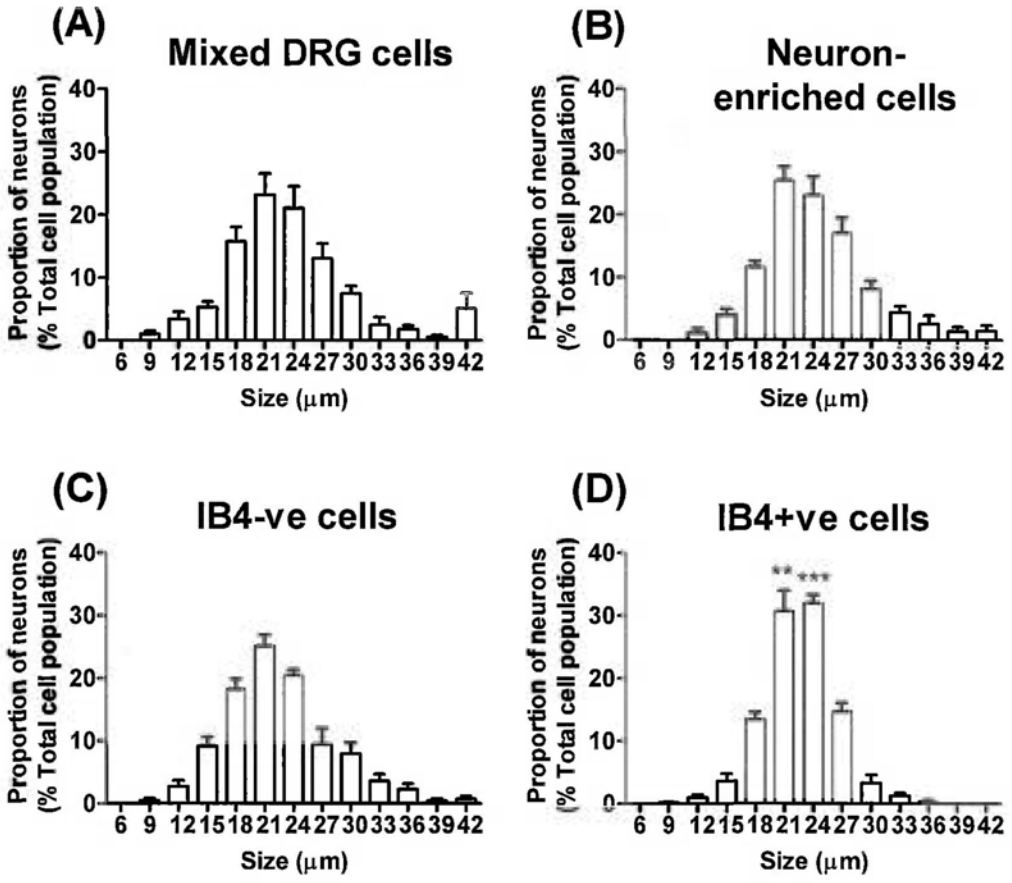

Fig 4.5. Neuronal size distribution in DRG cell, Size distributions of neurons in (A) mixed DRG cells, (B) neuron-enriched cells, (C) IB4-negative cells and (D) IB4-positive cells were determined on assay day (2 DIV) by measuring the diameters of cell bodies, from 6 wells in 2 independent experiments. ** $p < 0.01$ compared with mixed DRG cell cultures using two-way ANOVA with Bonferroni's *post hoc* tests. # $p < 0.05$, ### $p < 0.001$ compared with mixed DRG cell cultures using one-way ANOVA with Bonferroni's *post hoc* tests.

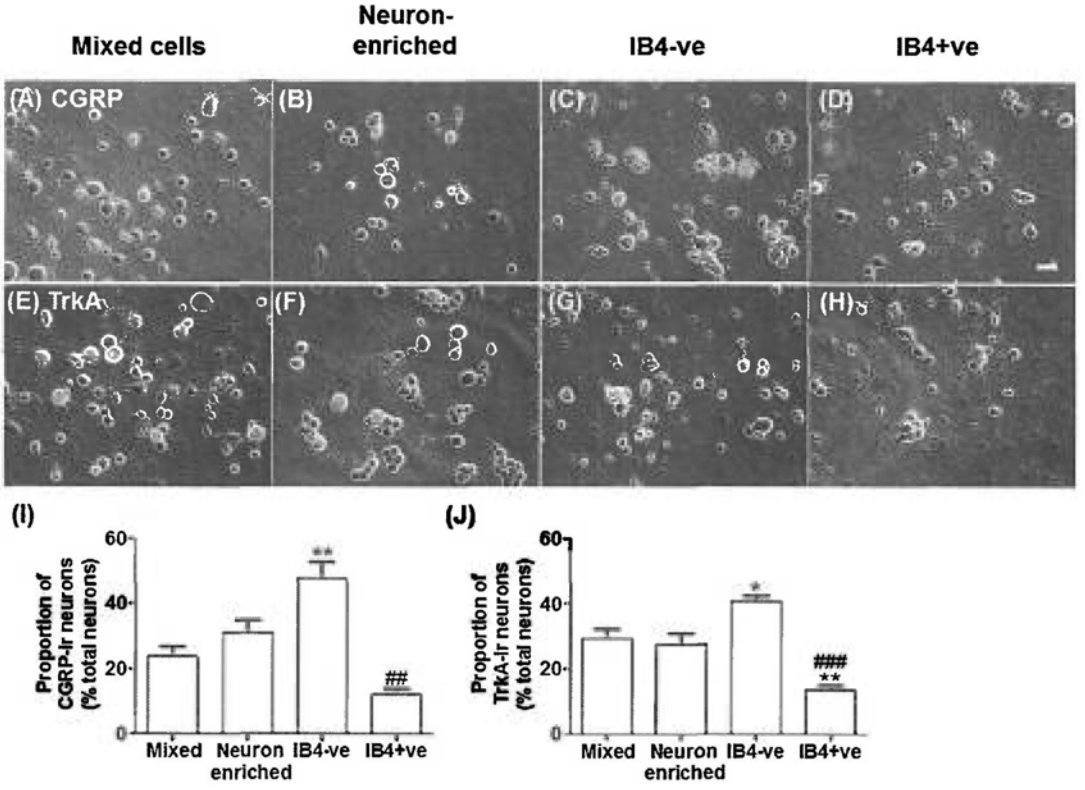

Fig. 4.6. Different DRG cell preparations express different neuronal cell markers (CGRP and TrkA). Neurons were identified on assay day (2 DIV) with phase contrast and fluorescence microscopy, and the number of neurons expressing CGRP (A – D; Cy3 secondary antibodies; red), TrkA (E – H; Cy3 secondary antibodies; red) was determined. Scale bar is 25 μm. Data in I and J are presented as means ± SEM of three to four independent experiments. * $p < 0.05$, ** $p < 0.01$ compared with mixed DRG cell cultures; ## $p < 0.01$, ### $p < 0.001$ compared with IB4-negative cell cultures using one-way ANOVA with Bonferroni's *post hoc* tests.

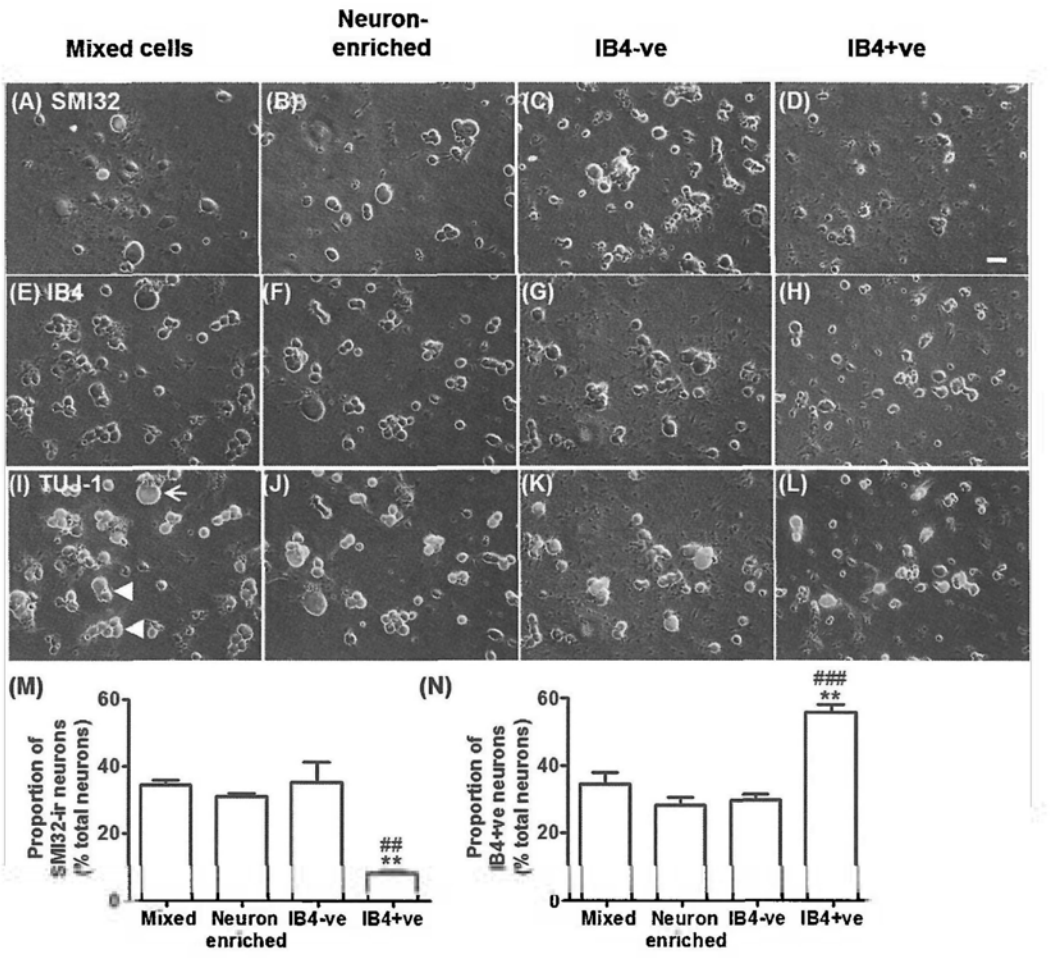

Fig. 4.7. Different DRG cell preparations express different neuronal cell markers (SMI32 and IB4). Neurons were identified on assay day (2 DIV) with phase contrast and fluorescence microscopy, and the number of neurons expressing SMI32 (A – D; FITC secondary antibodies; green) or binding IB4 (E – H; AMCA secondary antibodies; blue) was determined. TUJ-1 staining (FITC secondary antibodies; green) in neurons corresponding to panels E – H is shown in panels I – L, with small diameter neurons (cell body < 30 mm) marked with arrowheads, and a large diameter neuron (cell body > 30 mm) marked with an arrow (panel I). Scale bar is 25 μm. Data in panels M and N are presented as means ± SEM of three to four independent experiments. ** $p < 0.01$ compared with mixed DRG cell cultures; ## $p < 0.01$, ### $p < 0.001$ compared with IB4-negative cell cultures using one-way ANOVA with Bonferroni's *post hoc* tests.

Chapter 5

PTx-sensitive stress-dependent neurite retraction

5.1 Introduction

When injured, the peripheral terminals of DRG neurons can regenerate whereas the central terminals usually die unless provided with a conditioning lesion (Lu *et al.*, 1991; Wu *et al.*, 2007). Thus, dissociated DRG cells are useful tools for studying factors and pathways that control neurite extension and recovery (Kimpinski *et al.*, 2001; Leclere *et al.*, 2007; Lindsay, 1988).

We have previously shown that PGE_2 can stimulate neurite retraction in rat DRG neurons by activating EP_3 receptors (Wise, 2006). To determine whether the EP_3 receptor-dependent response was mediated through coupling to $G_{i/o}$ or $G_{12/13}$ proteins, we pretreated the DRG cell cultures with PTx to inhibit $G_{i/o}$ proteins. When DRG cell cultures were repeatedly removed from the cell culture incubator for quantifying neurite lengths, we noticed that the number of neurons expressing neurites in PTx-treated cells decreased one hour after the start of the experiment. The current study was designed to investigate the nature of this PTx-dependent neurite retraction response observed in DRG neurons.

PTx consists of an A-promoter and a B-oligomer. The PTx B-oligomer binds with a cell surface receptor (most likely contain carbohydrate), facilitating entry of the A-promoter into the cell which inactivates G-proteins of the $G_{i/o}$ family by ADP-ribosylation. However, the PTx B-oligomer of PTx has been reported to have biological activities independent of G-protein inactivation (Kaslow *et al.*, 1992). PTx favoured neurite outgrowth from adult retinal ganglion cells by acting on olfactory ensheathing cells (OEC) monolayer (Hayat et al., 2003). However, the PTx B-oligomer was responsible for altering the parallel alignment of neurite regrowth

from retinal ganglion cells on the OEC monolayer, which is due to a disruption of neuronal guidance mechanisms and not due to any intracellular effect on the function of OECs. The PTx B-oligomer showed no effect on rate of neurite outgrowth (Hayat et al., 2003). It is also reported that the PTx B-oligomer is responsible for inhibiting growth cone guidance independent of direct G-protein inactivation. The PTx B-oligomer inhibits both the guidance by growth promoting laminin and growth cone collapsing brain membrane-derived factor (Kindt *et al.*, 1995). In our studies, this potential effect which is independent of direct G-protein inactivation was investigated by pretreating DRG cells with the PTx B-oligomer.

5.1.1 Aim of study

Given the heterogeneous nature of a typical preparation of DRG cells, this study aimed to identify whether the PTx-dependent neurite retraction response was specific to any one of the three subpopulations of neurons (large diameter neurons, small diameter peptidergic neurons, and small diameter non-peptidergic neurons). Moreover, we were interested to know whether the PTx-dependent neurite retraction response is mediated by its ability to inactivate $G_{i/o}$ proteins or its binding to the cell surface via the PTx B-oligomer.

During the study, we prepared purified cultures of DRG cells followed by separating into subpopulations of DRG neurons (i.e. IB4-positive and IB4-negative cells). As a result, we discovered that the glial cells were involved in regulating this response, since PTx-dependent neurite retraction response was lost after removal of glial cells in culture. There we aimed to investigate how glial cells interacted with neurons to regulate this neurite retraction response. We tested our hypothesis that glial cells release soluble factors to promote neurite retraction in PTx-treated neurons. After elucidating the effect of glial cells in PTx-dependent neurite retraction, we finally moved back to identify which subpopulations of neurons were

demonstrated for this neurite retraction response.

5.2 Results

5.2.1 PTx-dependent neurite retraction in mixed DRG cell culture

In all experiments, neurites started to grow on day 1 before addition of PTx or PTx B-oligomer. Overnight pretreatment of mixed DRG cell cultures with PTx or PTx B-oligomer did not alter the intrinsic neurite outgrowth ability (Fig. 5.1A,B). The proportion of neurite-bearing neurons was 67 ± 3% for the control group, 69 ± 3% for PTx group and 68 ± 3% for the PTx B-oligomer group. Interestingly, once after stress induction, we saw a trend of decrease in the proportion of neurite-bearing neurons in PTx treated cells, but not in the PTx B-oligomer treated cells (Fig. 5.1A,B). In order to control for the variations of basal proportions of neurite-bearing cells between each well, data were reexpressed by normalizing with corresponding basal values for each well. We observed a maximal and significant decrease in the proportion of neurite-bearing neurons in the PTx pretreated cells (14 ± 4% less neurite-bearing neurons compared to control) which then recovered over the remaining 5 h of observation (Fig. 5.1C). In contrast, no neurite retraction response was observed in the PTx B-oligomer pretreated cells (Fig. 5.1D). In order to visualize the neurite retraction response, DRG cells were fixed at 1 h after stress induction (time for maximal response) and stained with TUJ-1 antibody. Under control conditions, neurites were extensively expressed on all types of DRG neurons (Fig. 5.1E). However, those neurites of large diameter neurons retracted in the PTx pretreated group (Fig. 5.1F).

5.2.2 No PTx-dependent neurite retraction response in purified cultures

To determine whether all three major neuronal subtypes were affected by PTx, we prepared IB4-negative and IB4-positive cells. So we started with preparing

neuron-enriched DRG cell cultures. The neuron-enriched cultures were further separated into IB4-negative and IB4-positive cells. However, none of these neuron-enriched DRG cell preparations displayed the PTx-dependent neurite retraction response observed previously in the mixed DRG cell cultures (Fig. 5.2 A-C).

5.2.3 Reoccurrence of PTx-dependent neurite retraction response in IB4-negative cells with additional glial cells

From the comparison between mixed DRG cell cultures and purified cultures, we hypothesized that glial cells were essential for the PTx dependent neurite retraction response. So we set up an experiment in which glial cells were added back to those purified cultures (IB4-negative and IB4-positive cells) to mimic the glial cell environment of mixed DRG cells. In the presence of additional glial cells, the proportion of neurite-bearing neurons significantly decreased by 16% ($p < 0.05$) in PTx pretreated IB4-negative cells. However, no response was observed in the IB4-positve cell preparations with additional glial cells (Fig. 5.3).

5.2.4 Conditioned medium from glial cells facilitates the PTx-dependent neurite retraction in IB4-negative cells

After proving the importance of glial cells in facilitating the PTx-dependent neurite retraction response, we proceeded to explore the means of this neuron-glia interaction. There are two possible means for neuron-glia interactions which are soluble factors and direct cell-cell contact. In order to determine whether physical contact was essential for the PTx-dependent neurite retraction response, we tested the effect of medium conditioned by glial cells on IB4-negative and IB4-positive cells. In addition, in order to test whether the release of soluble factor is dependent on stress-induction, the effect of conditioned medium from stressed and unstressed glial cells were also tested. Our results showed that conditioned medium from both

unstressed and stressed glial cells were able to facilitate the PTx-dependent neurite retraction response in IB4-negative neurons (Fig. 5.4A,B), but not in IB4-positive neurons (Fig. 5.4C,D). The proportion of neurite-bearing IB4-negative neurons decreased significantly after 1 h by 17 and 16% ($p < 0.01$ and $p < 0.05$ respectively; (Fig. 5.4A,B) in the presence of conditioned medium from unstressed and stressed glial cells, respectively.

5.2.5 The PTx-dependent neurite retraction is only observed in large diameter IB4-negative neurons

IB4-negative cell culture consists of large diameter neurons and small diameter peptidergic neurons, which are responsible for different physiological functions. Large diameter neurons are responsible for proprioception, while small diameter neurons are responsible for nociception. So we proceeded to investigate which subpopulation was responsible for the PTx-dependent neurite retraction response by analyzing the size of neurons which retracted their neurites in Fig. 5.5A,B. The proportion of large diameter (> 30 μm) IB4-negative neurons expressing neurites decreased significantly from 49 ± 3 to 24 ± 2% ($p < 0.001$; Fig. 5.5A). In addition, the average length of the longest neurite was significantly decreased from 33 ± 2 to 19 ± 3 μm in the large diameter IB4-negative neurons ($p < 0.001$, Fig. 5.5B). As these data were taken from IB4-depleted cell populations with medium conditioned by glial cells, we performed a similar analysis on the PTx pretreated mixed populations of cells and obtained a similar profile of responses (Fig. 5.5C,D). The proportion of large diameter (> 30 μm) neurons expressing neurites decreased significantly from 64 ± 3 to 34 ± 3% ($p < 0.001$, Fig.5.5C), while the average length of the longest neurite was significantly decreased from 52 ± 9 to 41 ± 7 μm ($p < 0.05$, Fig. 5.5C).

5.3 Discussion

PTx inhibits $G_{i/o}$-proteins by ADP-ribosylation of the $G\alpha_{i/o}$-subunit (Tamura *et al.*, 1982) and is therefore a useful tool to investigate the role of $G_{i/o}$-protein dependent cell signalling pathways. When used to determine whether the EP_3 receptor-dependent retraction of DRG neurites was mediated through coupling to $G_{i/o}$ or $G_{12/13}$ proteins (Wise, 2006), we noticed that the number of neurite-bearing neurons was reversibly decreased in PTx-treated cells. Therefore the first part of my study was designed to investigate this PTx-dependent neurite retraction response and to determine whether this response was specific to any particular subset of DRG neurons. Our data clearly shows that neurites retract in approximately 15% of PTx-treated cells, and that this effect appears to be reversible. Moreover, PTx-treatment alone is not sufficient to generate this response, as the proportion of neurite-bearing neurons was not affected at the start of the experiment. The stimulus for this PTx-dependent neurite retraction response was simply removing the cells from the incubator in order to monitor neurite outgrowth over time. And, while the cells responded to the initial stimulus, they appeared to become resistant to subsequent stimuli over the course of 6 h of observation. Although it is possible that the cells which retracted their neurites subsequently died, thus leaving the viable neurons to continue to express neurites, we saw no evidence of substantial cell death in these experiments. We have therefore referred to this stimulus simply as a stress response as we have not presently investigated the multifactorial process involved and we focused on the factor/s regulating the neurite retraction response.

PTx consists of two subunits; the PTx B-oligomer helps to anchor the toxin to the cell surface allowing for internalization of the A-promotor and subsequent ADP-ribosylation of $G\alpha_i$-subunits (Wong *et al.*, 1996). However, it was suggested that the PTx B-oligomer is not inert and has been shown to block growth-cone

collapse in embryonic chick DRG cells (Kindt *et al.*, 1995). In order to distinguish whether the effect of PTx was dependent on $G_{i/o}$-protein inhibition, DRG cells were also tested with PTx B-oligomer. Our results showed that the PTx B-oligomer pretreatment had no effect on neurite outgrowth in the current study. Therefore, we conclude that the PTx-dependent neurite retraction response involves direct inhibition of $G\alpha_{i/o}$-proteins.

This PTx-dependent neurite retraction response occurred in approximately 15% of the whole DRG neuron population. To investigate whether this response was specific to any particular subset of DRG neurons, we prepared neuron-enriched cultures which were further enriched with IB4-positive and IB4-negative cells. Full characterization of our DRG cell preparations showed that the cell size distribution (i.e. proportion of small and large diameter neurons) and the expression of neuron-specific markers (CGRP, TrkA and SMI32 immunoreactivity, and IB4-binding) were similar in mixed DRG cell cultures and neuron-enriched cell preparations. With the use of MACS technology, as described by Tucker et al. (2005), we generated a cell population enriched in IB4-positive neurons. In agreement with previous reports (Bennett *et al.*, 1998; Molliver *et al.*, 1997; Snider *et al.*, 1998; Stucky *et al.*, 1999), the IB4-positive neurons were predominantly small diameter non-peptidergic neurons, and the IB4-negative cells were predominantly small diameter peptidergic neurons and large diameter non-peptidergic neurons expressing heavy neurofilament (Fig. 4.3 & 4.4). According the immunocytochemistry result on mixed DRG cell cultures, IB4-binding neurons represent a fraction (35%) of total DRG neurons population. Although the MACS procedure clearly enriched the proportion of small diameter, IB4-binding neurons, we were unable to generate cell populations in excess of 60% purity. Moreover, our data would suggest that the collected IB4-positive neurons represent a small fraction

of total DRG neurons as the percentage of IB4-binding neurons in IB4-negative cultures was not significantly altered by MACS. And in this collected IB4-positive fraction, the CGRP-IR, TrkA-IR and SMI32-IR cells were significantly reduced. On the other hand, IB4-negative cells contained two major fractions, which are CGRP/TrkA-positive neurons (24 – 29%) and SMI32-positive neurons (34%). MACS procedure was able to enrich CGRP/TrkA-positive neurons by 10 – 15%. Furthermore, morphometric analysis showed that only 10% of neurons in the IB4-negative cell population were >30 μm in diameter, yet approximately 34% were SMI32-positive. This discrepancy might be due to binding of anti-heavy neurofilament antibodies to IB4-positive neurons (Leclere *et al.*, 2007). DRG neurons from adult rats do not require exogenous growth factors (Lindsay, 1988), and as a significantly greater proportion of IB4-negative cells expressed TrkA-immunoreactivity, this is likely responsible for the more rapid neurite extension observed in these cells than GDNF-responsive IB4-positive cells. In contrast, the IB4-positive cells required an extra day in culture to generate a comparable number of neurite-bearing neurons. The slower extension of neurites by GDNF-responsive cells compared to NGF-responsive cells has been previously reported (Leclere *et al.*, 2007; Tucker *et al.*, 2006).

In contrast to our observations of a PTx-dependent neurite retraction response in mixed DRG cell cultures, no such response was seen in any of the three neuron-enriched cell cultures. We used a differential adhesion and replating method to prepare these neuron-enriched cell cultures, but this procedure is unlikely to alter the general properties and responsiveness of neurons (Heblich *et al.*, 2001), except for the rate of neurite extension. When plated on culture surfaces, neurons harvested by differential adhesion showed a more rapid neurite extension than neurons in mixed cell cultures. On the assay day (2 DIV), the proportions of neurite-bearing

neurons in neuron-enriched cells (undisturbed for 1 day) were comparable to that in mixed DRG cell cultures (undisturbed for 2 days). On the other hand, neurite outgrowth was similar in mixed and neuron-enriched cell cultures, therefore we hypothesized that the removal of 'contaminating' glial cells did not alter the intrinsic neurite outgrowth capacity and had caused the loss of the PTx-dependent neurite retraction response in the neuron-enriched cell cultures. Studies have shown that glial cells contribute to the normal function of neurons, such as substance P release, bradykinin evoked inward currents and pain behaviour (Dublin *et al.*, 2007; Heblich *et al.*, 2001; Tang *et al.*, 2007). Therefore, to verify this hypothesis, harvested glial cells were added back to the neuron-enriched cultures. Interestingly, after supplementation with glial cells, the PTx-dependent neurite retraction response was restored, but only in the IB4-negative cell fraction. This result confirmed our hypothesis and revealed an important role for glial cells in facilitating PTx-dependent neurite retraction in DRG cell culture.

In studies of glial cells of the central nervous system, soluble factors such as ATP, cytokines, glutamate, nitric oxide and PGE_2 derived from glial cells can sensitize neurons (Milligan *et al.*, 2009; Scholz *et al.*, 2007; Zheng *et al.*, 2007). In contrast, direct contact with SGCs was reported to be essential for bradykinin-evoked currents in cultured neonatal DRG neurons (Heblich *et al.*, 2001), and for pain and injury-associated gap junction coupling between cultured trigeminal neurons and SGCs (Dublin *et al.*, 2007; Suadicani *et al.*, 2009). In addition, adhesion molecules clearly play a role in central nervous system tripartite synapse formation and neuron-glia interactions (Togashi *et al.*, 2009), and membrane-membrane interactions between neurons and astrocytes (Hatten, 1987) or Schwann cells (Salzer *et al.*, 1980) was essential for inhibition of glial cell proliferation *in vitro*. In order to investigate whether direct cell-cell contact between

glial cells and neurons is required for regulating neurite extensions, the effect of conditioned medium collected from purified glial cell cultures was tested. Our studies clearly demonstrated that direct cell–cell contact was not required for the effect of glial cells, as addition of medium conditioned by glial cells also allowed for detection of the PTx-dependent neurite retraction in IB4-negative cells. Furthermore, there was no difference in the extent of this effect if the stress stimulus was applied directly to the glial cells rather than to the neuronal cells. Therefore, we concluded that the stimulus was acting on neurons instead of glial cells. The cultured DRG neurons were able to sense the initial removal from the incubator for 20 min (at time -1 h), which was sufficient to initiate the neurite retraction response. Although the stress stimulus appears to directly affect the neuronal cells, under control conditions no dramatic effect is observed on cell morphology. However, when $G_{i/o}$-proteins were inhibited by PTx then factor/s constitutively released by glial cells caused retraction of neurites following this stress stimulus. At the present time, we are unable to separate the SGCs and Schwann cells to produce the pure cell preparations needed to identify the cellular source of such constitutively released factor/s.

Of the two readily separable neuronal cell populations, only the IB4-negative cells display this PTx-dependent neurite retraction response. The IB4-negative cell fraction includes large diameter proprioceptive neurons and small diameter peptidergic nociceptors (Fang *et al.*, 2006; Julius *et al.*, 2001). Cell size analysis showed that the large diameter IB4-negative cells were the principal cell types responsive to PTx. Interestingly, large diameter NF200-positive neurons are more susceptible to injury as they require both peripheral and central neurotrophic factors to survive. NF200-positive neurons were reduced substantially after either dorsal rhizotomy (central) or peripheral axotomy, whereas IB4-positive neurons decreased only after combined injury (Guseva *et al.*, 2006). While our large diameter

IB4-negative neurons in culture may lack crucial neurotrophic factors from central and peripheral terminals, this deprivation of neurotrophic factors is unlikely to be the primary cause of the PTx-dependent neurite retraction response because our cells lose this response over time and there is no evidence of cell death. In addition, we proposed that IB4-negative large diameter neurons, but not glial cells, were the target of PTx. If glial cells were affected by PTx treatment, we would not see the neurite retraction in our conditioned medium studies where glial cells were not treated with PTx. In our studies, stress induced PTx-treated IB4-negative neurons to reversibly retract their neurites under the influence of soluble factors derived from glial cells. Based on the fact the conditioning injury elevates cAMP level in neurons and promotes neurite outgrowth. We expect the PTx treatment to do the same. In theory, PTx inhibits Gi/o-protein signaling pathway to elevate the cAMP level in DRG neurons and in turns promotes neurite outgrowth. Interestingly, we found that PTx do the opposite in mixed DRG cell cultures. In later chapter, the PTx treatment on mixed DRG cell cultures reduced cAMP production. As we showed that PTx reduced the cAMP level, so it is possible for PTx to determine the outgrowth of neurite by reducing cAMP level. However, detailed role in actions of PTx on neurite outgrowth remains to be elucidated.

In conclusion, we have identified a multifactorial regulatory response, mediated by $G_{i/o}$-proteins, which prevent retraction of neurites in large diameter IB4-negative cells of adult rat DRG. The glial cells of adult rat DRG constitutively release factor/s that can stimulate neurite retraction of a subset of isolated DRG neurons, but this property of glial cells is only observed when the $G_{i/o}$-proteins of large diameter IB4-negative cells are inhibited. The neurite outgrowth is like having multiple factors acting on a balance. Neurite retraction was observed only when we offset the balance by taking away the factors that prevent retraction and introducing factors

that favour neurite retraction. Interestingly, the interaction between glial cells and neurons can only be observed under this condition where $G_{i/o}$-protein signalling is inhibited. Therefore, our studies revealed a neuron-glial interaction in which glial cells played an important role in influencing neurite outgrowth of DRG neurons.

5.4 Summary

In this study, we show that glial cells are essential for the PTx-dependent neurite retraction response in IB4-negative large diameter neurons. Large diameter neurons appear to be more susceptible to stress stimulus and transiently retract their neurites upon initial stimulus of removal from the incubator. Lack of response in PTx B-oligomer treated cells confirmed that the neuroprotective pathway is a $G_{i/o}$-protein signalling pathway. Moreover, the effect of conditioned medium from both stressed and unstressed glial cells suggested that glial cells constitutively release soluble factor(s) to regulate neurite outgrowth. To conclude, this neurite retraction response is facilitated by glial cell-derived soluble factor(s) and counterbalanced by a neuroprotective $G_{i/o}$-protein signalling pathway. From this study, we clearly demonstrate a neuron-glia interaction in which glial cells regulate the neurite outgrowth properties of DRG neurons.

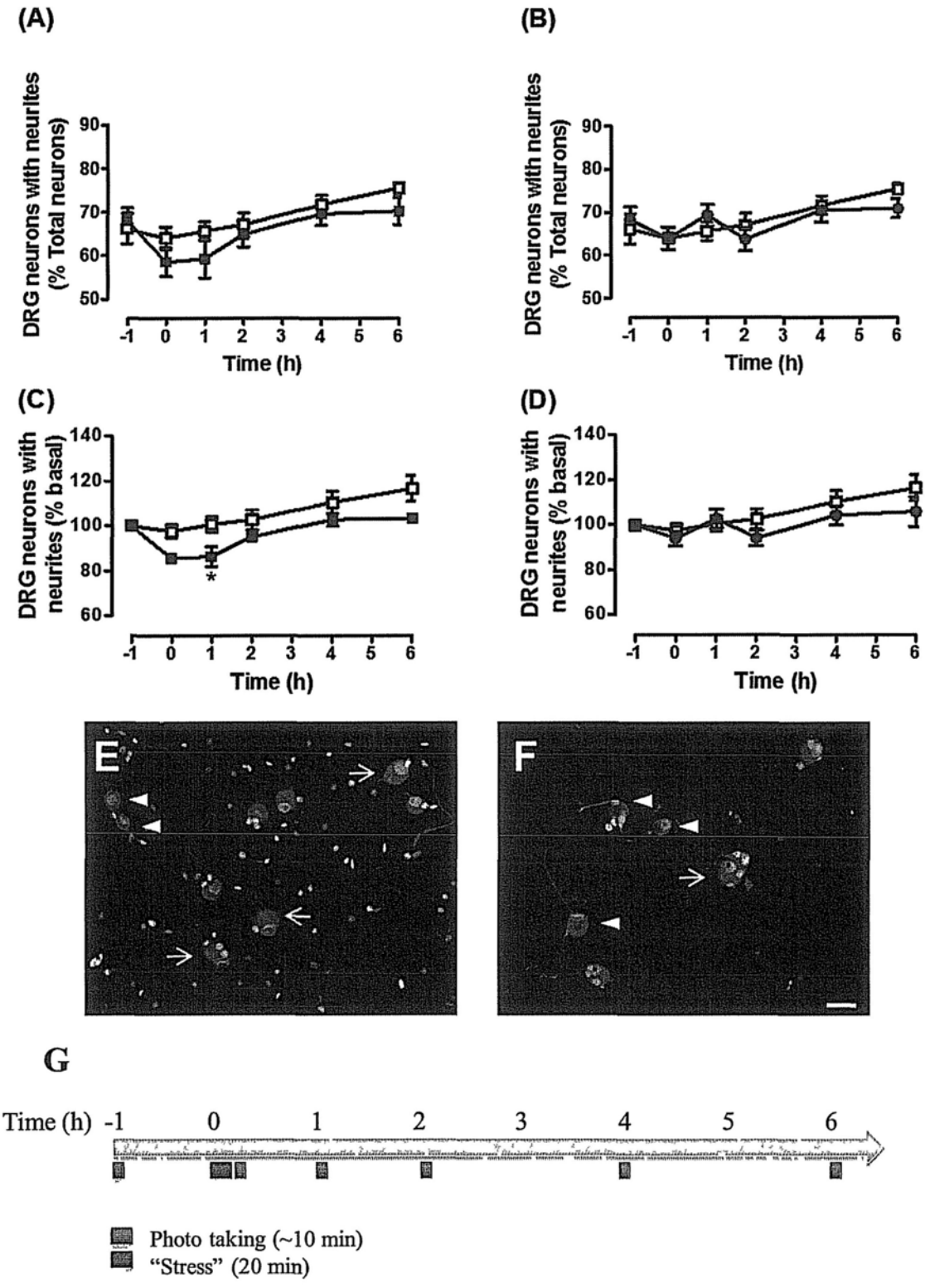

Fig. 5.1. PTx pretreatment causes neurites to retract in mixed DRG cell cultures. Cells were incubated in control solution (Ham's F14 medium, □), with or without PTx (100 ng/ml, ■) or PTx B-oligomer (100 ng/ml, ●) added 16 h before start (time = -1 h). Cells were removed from incubator for 20 min at time 0 to induce stress

(time = 0 h). The proportion of cells with neurites was determined over the following 6 h. (A,B) Raw data showing the proportion of neurons expressing neurites, and (C,D) data normalized for each well of cells related to their initial values at time = -1 h (% basal). Data are presented as means ± SEM of ten wells from five independent experiments. * $p < 0.05$ compared with control group. (E,F) Representative immunofluorescence images of control and PTx pretreated cells, respectively, at time = 1 h. Neurons were visualized with anti-TUJ-1 antibodies (Cy3 secondary antibodies; red) and nuclei were stained with Hoechst 33342 stain (blue). Small diameter neurons (cell body < 30 μm) are marked with arrow heads, and large diameter neurons (cell body > 30 μm) are marked with arrows. Scale bar is 25 μm. (G) Schematic diagram showing the time line for neurite assay.

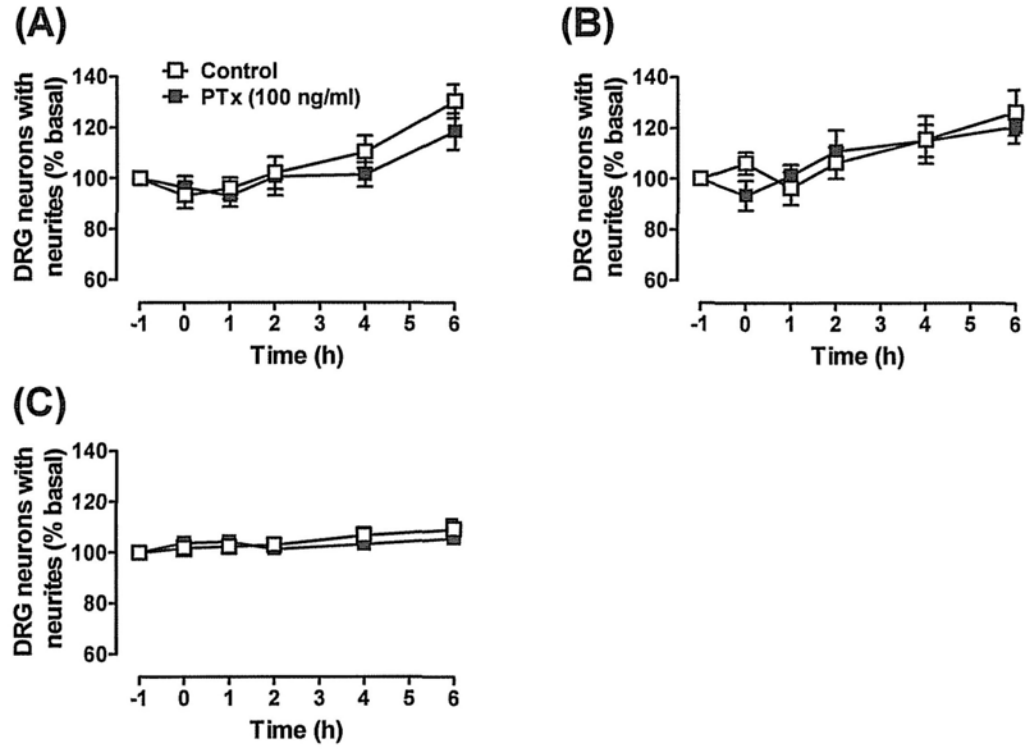

Fig. 5.2. No neurite retraction response was observed in purified DRG cell cultures. The time course effect of stress on neurite retraction by DRG neurons in (A) neuron-enriched, (B) IB4-negative and (C) IB4-positive cell cultures. Cells were incubated in control solution (Ham's F14 medium, □), with or without PTx (100 ng/ml, ■) added 16 h before start (time - 1 h). The proportion of neurons with neurites has been normalized for each well of cells related to their initial values at time – 1 h (% basal). Initial proportion of neurite-bearing neurons for control and PTx-pretreated cells, respectively, were 53 ± 4 and 56 ± 5% for neuron-enriched cell cultures, 52 ± 4 and 48 ± 4% for IB4-negative cell cultures and 70 ± 4 and 67 ± 4% for IB4-positive cell cultures. Data are presented as means ± SEM of 12 wells from six independent experiments.

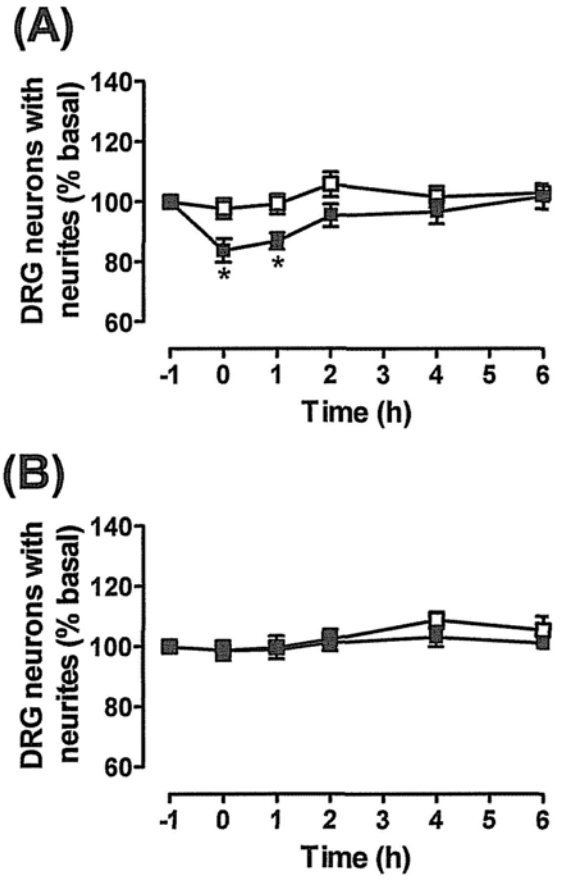

Fig. 5.3. PTx-dependent neurite retraction response reoccurred in IB4-negative cells with additional glial cells, but not in IB4-positive cells. Glial cells were added back to purified cultures, (A) IB4-negative cells and (B) IB4-positive cells, to mimic conditions in Fig. 5.1. Cells were incubated in control solution (Ham's F14 medium, □), with or without PTx (100 ng/ml, ■) added 16 h before start (time = -1 h). The proportion of neurons with neurites has been normalized for each well of cells related to their initial values at time = -1 h (% basal). Initial values for control and PTx-treated cells, respectively, were 73 ± 5 and 75 ± 2% for IB4-negative cells, and 69 ± 4 and 65 ± 4% for IB4-positive cells. Data are means ± SEM of six wells from three independent experiments. * $p < 0.05$ compared with control group.

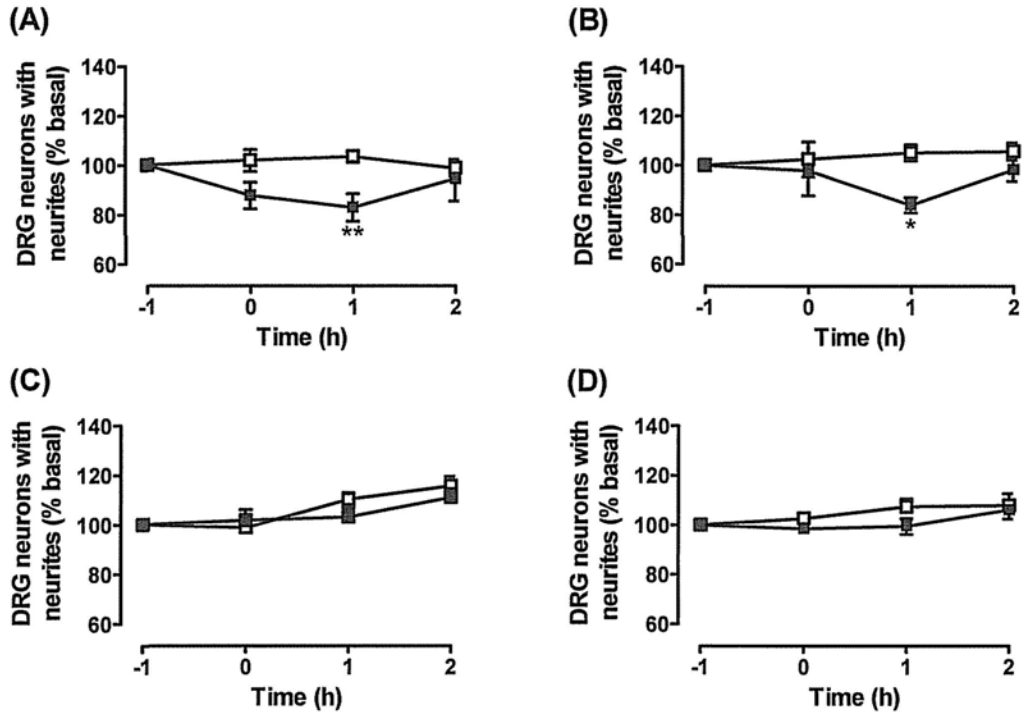

Fig. 5.4. Non-neuronal cells constitutively release factor/s facilitating PTx-dependent neurite retraction. The time course effect of conditioned medium derived from unstressed or stressed glial cell on neurite retraction by DRG neurons in IB4-negative (A,B) and IB4-positive cell cultures (C,D). Cells were incubated in control solution (Ham's F14 medium, □), with or without PTx (100 ng/ml, ■) added 16 h before start (time = -1 h). Conditioned medium derived from both unstressed (A,C) and stressed (B,D) glial cells allowed PTx-dependent neurite retraction only in IB4-negative cells. The proportion of neurons with neurites has been normalized for each well of cells related to their initial values at time = -1 h (% basal). Initial values for control and PTx-treated cells, respectively, were 70 ± 2 and 75 ± 2% for IB4-negative cells, and 67 ± 5 and 78 ± 1% for IB4-positive cells. Data are means ± SEM of seven to nine wells from three independent experiments. * $p < 0.05$, ** $p < 0.01$ compared with control group.

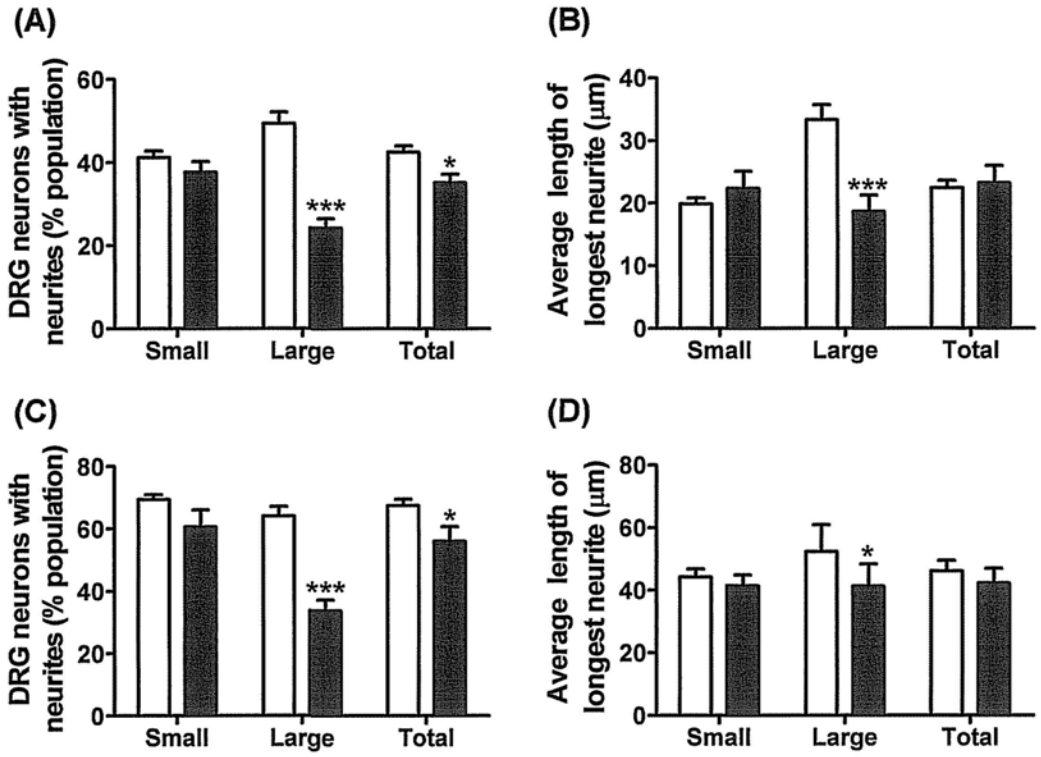

Fig. 5.5. Only large diameter neurons display PTx-dependent neurite retraction. Size analysis shows the proportion of small and large diameter neurons expressing neurites and the length of the longest neurite in (A,B) IB4-negative cells (data from Fig. 5.4A), and (C,D) mixed cell populations (data from Fig. 5.1A). Data was collected at time -1 h (open bars) and at 1 h (filled bars). Data are presented as means ± SEM of eight wells (A,B) and four wells (C, D) from three independent experiments with a minimum of 100 cells counted per well. * $p < 0.05$, *** $p < 0.001$ compared with time -1 h of each group using two-way ANOVA with Bonferroni's *post hoc* tests.

Chapter 6

Expression of functional EP4 and IP receptor in both cultured adult rat DRG neurons and glial cells

6.1 Introduction

In addition to the study on neurite outgrowth, cultures of DRG neurons have long been used as a model to study the mechanism underlying nociception and hyperalgesia (Gold *et al.*, 1996; Smith *et al.*, 2000; Southall *et al.*, 2001). In DRG cell cultures, PGE_2 or PGI_2 were shown to sensitize DRG neurons to stimulation by capsaicin, ATP, histamine and bradykinin (Lopshire *et al.*, 1998; Nicolson *et al.*, 2007; Stucky *et al.*, 1996; Wang *et al.*, 2007). While some of the effects of PGE_2 are protein kinase C-dependent (Sachs *et al.*, 2009), the majority of potentiating effects of PGE_2 and PGI_2 are PKA-dependent (Ferreira *et al.*, 1978; Hingtgen *et al.*, 1995; Lopshire *et al.*, 1998). Previous reports on corresponding receptor subtypes mediating the effect of PGE_2 are varied. PGE_2 receptor subtype EP_4 and the PGI_2 receptor (IP) has been identified as the principal G_s-coupled prostanoid receptors likely to mediate the PKA-dependent effects of these prostanoids (Bley *et al.*, 1998; Rowlands *et al.*, 2001; Wise, 2006). However, Southall and Vasko (2001) reported that the EP_3 receptor also plays an important role in mediating PKA-dependent effects of PGE_2. With the availability of the EP_4 receptor selective antagonist ONO-AE3-208 (Kabashima *et al.*, 2002) and the IP receptor selective antagonist RO1138452 (also known as CAY10441; (Bley *et al.*, 2006)), we can investigate the EP_4 and IP receptor-dependent signalling in DRG cells.

The DRG cell cultures comprise both neurons and glial cells. In DRG slices, in situ hybridization studies revealed the mRNA expression of EP_4 and IP receptors (Oida *et al.*, 1995; Sugimoto *et al.*, 1994) and EP_4 protein (Lin *et al.*, 2006) in dorsal

root ganglion neurons, but not in surrounding SGCs. These results provided the rationale that PGE_2 and PGI_2 only act on neurons, but not on those associated glial cells. From our previous study, we discovered that DRG glial cells inhibited neurite outgrowth by DRG neurons. This neuron-glia interaction required inhibition of $G_{i/o}$-dependent signalling but not direct cell-cell contact (Ng *et al.*, 2010). In contrast, cell-cell contact between DRG neurons and glial cells is essential for bradykinin-mediated inward currents (Heblich *et al.*, 2001) and capsaicin and KCl-stimulated release of substance P (Tang *et al.*, 2007). Thus, any effect on neurons is likely to be heavily influenced by associated glial cells. Recently, there is a trend of growing interest in neuron-glia interactions from *in vitro* studies and in animal models of inflammatory and neuropathic pain (Chen *et al.*, 2008; Takeda *et al.*, 2007; Vit *et al.*, 2008). However, the neuron-glia interactions in prostanoid receptor-mediated signalling activity in DRG neurons have not yet been elucidated. Moreover, it is too early to discount the prostanoid signalling in glial cells *in vivo*, since the absence of EP_4 and IP receptor mRNA in glial cells may be due to the insensitivity of the tools to study the mRNA expression in small cells such as SGCs. Moreover, expression of prostanoid receptors may be upregulated during pathological conditions which may be reflected on *in vitro* DRG cultures (Zheng *et al.*, 2007). With the technique of isolating glial cells from DRG cell cultures, we can investigate for prostanoid receptor-dependent activity in DRG glial cells.

6.1.1 Aims of study

With the availability of selective antagonists for EP_4 and IP receptors, we started by aiming to confirm these receptor subtypes are responsible for PGE_2 and cicaprost (PGI_2 mimetic) stimulated cAMP signalling in mixed DRG cell cultures. As described in the previous chapter, we generated cultures enriched in neurons or glial cells by differential adhesion, and cultures enriched in IB4-positive or IB4-negative

cells by MACS. Representative images of the DRG cell cultures used in this study is shown in Fig. 6.1. Given the heterogeneous nature of a typical preparation of DRG cells, we would like to check the contributions of subpopulations of DRG neurons and whether glial cells are involved in the prostanoid receptor-dependent signalling in DRG cell cultures. Interestingly, we found that glial cells responded to PGE_2 and cicaprost (PGI_2 mimetic) by stimulating cAMP signalling. Moreover, responses from purified glial cells were much higher than cultures containing neurons. Therefore we hypothesized that there is a neuron-glia interaction regulating the adenylyl cyclase activities of glial cells in cultures. So, towards the end of this chapter, we have explored neuron-glia interactions using different coculture systems.

6.2 Results

6.2.1 EP_4 and IP receptors mediate activation of adenylyl cyclase in DRG cultures

Agonist-based analysis in typical mixed DRG cell culture was consistent with previous findings (Wise, 2006) with cicaprost more potent in cAMP production than PGE_2 and ONO-AE1-329 (EP_4 receptor agonist (Cao *et al.*, 2002; Shibuya *et al.*, 2002; Suzawa *et al.*, 2000)). The pEC_{50} values were 7.38 ± 0.08, 6.93 ± 0.24 and 7.04 ± 0.09 respectively (Fig. 6.2A). Maximal response to cicaprost was also higher than that to PGE_2 and ONO-AE1-329 ($p < 0.05$).

In order to study the IP receptor-dependent cAMP production in DRG cell cultures, the IP receptor antagonist RO1138452 was used. Since RO1138452 has a p*K*i value of 9.0 for inhibition of cAMP accumulation in CHO-K1 cells stably expressing the human IP receptor (Bley *et al.*, 2006) and a pA_2 value of 8.2 in human pulmonary artery (Jones *et al.*, 2006), a single concentration of 100 nM of RO1138452 was used to selectively inhibit IP receptors. Pretreating mixed DRG cell

cultures with RO1138452 shifted the cicaprost log concentration-response curve to the right (pEC_{50} values = 6.02 ± 0.21; $p < 0.001$), with an estimated pA_2 value of 8.3 (Fig. 6.2B). This estimated pA_2 value was calculated using Schild equation. ($dr - 1 = [B] / K_B$). The selectivity of RO1138452 (100 nM) was revealed as it showed no effect on response to PGE_2 (Fig. 6.2C; pEC_{50} = 6.96 ± 0.04) or ONO-AE1-329 (Fig. 6.2D; pEC_{50} = 7.27 ± 0.15).

In a parallel study, ONO-AE3-208 was used for studying the EP_4 receptor-dependent signalling. ONO-AE3-208 is a potent EP_4 receptor antagonist with a p*K*i value of 8.9 (Kabashima *et al.*, 2002), therefore it was also used at 100 nM. Pretreatment of cells with ONO-AE3-208 shifted the PGE_2 log concentration-response curve to the right (Fig. 6.2C; pEC_{50} = 5.61 ± 0.02; $p < 0.01$), with an estimated pA_2 value of 8.3 (using Schild equation). Moreover, responses to ONO-AE1-329 were completely antagonised by ONO-AE3-208 (Fig.5.2D). The selectivity of ONO-AE3-208 (100 nM) was revealed by lack of inhibition of cicaprost-stimulated responses (Fig. 6.2B). Curve-fitting analysis revealed that there was no significant difference in the maximal responses to PGE_2 in the presence and absence of ONO-AE3-208. However such analysis was not possible for responses to ONO-AE1-329, since the curve-fitting for ONO-AE1-329 in the presence of ONO-AE3-208 is ambiguous.

Under high concentration of PGE_2 (10 μM), the presence of ONO-AE3-208 could not completely abolish the response. We speculated that the residual response may due to the activation of EP_2 receptors, which are another G_s-coupled prostanoid receptor. Therefore, we tested whether the EP_1/EP_2 receptor antagonist (AH6809) could inhibit the cAMP production by high concentration of PGE_2. As shown in Fig 6.3A, PGE_2 (10 μM) stimulated responses in DRG cell cultures could not be inhibited by pretreating with AH6809 (100 nM) nor treating with both AH6809 and

ONO-AE3-208 (100 nM). Moroever, neither EP_2 agonist (ONO-AE1-259-01; 100 nM) nor EP_3 agonist (ONO-AE-248; 100 nM) can significantly increase the cAMP production in mixed DRG cell cultures (Fig. 6.3 B).

6.2.1.1 Pharmacological evidence for EP_4 and IP receptor-mediated activation of adenylyl cyclase in DRG cultures

After confirming that EP_4 and IP receptors are responsible for the PGE_2- and cicaprost-stimulated cAMP production in mixed DRG cell cultures, we proceeded to investigate the contribution of neurons and their associated glial cells in cultures. The EP_4 and IP receptor-mediated cAMP signalling in DRG cell cultures is expected to arise from activity in neurons, since EP_4 and IP receptor mRNA was identified exclusively on neurons of rodent DRG (Matsumura *et al.*, 1995; Oida *et al.*, 1995). In our mixed DRG cell preparation, DRG neurons mixed with a similar proportion of glial cells on the day of isolation (50 ± 1% of total cell population). However, the proportion of neurons is reduced to 16 ± 1% after 2 days due to proliferation of glial cells, and even incubation with arabinoside C (10 μM), 5-fluoro-2'-deoxyuridine (50 μM) and uridine (150 μM) failed to have any marked effect on glial cell numbers at 2 DIV (data not shown). By using the differential adhesion properties of neurons and glial cells (Lindsay, 1988), we generated a neuron-enriched fraction (96 %) and a purified glial cell preparation (98 %) on day of isolation. In order to study the relative contribution of subpopulation of DRG neurons, the neuron-enriched fraction was further separated into IB4-negative and IB4-positive fraction by MACS.

To compare adenylyl cyclase activity in various DRG cell cultures, single concentrations of agonists were selected to produce equi-effective responses in the mixed DRG cell preparation. According to the log concentration-response curve in Fig. 6.2A, the EC_{50} concentration of cicaprost (IP agonist; 40 nM) and near-maximally effective concentration of PGE_2 (1 μM) and ONO-AE1-329 (EP_4

agonist; 1 μM) significantly increased [^{3}H]cAMP production to a similar extent. Pretreatment of mixed DRG cells with ONO-AE3-208 (EP_4 antagonist; 100 nM) significantly inhibited PGE_2 and ONO-AE1-329-stimulated responses (Fig. 6.4A). Similarly, pretreatment with RO1138452 (100 nM) significantly inhibited cicaprost-stimulated responses (Fig. 6.4A). Surprisingly, these EP_4 and IP receptor-dependent responses were also shown in the purified glial cell preparation (Fig. 6.4B). In contrast, the responses of the IB4-negative and IB4-positive cell fractions to PGE_2, ONO-AE1-329 and cicaprost were relatively weaker than the responses of the mixed DRG cell cultures and purified glial cell cultures (Fig. 6.4C-D). Similarly, the pattern observed in mixed DRG cell cultures, the agonist-stimulated adenylyl cyclase activity in IB4-negative cultures, IB4-positive cultures and purified glial cell cultures was selectively inhibited by the receptor specific antagonists (Fig. 6.4B-D).

6.2.1.2 Identification of EP_4 and IP receptor expression in neurons and glial cells (ICC and RT-PCR experiment)

Given the unexpected EP_4 and IP receptor-dependent adenylyl cyclase activity in glial cells, we aimed to confirm the expression of EP_4 and IP receptor protein and mRNA by immunocytochemistry and RT-PCR, respectively. Specific EP_4-immunoreactivity (EP_4-IR) and IP-immunoreactivity (IP-IR) were readily detected in all cell types (Fig. 6.5 & 6.6). Both EP_4-IR and IP-IR were detected in plasma membrane and cytoplasm of DRG neurons, as shown in the graphs as red rings surrounding the yellow cores (Fig. 6.5). The yellow cores represented the colocalization of receptor proteins and βIII-tubulin in cytosol, while the red rings revealed the expression of receptor proteins on the plasma membrane. Moreover, no observable difference in staining pattern and intensity was observed for neurons in mixed DRG cell cultures and neuron-enriched cultures. Similar expression patterns

were also found in glial cells, which indicated the expression of EP_4 and IP receptor proteins in the plasma membrane and cytosol of glial cells (Fig. 6.6). Also, there is no observable difference in staining pattern and intensity for glial cells in mixed DRG cell cultures and glial cell cultures. These findings suggested that prostanoid receptors such as EP_4 and IP receptors are expressed in both neurons and glial cells *in vitro*. Moreover, since there is no observable difference in staining pattern and intensity for neurons or glial cells in mixed DRG cell cultures and enriched cultures, it is unlikely that the expression of EP_4 and IP receptors on glial cells are affected by neurons, or vice versa.

Semi-quantitative RT-PCR showed EP_4 and IP mRNA expression in both mixed DRG cell cultures and pure glial cell cultures, with expression of both EP_4 and IP receptors relative to GAPDH mRNA appearing greater in the mixed DRG cell population. For the EP_4 receptor, densitometry readings relative to GAPDH were 0.57 ± 0.17 and 0.52 ± 0.11 for mixed DRG cell cultures and glial cell cultures respectively; while for the IP receptor, densitometry readings relative to GAPDH were 0.50 ± 0.02 and 0.16 ± 0.10, respectively (means ± SEM, n = 3; Fig. 6.7). Since we could not achieve 100% neuronal cell purity in the neuron-enriched cultures, the EP_4 and IP mRNA expression from neuron-enriched cultures was compared to the mRNA generated from the estimated glial cell component contaminating these cultures. Semi-quantitative RT-PCR showed EP_4 and IP mRNA expression in neuron-enriched cultures with densitometry readings relative to GAPDH of 0.62 ± 0.07 and 0.39 ± 0.06, respectively (means ± SEM, n = 3; Fig. 6.7). IP mRNA expression in glial cells was low with densitometry reading relative to GAPDH as low as 0.04 ± 0.02 (means ± SEM, n = 3; Fig. 6.7). In contrast, EP_4 mRNA expression on glial cells (0.85 ± 0.1 relative to GAPDH; means ± SEM, n = 3; Fig. 6.7) was comparable to that on neuron-enriched cells.

6.2.2 Discovery of inhibitory effect from neurons on adenylyl cyclase activity in glial cells

According to data in Fig. 6.4, the basal activities for the four DRG cell cultures were different. ELISA was used to prove the basal activity in different DRG cell cultures were different and suggested that the lower basal [^{3}H]cAMP production in glial cells was not an artefact of the assay technique (Fig. 6.8). Basal adenylyl cyclase activity in glial cells was significantly lower than that in mixed DRG cell cultures (0.09 ± 0.01 and 0.28 ± 0.03% conversion, respectively; $p < 0.05$, two-way ANOVA; Fig. 6.8), and this might affect the interpretation on agonist-stimulated responses in glial cells. When assayed by an ELISA method, cAMP levels were also lower in glial cell cultures (24 ± 3 and 39 ± 10 pmol/well for glial cells and mixed cell cultures, respectively; Fig. 6.8), suggesting that the lower basal [^{3}H]cAMP production in glial cells was not an artefact of the radioactive assay technique. The cAMP levels of IB4-negative cells and IB4-positive cells were in between that of glial cells and mixed cell cultures (32 ± 8 and 25 ± 7 pmol/well respectively; Fig. 6.8).

In order to account for this different in intrinsic adenylyl cyclase activities, data was expressed as fold basal (i.e. agonist-stimulated response/basal response). After that, the glial cell responses were notably higher than those in the other cell groups. For example, cicaprost (40 nM)-stimulated activity in mixed DRG cell cultures was 2.47 ± 0.49 fold basal, in IB4-negative cell cultures was 2.57 ± 0.94 fold basal, and in IB4-positive cell cultures was 2.31 ± 0.19 fold basal. In contrast, cicaprost-stimulated activity in glial cell cultures was 8.07 ± 1.29 fold basal ($p <$ 0.01 compared with the other three DRG cell cultures; one-way ANOVA).

In the previous section, we provided evidence that glial cells express EP_4 and IP receptors. Therefore, any adenylyl cyclase activity detected in mixed DRG cell cultures can be contributed by both neurons and glial cells. In order to evaluate the

relative contribution by DRG neurons and glial cells, EP_4 and IP-stimulated adenylyl cyclase activity in DRG cells was fully characterized. Full log agonist concentration-response curves were generated to compare the parent mixed DRG cultures with the glial cell culture and neuron-enriched cultures (Fig. 6.9). Because of the weak agonist responses in neuron-enriched cultures, data was combined from three independent experiments for pEC_{50} calculation. pEC_{50} values for PGE_2 were similar in all three cell groups (mixed: 6.72 ± 0.49; glial: 6.42 ± 0.26, neuron-enriched: 6.75). Comparably, pEC_{50} values for cicaprost were also similar in all three cell groups (mixed: 7.50 ± 0.46; glial: 7.23 ± 0.28, neuron-enriched: 7.62).

As observed previously in mixed cell cultures (Wise, 2006), maximal responses to PGE_2 in glial cells were significantly lower than responses to cicaprost ($p < 0.001$). Furthermore, maximal PGE_2 responses of mixed DRG cells were 50% of responses in glial cells, and maximal cicaprost responses of mixed DRG cells were 23% ($p < 0.001$) responses in glial cells, despite comparable numbers of glial cells in both cell groups. The maximal responses of glial cells to PGE_2 and cicaprost were 1.49 ± 0.18% conversion and 5.01 ± 0.16% conversion, respectively. In addition, maximal responses of mixed DRG cells to PGE_2 and cicaprost (0.75 ± 0.16% conversion and 1.18 ± 0.24% conversion, respectively) were greater than responses of neuron-enriched cultures (0.46 ± 0.16% conversion and 0.33 ± 0.06% conversion, respectively). In contrast, the receptor-independent stimulation by forskolin significantly increased [^{3}H]cAMP production in both mixed cell and glial cell cultures to a similar level. Moreover, forskolin responses of both mixed cell and glial cell cultures were significantly higher than that of neuron-enriched cultures (Fig 6.9).

Although both the mixed cell cultures and the glial cell cultures represent cells on 2 DIV, the glial cells and neurons were replated after 1 day and then assayed after

another day in culture. Nevertheless, when an equivalent number of glial cells were assayed after a further day in culture (i.e., 2 days undisturbed), their responses to cicaprost, PGE_2 and forskolin were similar and still greater than seen for the mixed cell cultures (data not shown). The relatively low level of agonist-stimulated adenylyl cyclase activity in neuron-enriched cultures is also unlikely to be an artefact of the cell preparation methodology. Despite a shorter time in culture, immunostaining for TUJ-1 showed that neurite outgrowth was comparable in mixed DRG cultures and in neuron-enriched cultures (Ng *et al.*, 2010).

Interestingly, we also observed a progressive increase in agonist-stimulated [^{3}H]cAMP production as the proportion of glial cells in the different cell fractions increased (Fig. 6.4). In contrast, basal and forskolin responses were not regulated in a similar manner. Further examination of the data in Fig. 6.4 showed that agonist-stimulated responses were greatest in cultures plated with higher ratios of glial cells to neurons (e.g., 55:1 in glial cultures vs. 1:1 for mixed DRG cells). Despite the presence of similar numbers of neurons in the IB4-positive and IB4-negative cell fractions, the increase in [^{3}H]cAMP production by the IB4-positive cells was the lowest, and this fraction contained the lowest proportion of glial cells (23% vs. 37%). In a population of mixed DRG cells on the day of assay, the proportion of glial cells is approximately 80%. We therefore proposed that most of the [^{3}H]cAMP response determined in mixed DRG cell cultures derived not from neurons but from glial cells. Furthermore, because [^{3}H]cAMP production decreased in neuron-containing cultures, we hypothesized that this glial response was inhibited by the presence of DRG neurons. To test this hypothesis, adenylyl cyclase activity was assayed in conditions where increasing numbers of glial cells were incubated in the presence or absence of a fixed number of neurons, and increasing numbers of neurons were incubated in the presence or absence of a fixed number of glial cells.

Neurons and glial cell numbers were chosen to represent conditions above and below those normally assayed in mixed DRG cell preparations (i.e., 5000 neurons and 20000 glial cells on day of assay).

6.2.2.1 Increasing numbers of glial cells were incubated in the presence or absence of a fixed number of neurons

Adenylyl cyclase activity in glial cells (200 – 60000 cells/well), whether assayed in the absence of agonists (i.e., basal activity) or in response to receptor-dependent stimuli (PGE_2 and cicaprost) or in response to receptor-independent stimuli (forskolin), appeared to saturate at 10000 – 20000 glial cells/well (Fig. 6.10; open symbols). The addition of 5000 neurons tended to increase basal and forskolin-stimulated [^{3}H]cAMP production in an additive manner (Fig. 6.10A,C). In contrast, the presence of 5000 neurons appeared to inhibit cicaprost and PGE_2-stimulated glial cell responses (Fig. 6.10B,D). Thus, the presence of 5000 neurons significantly inhibited cicaprost and PGE_2-stimulated [^{3}H]cAMP production by an estimated 60000 glial cells ($p < 0.05$ and $p < 0.001$ for cicaprost and PGE_2, respectively; two-way ANOVA) while significantly increasing the response to forskolin ($p < 0.05$; two-way ANOVA).

6.2.2.2 Increasing numbers of neurons were incubated in the presence or absence of a fixed number of glial cells

Adenylyl cyclase activity in neurons similarly appeared to saturate with increasing numbers of cells (100 – 10000 neurons/well) (Fig. 6.11; open symbols). On the day of assay, we would expect a contribution to the measured [^{3}H]cAMP from glial cells contaminating the DRG neuron fraction, but these would amount to merely 4, 40, 200 and 400 glial cells on the day of assay from plating 100, 1000, 5000 and 10000 DRG neurons/well. To these groups we added a fixed number (10000) of glial cells which will have doubled in number by the time of assay. The presence of this

additional 20000 glial cells on the day of assay increased basal and forskolin-stimulated [^{3}H]cAMP production, but less than expected from a simple additive response (Fig. 6.11A,C). For both cicaprost and PGE_2, the statistically significant increase in [^{3}H]cAMP production with the lower numbers of DRG neurons plus a fixed number of glial cells ($p < 0.001$; two-way ANOVA), was lost as the number of neurons reached 10000 cells/well (Fig. 6.11B,D).

6.2.2.3 Individual labelling of neurons and glial cells reveals the inhibitory effect from neurons

The co-culture data represented in Figs. 6.10 and 6.11 reflects a composite of [^{3}H]adenine uptake and adenylyl cyclase turnover properties of the different cell types. Therefore, in order to confirm our hypothesis that neurons inhibit glial cells, we needed to individually label each DRG cell type. Therefore, the effect of neurons on adenylyl cyclase activity of glial cells was assessed by coculturing [^{3}H]adenine-labelled glial cells with unlabelled neurons and vice versa. The cell mixtures were selected to represent the data points at the far right of the graphs in Fig. 6.11, where the inhibition of agonist-stimulated [^{3}H]cAMP production was the strongest. Absolute [^{3}H]cAMP production (% conversion) values in Fig. 6.13 are therefore not directly comparable to those in previous figures because of the different [^{3}H]adenine-labelling protocol (Fig 6.12) required to maintain sufficient [^{3}H]ATP inside the neurons after two days in culture.

Cicaprost, PGE_2 and forskolin all significantly increased [^{3}H]cAMP production in [^{3}H]adenine-labelled glial cells (20000 cells/well) (Fig. 6.13A; $p < 0.05$, two-way ANOVA). In the presence of 10000 unlabelled DRG neurons, both cicaprost and PGE_2-stimulated responses were decreased (from 4.39 ± 0.15 to 2.53 ± 0.51% conversion for cicaprost, $p < 0.01$, two-way ANOVA; and from 1.98 ± 0.24 to 1.13 ± 0.16% conversion for PGE_2), while that to forskolin was unchanged (3.00 ± 0.50 to

3.80 ± 0.58% conversion) (Fig. 6.13A). Conversely, only forskolin significantly increased [^{3}H]cAMP production in [^{3}H]adenine-labelled neurons (10000 cells/well), and these responses were not affected by the presence of 20000 unlabelled glial cells (Fig. 6.13B; two-way ANOVA).

6.2.3 Mode of inhibitory effect from neurons

6.2.3.1 Soluble factor vs cell-cell contact

We have shown that co-culturing glial cells with neurons resulted in inhibition of prostanoid-stimulated adenylyl cyclase activity in glial cells. This interaction between neurons and glial cells in culture could be direct through cell-cell contact or indirect by the release of soluble factors. In order to elucidate the mode of interaction in the co-cultures, glial cell cultures were treated with conditioned medium generated from neuron-enriched cultures and we looked for any inhibitory effect due to soluble factors in the conditioned medium. Conditioned medium was harvested from neuron-enriched cultures after 24 h, then centrifuged to eliminate cell debris before addition to glial cell cultures. In this experiment, we kept the number of glial cells and neurons in culture equivalent to that in mixed DRG cultures on their assay day (i.e., 5000 neurons and 20000 glial cells). As we have shown an inhibitory effect of neurons in cell cultures where either or both cell types have been labelled with [^{3}H]adenine, we tested the effect of conditioned medium in cultures where all cells were labelled and thus avoided the need to perform 2 steps of differential adhesion (Fig. 6.12). As seen above, co-culturing glial cells with neurons significantly inhibited cicaprost-stimulated [^{3}H]cAMP production (2.57 ± 0.46 to 1.21 ± 0.22% conversion, means ± SEM, n = 4; $p < 0.01$, two-way ANOVA) and inhibited PGE_2-stimulated [^{3}H]cAMP production (1.36 ± 0.21 to 0.59 ± 0.08% conversion, means ± SEM, n = 4), without affecting basal or forskolin-stimulated [^{3}H]cAMP production (Fig. 6.14). However, treating glial cell cultures with

conditioned medium derived from neuron-enriched cultures did not have any effect on their adenylyl cyclase activities. The PGE_2 and cicaprost-stimulated [^{3}H]cAMP production for 15 min conditioned medium treatment are 1.75 ± 0.27% and 3.34 ± 0.38 respectively; while those responses for 16 h treatment are 1.12 ± 0.07% and 2.31 ± 0.64% respectively.

The lack of response from conditioned medium may be due to insufficient treatment time in acute treatment group (15 min) or instability of the soluble factor in chronic treatment group (16 h). Therefore we cannot discount the contribution of soluble factor/s. In order to study the effect of soluble factors derived from neurons, glial cells and neurons were separated by a transwell membrane using 12-well transwell plates with 6.5 mm diameter inserts (0.4 μm pore size; polyester). Glial cells were plated in the wells and neurons were plated in the membrane inserts (Fig. 6.15). As a result, any soluble factor released from neurons can freely diffuse across the membrane, while physical contact between neurons and glial cells cannot be established. Moreover, in order to study whether the release of soluble factor/s from neurons is dependent on physical contact with glial cells, we also added glial cells to the membrane inserts and allowed physical contact to occur in the inserts. Cells grown in transwell inserts were removed before adding cicaprost (40 nM) or forskolin (1 μM) to glial cells in wells for the [^{3}H]cAMP assay. In this study, we showed a tendency that adenylyl cyclase activities of glial cells were reduced by soluble factor/s which was constitutively released from neurons. The release of factor from neurons is independent of the physical contact with glial cells. As seen above, co-culturing glial cells with neurons (group B) significantly inhibited cicaprost-stimulated [^{3}H]cAMP production by 62% (3.08 ± 0.59% to 1.18 ± 0.24% conversion; $p < 0.01$ comparing with group A), without reducing forskolin-stimulated [^{3}H]cAMP production (2.57 ± 0.26% to 3.83 ± 0.54%

conversion; Fig. 6.16). When glial cells were separated from neuron-enriched fractions by a transwell membrane (group C), both cicaprost (2.17 ± 0.42% conversion) and forskolin responses (1.92 ± 0.17 % conversion) for glial cells in the wells underneath were reduced by 30% and 25%, respectively (Fig. 6.16 C). Similarly, when there is physical contact between neurons and glia cells in membrane inserts (group D), both cicaprost (2.04 ± 0.42% conversion) and forskolin responses for glial cells in the wells underneath (2.11 ± 0.17 % conversion) were similarly reduced by 34% and 19%, respectively (Fig. 6.16D).

6.2.3.2 Role of Gi/o-protein in inhibiting adenylyl cyclase activity in glial cells

We have observed that receptor-specific adenylyl cyclase activity in glial cells can be inhibited by the presence of DRG neurons. One possible cause of this interaction is that neurons activate a $G_{i/o}$ protein-coupled signalling pathway in glial cells and inhibit the adenylyl cyclase activity, although lack of the inhibition of forskolin-stimulated [^{3}H]cAMP might argue against this. To investigate the potential role of $G_{i/o}$ proteins in mediating this inhibitory effect of neurons, we compared the effect of PTx (100 ng/ml overnight) on receptor-dependent adenylyl cyclase activity in DRG glial cells, neurons and mixed cell cultures. Pretreatment of cells with PTx had no significant effect on PGE_2 or cicaprost-stimulated [^{3}H]cAMP production in cultures enriched in neurons or glial cells (Fig. 6.17C-F). For neuron-enriched cultures, pEC_{50} values for cicaprost were estimated at 7.82 and 7.57 in the absence and presence of PTx, respectively; while pEC_{50} values for PGE_2 in neuron-enriched cultures were estimated at 6.41 and 6.22 in the absence and presence of PTx, respectively. For glial cell cultures, pEC_{50} values for PGE_2 were 6.32 ± 0.11 and 6.24 ± 0.60 in the absence and presence of PTx, respectively; while pEC_{50} values for cicaprost were 7.31 ± 0.11 and 7.31 ± 0.18 in the absence and presence of PTx, respectively. In contrast, although PTx had no significant effect on agonist affinities

in mixed DRG cell cultures (pEC_{50} values for PGE_2 were 6.85 ± 0.29 and 6.55 ± 0.16, and for cicaprost were 7.48 ± 0.09 and 7.28 ± 0.04, in the absence and presence of PTx, respectively), it slightly inhibited agonist-stimulated responses in mixed DRG cell cultures (Fig. 6.17A-B). PTx attenuated responses in mixed DRG cells to PGE_2 (55% inhibition at 100 nM) and cicaprost (35% inhibition at 100 nM), but did not affect the basal activity. The maximal cicaprost-stimulated response was significantly reduced by PTx pretreatment from 1.26 ± 0.19% to 0.94 ± 0.15% conversion (means ± SEM, n = 4; $p < 0.05$), while the maximal PGE_2-induced response was slightly reduced from 0.75 ± 0.12% to 0.62 ± 0.05% conversion (means ± SEM, n = 4). Moreover, PTx pretreatment also unexpectedly reduced the forskolin-stimulated [^{3}H]cAMP production in glial cell cultures (1.84 ± 0.11% to 0.88 ± 0.19% conversion, means ± SEM, n = 3; $p < 0.01$), and reduced [^{3}H]cAMP production in mixed DRG cell cultures (3.06 ± 0.43% to 2.35 ± 0.45% conversion, means ± SEM, n = 3, Fig. 6.18A,C). In contrast, the PTx pretreatment did not affect the forskolin-stimulated responses in neuron-enriched cultures (Fig. 6.18B).

Given the unexpected inhibitory response produced by PTx, we speculated that a mechanism other than $G_{i/o}$-protein inhibition was involved. While it is the A-promoter of PTx by which ADP-ribosylates $G_{i/o}$-proteins, it is the PTx B-oligomer which anchors the toxin to the cell surface and facilitates its internalization. This PTx B-oligomer is reported to have biological function independent of $G_{i/o}$-protein coupled signalling (Wong and Rosoff 1996; Hayat *et al.*, 2003). Pretreatment of cells with PTx B-oligomer (100 ng/ml overnight) had no effect on PGE_2, cicaprost or forskolin-stimulated [^{3}H]cAMP production in mixed DRG cell cultures and neuron-enriched cultures (Fig. 6.18A,B). Interestingly, PTx B-oligomer significantly reduced the forskolin-stimulated [^{3}H]cAMP production in glial cell cultures (1.84 ± 0.11% to 1.09 ± 0.06% conversion, means ± SEM, n = 3; $p < 0.05$), marginally

reduced cicaprost-stimulated responses (4.93 ± 1.2% to 3.63 ± 0.83% conversion, means ± SEM, n = 3), but had no observable effect on PGE_2-stimulated [^{3}H]cAMP production in glial cell cultures (Fig. 6.18C).

6.3 Discussion

In our previous studies, using EP and IP receptor specific agonists, we have demonstrated that DRG cells of adult rats express EP_4 and IP receptors *in vitro* (Rowlands *et al.*, 2001; Wise, 2006). Herein we confirm this conclusion using the EP_4 receptor antagonist ONO-AE3-208 (Kabashima *et al.*, 2002) and the IP receptor antagonist RO1138452 (Bley *et al.*, 2006). ONO-AE3-208 competitively inhibited PGE_2-stimulated [^{3}H]cAMP production, with an estimated pA_2 value of 8.4 which is comparable with data from Kabashima et al. (2002) and helps confirm that PGE_2 is acting on EP_4 receptors to stimulate adenylyl cyclase activity. Both PGE_2 and the EP_4 receptor agonist ONO-AE1-329 produced comparable maximal stimulation of adenylyl cyclase activity, further suggesting that PGE_2 acts only on the EP_4 receptor subtype in rat DRG cells. However, despite the comparable responses to PGE_2 and ONO-AE1-329, a residual response remained for PGE_2 even in the presence of ONO-AE3-208 at a concentration which completely inhibited adenylyl cyclase activity stimulated by the EP_4 receptor specific agonist. It would appear unlikely though that PGE_2 is stimulating EP_2 receptors in these mixed cell cultures as the EP_2 receptor specific agonist (ONO-AE1-259) failed to significantly increase [^{3}H]cAMP production and the EP_1/EP_2 receptor antagonist (AH6809) failed to inhibit PGE_2-stimulated responses.

RO1138452 is highly selective for IP receptors, but is also a potent antagonist at non-prostanoid receptors such as α_{2A}-adrenoceptors, imidazoline I_2 and platelet activating factor receptors (Bley *et al.*, 2006; Jones *et al.*, 2006), but such activities

are not expected to affect cicaprost-stimulated responses in DRG cells. RO1138452 (100 nM) gave an estimated pA_2 value of 8.4, which is comparable to reported values in other tissues (Bley *et al.*, 2006; Jones *et al.*, 2006). Although higher concentrations of cicaprost may have surmounted the inhibitory effect of RO1138452, curve fitting analysis suggested that the maximum response to cicaprost was significantly inhibited by RO1138452. Such insurmountable inhibition has been observed previously in other systems, either due to agonist-dependent functional antagonism via EP_3 receptor (Jones *et al.*, 2006) or ascribed to pseudo-irreversible orthostatic antagonism (Ayer *et al.*, 2008). Our previous failure to detect EP_3 receptor-dependent inhibition of adenylyl cyclase activity in DRG cells (Wise, 2006) and the lack of EP_3 agonist-stimulated response in DRG cells suggests that the response profile of RO1138452 shown herein is more likely due to pseudo-irreversible orthostatic antagonism.

Both PGE_2-stimulated EP receptors and PGI_2-stimulated IP receptors have been well characterised in isolated DRG cells as both are nociceptor sensitizing agents (Bley *et al.*, 1998; Smith *et al.*, 2000), but the presumption has been that only the neuronal cells are involved. This is presumably because the early studies of prostanoid receptor mRNA expression in DRG slices from normal mice found EP and IP receptors in DRG neurons, but not in glial cells (Oida *et al.*, 1995; Sugimoto *et al.*, 1994). However, DRG glial cells are not passive bystanders and can modulate functional responses of DRG neurons in slices (Thippeswamy *et al.*, 2005; Zheng *et al.*, 2007) and in isolated cell cultures (Heblich *et al.*, 2001; Ng *et al.*, 2010; Suadicani *et al.*, 2009; Tang *et al.*, 2007). Typical DRG cell cultures from adult rats tend to be composed of more glial cells than neurons, and we can generate neuron-enriched and purified glial cell fractions by differential adhesion. We also looked for EP_4 and IP receptors expression in isolated DRG glial cells. We were

therefore surprised to discover both EP_4 and IP receptors in isolated DRG glial cells using EP_4 and IP receptor-specific agonists and antagonists. PGE_2 and ONO-AE1-329-stimulated [^{3}H]cAMP production was inhibited by the EP_4 receptor antagonist ONO-AE3-208 but not by the IP receptor antagonist RO1138452, and cicaprost-stimulated [^{3}H]cAMP production was inhibited by RO1138452 but not by ONO-AE3-208. Furthermore, agonist affinities were similar in both cell groups.

In whole DRG, the SGCs normally form a tight sheath surrounding the sensory neurons and control the neuronal environment (Hanani 2005), while myelin-expressing S100β-positive Schwann cells and GFAP-expressing Schwann cells ensheath the neurons (Campana, 2007). Schwann cells in rat sciatic nerve segments do not express EP receptors (Ma *et al.*, 2002), but isolated Schwann cells from rat sciatic nerve are reported to express IP receptors (Muja *et al.*, 2007). At the present time we are unable to distinguish SGCs from Schwann cells as both cell types express GFAP in culture (Scholz *et al.*, 2007) and SGCs in culture lose their specific expression of glutamine synthase (M. Hanani, personal communication). Nevertheless, the pharmacological evidence for the functional expression of EP_4 and IP receptors on DRG glial cells was further supported by evidence of EP_4 and IP receptors immunoreactivity and mRNA expression. The process of dissociation and culturing is well known to produce responses different from those obtained in whole ganglia (Buschmann *et al.*, 1998; Schoenen *et al.*, 1989), leading to the proposal that the dissociated DRG neuron is an injured neuron with 'neuropathic' properties (Zheng *et al.*, 2007). Therefore, EP_4 and IP receptors expression by SGCs and/or Schwann cells may be quiescent in intact ganglia, and only becomes evident on axotomy and subsequent dissociation of cells. Messenger RNA levels of μ-opioid receptor, TRPV1, TRPA1, $Na_v1.8$ and substance P have been shown to alter during culture of 'mixed' adult mouse DRG cells (Franklin *et al.*, 2009). It remains to be

determined whether EP_4 and IP receptor mRNA expression by adult rat DRG neurons and glial cells displays any similar time-dependent changes.

In DRG *in vivo*, more recent studies have demonstrated EP_4-IR in DRG neurons but not glial cells, but again in normal rats (Kopp *et al.*, 2004; Lin *et al.*, 2006). In a model of peripheral inflammation, Lin et al. (2006) reported an increase in EP_4-IR in DRG neurons with no reported expression in glial cells. However, injury to a peripheral nerve may produce a different profile of responses with glial cell hypertrophy (Lu *et al.*, 1991) and upregulation of GFAP expression in activated SGCs (Hanani, 2005) resulting in increased reactivity within the DRG. In the partial sciatic nerve ligation model of neuropathic pain, EP_4-IR is increased in macrophages infiltrating the injured nerve and in unidentified resident cells, presumed to be fibroblasts (Ma *et al.*, 2002), but EP_4-IR in associated DRG was not investigated. Therefore, despite the current lack of evidence for EP_4 and IP receptors expression by glial cells *in vivo*, studies of DRG in neuropathic pain models remain to be performed and the changes we describe herein could be characteristic responses of DRG cells following nerve injury.

Conventional wisdom holds that EP_4 and IP receptors are expressed by neurons in mouse and rat DRG, but not by their associated SGCs or Schwann cells (Oida *et al.*, 1995; Sugimoto *et al.*, 1994). Thus, when EP receptor subtypes were knocked down in adult rat DRG cell cultures, the conclusion that EP_{3C} and EP_4 receptors mediated cAMP accumulation and sensitization of sensory neurons presumed that PGE_2 was acting directly on the sensory neurons (Southall *et al.*, 2001). However, we have presented evidence that dissociated DRG glial cells also express EP_4 and IP receptors, and it is possible that previously quiescent SGCs may up-regulate expression of EP_4 and IP receptors following nerve injury. This work led us to hypothesize that most of the EP_4 and IP-receptor dependent cAMP responses

determined in mixed DRG cell cultures derived from glial cells, not from neuronal cells. Here we show that cicaprost and PGE_2-stimulated adenylyl cyclase activity in a neuron-enriched fraction of DRG cells is very weak compared to that seen in the mixed DRG cell culture, although the pEC_{50} values for these agonists were similar in both cell groups. By further separating these DRG neurons into two subsets (IB4-negative and IB4-positive cells), we showed a similar profile of EP_4- and IP receptor-dependent adenylyl cyclase activity when compared to the mixed DRG cell cultures. The mixed DRG cell preparation and the three neuron-enriched fractions tested all contained 5000 neurons, but the former is estimated to have 100-fold greater number of glial cells. Thus, when mixed DRG cells and fractions enriched in DRG neurons were assayed using identical numbers of neurons per well, there appeared to be progressive increase in [^{3}H]cAMP production as the proportion of glial cells in the different cell fractions increased. Finally, when directly comparing EP_4 and IP receptor-dependent responses, we could see that responses were greatest in the glial cells > mixed DRG cells > neuron-enriched cultures. In contrast, basal and forskolin-stimulated adenylyl cyclase activity was greatest in mixed DRG cells > glial cells > neuron-enriched cultures. Moreover, the total number of glial cells in the mixed DRG cell culture was similar to that in the purified glial cell cultures on the day of assay, yet agonist-stimulated activity in the glial cell preparation was significantly greater than in the mixed DRG cell cultures. Both mixed cells and glial cells were assayed after a total of 2 DIV, therefore were comparable in relation to the original axotomy. When glial cells were left for a further day *in vitro*, responses were unchanged and remained greater than observed in mixed cell cultures. These results therefore suggest that the presence of neurons is inhibiting agonist-stimulated responses in glial cells.

Taken together, our results clearly show a relatively weak EP_4 and IP

receptor-dependent increase in [^{3}H]cAMP production in neuron-enriched cultures, despite evidence of EP_4 and IP receptor protein expression on neurons and of EP_4 and IP mRNA expression in neuron-enriched cultures. When IP mRNA was determined in a fraction of glial cells estimated to represent glial cell numbers in neuron-enriched cell cultures, we discovered that IP mRNA expression was relatively low which suggests that the IP mRNA expression in neuron-enriched cultures came largely from neurons. In contrast, EP_4 mRNA expression on glial cells was comparable to that of neuron-enriched cells, which suggests that EP_4 mRNA expression in neuron-enriched cultures was largely due to the 'contaminating' glial cells. Given our evidence below that DRG neurons specifically inhibit EP_4 and IP receptor-dependent responses in DRG glial cells, it is possible that this high EP_4 mRNA expression in glial cells may be due to the absence of an inhibitory influence from DRG neurons. However, our immunocytochemistry result suggested that EP_4 and IP receptor expression on glial cells were not affected by coculturing with neurons. This result indicates that the inhibitory influence from neurons was not due to alteration of receptor mRNA or protein expression. Furthermore, functional EP_4 and IP receptors should be expressed on the membrane. Our data revealed that there is quite a large population of EP_4 and IP receptors protein expressed in the cytosol, which may represent the portion of prostanoid receptor being internalized, or being transported from the endoplasmic reticulum to the membrane. We hypothesize that neuronal cells are affecting receptor-effector signalling pathways in glial cells. For example, GPCR desensitization or internalization (Gainetdinov *et al.*, 2004). The cicaprost-stimulated cAMP responses in glial cell cultures were much greater than neuron-enriched cultures; while IP receptor mRNA was much lower in glial cell cultures. However the expression profile of receptor protein can be different from mRNA. Therefore, further investigation on IP receptor protein expression is needed.

Moreover, RT-PCR provided only semi-quantitative measurement for the receptor mRNA. Therefore, absolute quantification of receptor mRNA using real-time PCR may help to provide more information. In addition, differential expression of adenylyl cyclase subtypes in different cell types can contribute to different cAMP response. At this moment, there is no report for expression profile of adenylyl cyclase isoforms in DRG cells. So RT-PCR experiments on mRNA expression of adenylyl cyclases isoforms in neurons and glial cells are needed. Moreover, it is also interesting to study the effect of coculture on expression profile of adenylyl cyclase isoforms on DRG cells.

In our previous study, mixed DRG cells cultures required at least 2 days of incubation on a poly-DL-ornithine/laminin-coated surface before they could demonstrate EP_4 and IP receptor-dependent responses (Wise 2006). All three cell groups in the current study were assayed on 2 DIV, but the neuron-enriched cells and glial cells have been dislodged from poly-DL-ornithine-coated tissue culture plates after 1 day then replated onto poly-DL-ornithine/laminin-coated tissue culture plates for a further day in culture. Nevertheless, immunostaining for TUJ-1 showed that neurite outgrowth was comparable in both sets of cells, and we have shown previously that neurons in mixed DRG cell cultures, which were cultured for 2 days, had a similar proportion of neurite-bearing neurons compared to neurons in neuron-enriched cultures which had been cultured for 1 day. When neuron-enriched cultures were cultured for an additional day, all adenylyl cyclase responses were increased proportionately (data not shown). This increased [^{3}H]cAMP production could result from increased maturity of the neurons (reflected as an increase in adenylyl cyclase expression/activity) or from the contribution of increased numbers of contaminating glial cells. In neuron-enriched cultures, the proportion of glial cells will increase over time as the glial cells continue to proliferate. Therefore,

without being able to prepare a significantly purer neuronal cell preparation, we cannot know if DRG neurons from adult rats will increase their responses to cicaprost and PGE_2 if left for longer time periods in culture.

Our second hypothesis deriving from these observations was that adenylyl cyclase activity in glial cells was inhibited by the presence of DRG neurons. Increasing the number of glial cells or neuronal cells in culture did not increase [^{3}H]cAMP in direct proportion to the number of cells, instead we observed a saturation effect. This saturation response was independent of the maximal response and is therefore unlikely to be due to depletion of [^{3}H]ATP as substrate for generation of [^{3}H]cAMP. Furthermore, it is unlikely that the [^{3}H]cAMP response plateaus due to increased phosphodiesterase activity because of the inclusion of IBMX in the cAMP assay and because the asymptotes occur at different levels of [^{3}H]cAMP production. Therefore, the underlying cause of this saturation response is currently unknown, but this phenomenon does not compromise our observations that neurons inhibit adenylyl cyclase activity of glial cells. Even though all responses were already saturated in the group containing 60000 glial cells, co-culturing with 5000 neurons could still further suppress the EP_4 and IP receptor-dependent responses.

The addition of a fixed number of neurons to increasing numbers of glial cells showed a marked difference in response profiles for basal adenylyl cyclase and adenylyl cyclase activity stimulated by receptor-dependent agonists (PGE_2 and cicaprost), and receptor-independent stimuli (forskolin). We found that adding neurons to glial cell cultures increased basal and forskolin-stimulated [^{3}H]cAMP production but decreased cicaprost and PGE_2-stimulated [^{3}H]cAMP production by glial cells. On the other hand, the addition of increasing number of neurons in glial cell cultures showed an inhibitory effect on receptor-dependent stimulation of

adenylyl cyclase activity. In 2001, we reported that iloprost and PGE_2-stimulated [^{3}H]cAMP production was significantly increased in mixed DRG cultures with low numbers of neurons (500 neurons/well) compared to high numbers of neurons (15000 neurons/well), but that forskolin-stimulated activity was unaffected (Rowlands *et al.*, 2001). Extensive investigations at that time showed that the increased response in cultures with fewer neurons was not affected by treating the cells with indomethacin, nerve growth factor and anti-neurotrophin antibody. Moreover, the downregulation by high concentration of EP and IP receptor agonists were similar in cultures of high numbers of neurons and cultures of low numbers of neurons. Therefore the neuron-glia interaction, which inhibited the prostanoid receptor-dependent signalling, was independent of cyclooxygenase activity, independent of receptor down-regulation in high density culture, and independent of neurotrophins. At that time, the prostanoid receptors were presumed to be only present on the DRG neurons, but our earlier data is entirely consistent with that is the current report if we allow for EP_4 and IP receptor-mediated responses via glial cells. Thus, in the mixed DRG cell cultures with 15000 neurons/well, the neurons were also specifically inhibiting PGE_2 and iloprost-stimulated adenylyl cyclase activity from the 'contaminating' glial cells.

In the co-culture systems discussed so far, the measurement of [^{3}H]cAMP production will reflect a composite of [^{3}H]adenine uptake and adenylyl cyclase turnover rates which may be different for the different cell types. However, the same inhibitory effect of neurons was observed when unlabelled neurons were added to [^{3}H]adenine-labelled glial cells, but no obvious interactions were observed when unlabelled glial cells were added to [^{3}H]adenine-labelled neuron-enriched cell cultures. To achieve this cell specific labeling of neurons and glial cells, cultures were kept for one more day to achieve comparable co-culture conditions between

labelled and unlabelled cells. One may argue for potential leakage of radioactive materials from one cell type to another which might confuse the interpretation of the data. If this was the case however, cultures with [^{3}H]adenine-labelled neurons and unlabelled glial cells would produce an agonist-stimulated response different from that of [^{3}H]adenine-labelled neurons alone, since any glial cells which might have taken up some [^{3}H]adenine are more capable of producing [^{3}H]cAMP in response to cicaprost and PGE_2. Our results showed that responses from cultures with labelled neurons and unlabelled glial cells were no different from cultures with labelled neurons alone, therefore, there appears to be no leakage from neurons to glial cells.

In order to more fully understand the mode of inhibitory action of neurons in the current study, conditioned medium was generated from neuron-enriched cultures and added to glial cell cultures. However, neuron-conditioned medium failed to reduce prostanoid-stimulated [^{3}H]cAMP production by glial cells in assays where co-culture of neurons with glial cells was still effective. These results indicate that close contact between cultured neurons and glial cells is required for the interactions described herein, but cannot yet discount a role for biologically unstable soluble factors. In order to study whether physical contact in essential for the inhibitory action of neurons, glial cells and neurons in cultures were separated by transwell membranes which only allows soluble factors to pass through. Therefore, any soluble factor released from neurons plated on the membrane inserts can diffuse through the membrane and act on glial cells plated on the wells underneath. Moreover, we recreated the physical contact between neurons and glial cells in the inserts to see whether the release of soluble factor itself is dependent on physical contact. Our results suggested that soluble factors are released from neurons to reduce the adenylyl cyclase activities on glial cells by 30%. Since additional physical contact in the membrane inserts (group D in Fig. 6.15) did not further

reduce the cicaprost stimulated response in glial cells in the lower chamber, then the release of soluble factor from neurons is independent of physical contact with glial cells. Furthermore, the difference in response sizes of cicaprost-stimulated responses in (group A) glial cell alone cultures and (group B) neuron and glial cell cocultures is 1.9 % conversion (Fig. 6.16); while the difference in response size of (group A) glial cell alone cultures and (group C) neuron and glial cell cultures without physical contact is 0.9% conversion (Fig. 6.16). By comparing with the size of inhibitory response in coculturing glial cells with neurons (physical contact plus soluble factors), soluble factors from neurons only account for half of the inhibition on cicaprost stimulated responses. As a result, we believed that both soluble factors and physical contact between neurons and glial cells are required for the inhibitory response of neurons in our current studies. In contrast to all our previous studies, the forskolin response was also slightly, but not significantly, inhibited by soluble factor from neurons. This observation suggested that the inhibitory action of neurons may not be prostanoid receptor-specific. In our previous study, the inhibition on forskolin-stimulated response in glial cells may be masked by the forskolin stimulated response from neurons. In this transwell study, neurons plated on the membrane inserts were removed before testing the forskolin-stimulated response in glial cells, as a result forskolin response from the cultures is solely contributed by glial cells. Therefore, the inhibitory action on forskolin-stimulated adenylyl cyclase activities on glial cells was unveiled.

One possible candidate property of a paracrine inhibitory factor released by neurons is to activate $G_{i/o}$-coupled receptors on glial cells. IP receptors demonstrate cell-specific coupling to $G_{i/o}$ proteins (Kam *et al.*, 2001), and PTx-sensitive cAMP responses have been detected in HEK 293 cells expressing EP_4 receptors (Leduc 2009) and EP_4 receptors have been shown to couple to $G_{i/o}$ proteins resulting in

activation of PI3K (Fujino *et al.*, 2006). Thus, coupling of EP_4 receptors to G_s proteins may ordinarily dominate and prevent sufficient coupling to $G_{i/o}$ proteins for detection in native cells. It is also possible that coculturing with neurons would favour the $G_{i/o}$-protein coupling to prostanoid receptors in glial cells. Our hypothesis was that PTx might increase EP_4 and IP receptor-dependent responses in the mixed DRG cell preparation, but have no effect on the purer neuronal and glial cell preparations. Indeed, PTx had no effect on cicaprost or PGE_2-stimulated adenylyl cyclase activity in either neuron-enriched or glial cell cultures. Surprisingly, PTx actually inhibited rather than potentiated agonist-stimulated activity in the mixed DRG cell cultures, and in addition, significantly inhibited forskolin-stimulated adenylyl cyclase activity in glial cell cultures. Because of this unusual effect of PTx, we also tested the PTx B-oligomer which is reported to have biological activity not related to the $G_{i/o}$-signalling pathway (Hayat *et al.*, 2003; Wong *et al.*, 1996). Except for an inhibitory effect on forskolin-stimulated adenylyl cyclase activity in glial cells, the PTx B-oligomer had no effect on the mixed DRG cell or neuron-enriched cell cultures. Therefore, an effect of the PTx B-oligomer may account for the inhibitory effect of PTx in glial cells, but it is presently unclear why this effect is specific to agonist-independent stimulation of adenylyl cyclase. However, the inhibitory effect of PTx on agonist-stimulated adenylyl cyclase activity in mixed DRG cells does appear to depend on inactivation of $G_{i/o}$ protein, and this may proceed through a βγ-dependent pathway following the activation of $G_{i/o}$-coupled receptors (Halls *et al.*, 2006).

It is now appreciated that primary sensory neurons, and their axons terminating in the dorsal horn of the spinal cord, are heavily influenced by 'activated' Schwann cells, SGCs, astrocytes and microglial cells, which together play an important role in the development of chronic pain hypersensitivity (Campana, 2007; Ohara *et al.*,

2009; Vit *et al.*, 2006). As noted by Ohara et al. (2009), it is important to remember that SGCs are rarely subject to direct injury, therefore, any changes seen in SGCs *in vivo* must be driven by alterations to the neuron. This implies some active signalling mechanism between neurons and SGCs *in vivo*. The dissociated DRG cell preparations used in the present study may be considered to mirror the responses of cells following nerve injury, but at the present time we cannot conclude if the expression of EP_4 and IP receptors by DRG glial cells *in vitro* is part of a pro-inflammatory or anti-inflammatory process. We can suggest however that DRG neurons are able to inhibit EP_4 and IP receptor-dependent signalling by DRG glial cells, and it remains to be determined if other inflammatory receptors are similarly affected by neuron-glia crosstalk.

To conclude, our results suggested that both cultured DRG neurons and glial cells expressed EP_4 and IP receptors, while glial cells contribute to a large portion of prostanoid-stimulated response in the mixed DRG cell cultures. Moreover, we showed that the adenylyl cyclase activity on glial cells was inhibited by neurons in a receptor-dependent manner. Since, soluble factors only contributed to 50% of thr inhibition, we proposed that cell-cell contact was also essential for the observed inhibitory influence from neurons. In the past, when cultures of adult rat DRG cells were used to assess the nociceptor sensitization properties of PGE_2 and PGI_2, the presence of EP_4 and IP receptors on the associated glial cells was not recognised. In the future, it will be essential to consider that EP_4 and IP receptor agonists/antagonists may also affect the activity of the contaminating glial cells, and to consider that interactions between DRG neurons and glial cells may affect the functional responses under investigation.

From our studies, we have provided evidence of bidirectional interactions between neurons and glial cells. Firstly, glial cells constitutively release factors that

regulate neurite outgrowth, since deprivation of glial cells prevented stress-induced neurite retraction. Secondly neurons regulate prostanoid receptor-dependent adenylyl cyclase activity in glial cells. These results indicate that glial cells participate actively and work in concert with neurons, instead of being a passive bystander. On one hand, glial cells sense the signals from neurons and alter their own activities. On the other hand, glial cells can release signals that regulate the properties of neurons. Since dissociated DRG cell cultures can be separated into different cell types, we can study the properties of individual DRG cell subpopulations in enriched/purified cultures and also the changes in properties of DRG cells in coculture system. Therefore, all these *in vitro* studies serve as a platform for studying interaction between neurons and glial cells and provide a foundation to understand complex neuron-glia interaction *in vivo* which will eventually help to overcome obstacles in promoting neurite regeneration and treating hyperalgesia.

6.4 Summary

Prostanoid receptor agonists such as PGE_2 and cicaprost produce a hyperalgesic action mediated by activation of a cAMP/PKA pathway in sensory neurons. With the availability of EP_4 and IP receptors selective antagonists, we confirmed that it is EP_4 and IP receptors which mediate the response to PGE_2 and cicaprost, respectively. Contrary to popular belief, we also observed a response to PGE_2 and cicaprost in glial cell cultures. Since the agonist-stimulated adenylyl cyclase activity is greatest in pure glial cell cultures and weakest in neuron-enriched cultures, we then hypothesized that neurons inhibit adenylyl cyclase activity in glial cells in mixed DRG cell cultures. In order to test this hypothesis, cultures with different ratios of neurons to glial cells were generated by fixing the number of neurons with different

quantity of glial cells and vice versa. When glial cells were cocultured with neurons, prostanoid-stimulated responses were weaker. An increase in quantity of neurons led to a trend of decrease in cAMP production by prostanoids. In contrast, basal and forskolin-stimulated [^{3}H]cAMP production was not regulated in a similar manner. In addition, individual labelling of DRG cells provided evidence to confirm the inhibitory action from neurons, while glial cells were unlikely to affect the adenylyl cyclase activity on neurons. Furthermore, since conditioned medium derived from neuron-enriched cultures cannot inhibit the adenylyl cyclase activity of glial cells, we speculated that cell-cell contact is important for this neuron-glia interaction in regulating adenylyl cyclase on glial cells. PTx pretreatment was used to investigate for participation of $G_{i/o}$-protein coupled signalling. However, we cannot yet exclude the role of $G_{i/o}$-proteins in mediating the interaction between neurons and glial cells because PTx unexpectedly inhibited adenylyl cyclase activity in the mixed DRG cell cultures.

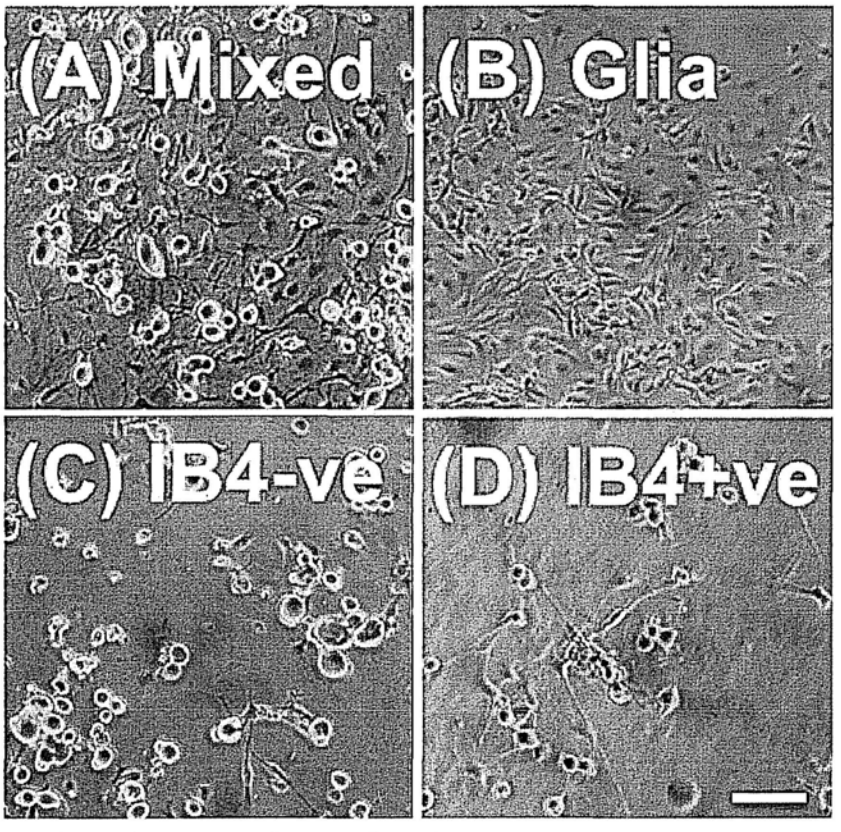

Figure 6.1. Representative phase contrast microscopic images of mixed DRG cell cultures. (A), glial cell cultures (B), IB4-negative cell cultures (C) and IB4-positive cell cultures (D). Note the reduction in number of glial cells (phase dark cells) in purified cultures (B – D) and elimination of large diameter neurons in IB4-positive cell cultures (D).Scale bar = 100 μm.

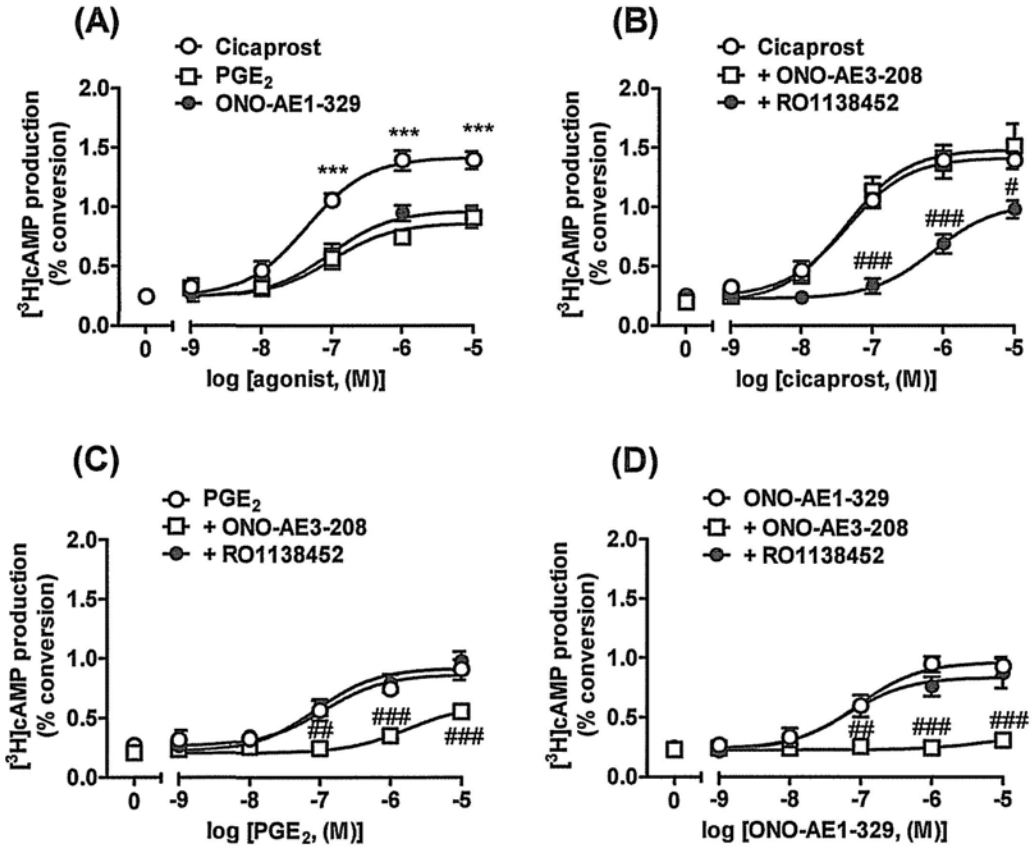

Figure 6.2. PGE_2 and cicaprost specifically stimulate EP4 and IP receptors, respectively, in mixed cultures of DRG cells. (A) Cells were incubated with increasing concentrations of the IP receptor agonist cicaprost, the EP receptor agonist PGE_2, or the EP4 receptor agonist ONO-AE1-329. (B,C,D) The effect of the IP receptor antagonist RO1138452 (100 nM) or the EP4 receptor antagonist ONO-AE3-208 (100 nM) on agonist concentration-response curves [○]. Data are presented as mean ± SEM, from 3 independent experiments. Error bars smaller than the symbol size are not shown. # $p < 0.05$, ## $p < 0.01$ and ### $p < 0.001$ compared with agonist alone group; ***$p < 0.001$ compared with PGE_2 group; two-way ANOVA.

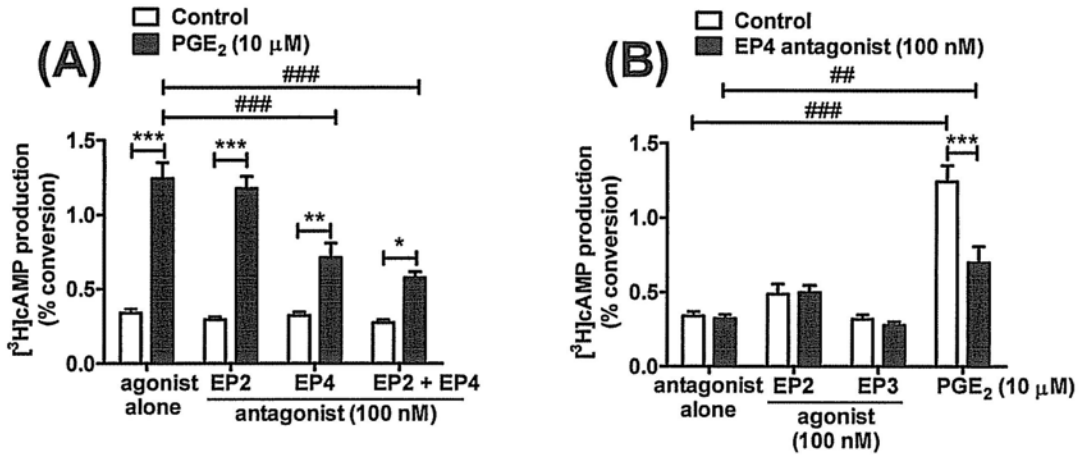

Fig 6.3. Investigation of responses induced by high concentration (10 μM) of PGE_2. (A) Adenylyl cyclase activity was determined in mixed DRG cells incubated with Control solution (assay buffer) or high concentration of PGE_2 (10 μM) either alone or following 15 min incubation with EP_2 receptor antagonist (100 nM; AH6809), EP_4 receptor antagonist (100 nM; ONO-AE3-208) or a combination of both EP_2 and EP_4 receptor antagonists. (B) Adenylyl cyclase activity was determined in mixed DRG cells incubated with Control solution (assay buffer), EP_2 receptor agonist (100 nM; ONO-AE1-259-01), EP_3 receptor agonist (100 nM; ONO-AE-248) or high concentration of PGE_2 (10 μM) either alone or following 15 min incubation with EP4 receptor antagonist (100 nM; ONO-AE3-208). Data are presented as means ± SEM, from 3 independent experiments. * $p < 0.05$, ** $p < 0.01$, *** $p < 0.001$, ## $p < 0.01$ and ### $p < 0.001$; 2-way ANOVA.

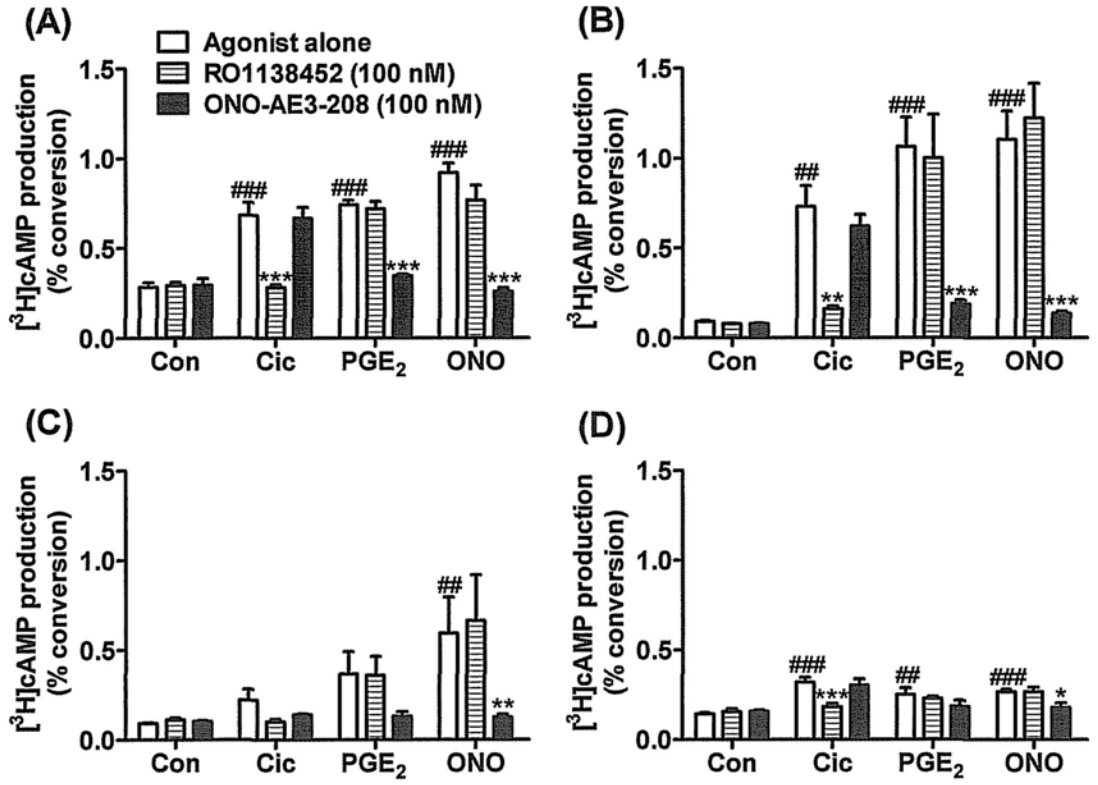

Figure 6.4. Evidence for EP_4 and IP receptor-dependent responses and neuronal inhibition in four DRG cell preparations, such as mixed DRG cells (A), glial cells (B), IB4-negative cells (C) and IB4-positive cells (D). Adenylyl cyclase activity was determined in DRG cells incubated with Control solution (assay buffer; Con), PGE_2 (1 μM; PGE_2), ONO-AE1-329 (1 μM; ONO) or cicaprost (40 nM; Cic) either alone or following 15 min incubation with RO1138452 (100 nM) or ONO-AE3-208 (100 nM). Data are presented as mean ± SEM, from at least 3 independent experiments. ## $p < 0.01$ and ### $p < 0.001$ compared with Control untreated group; **$p < 0.01$ and ***$p < 0.001$ compared with agonist alone group; two-way ANOVA.

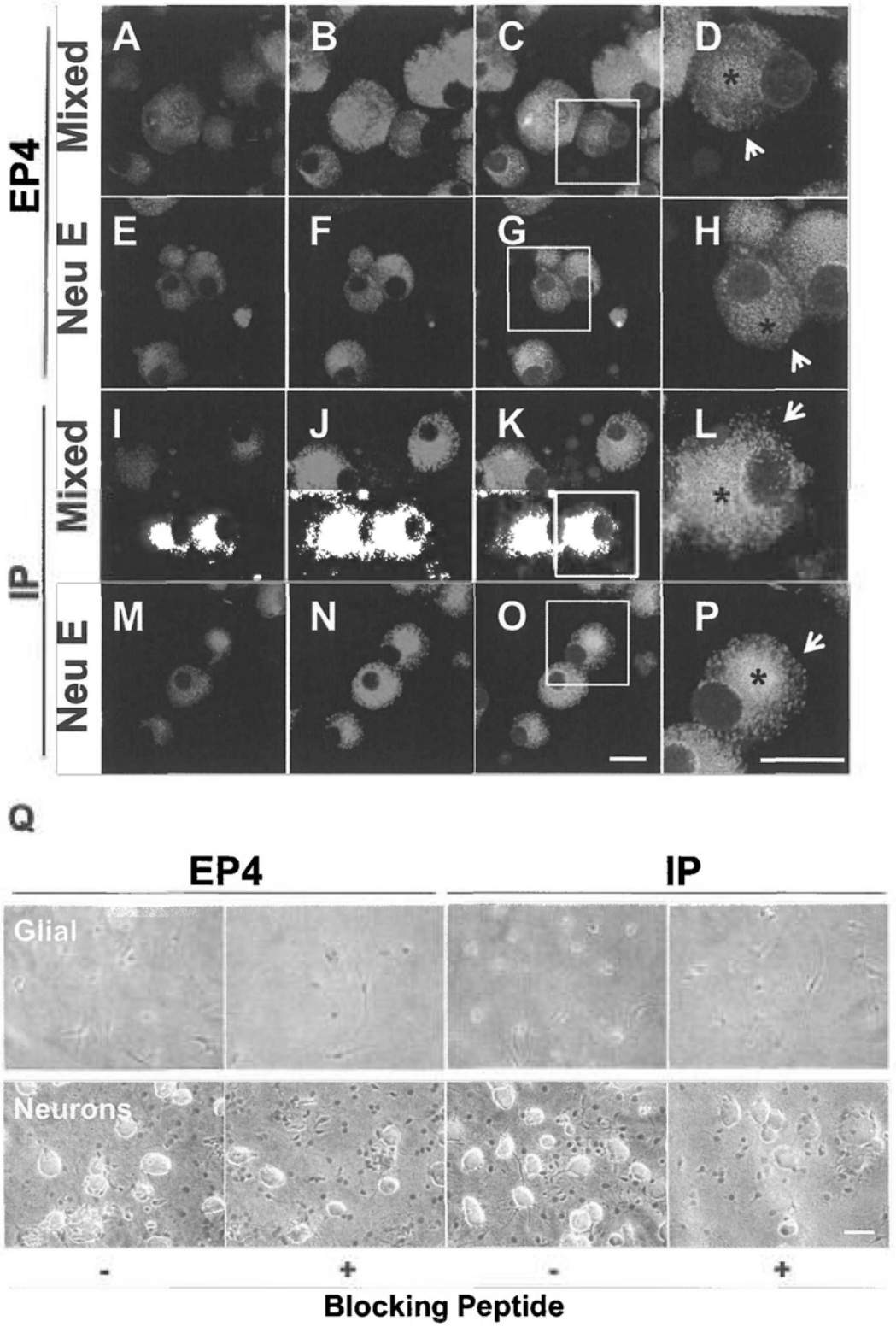

Figure 6.5. Investigation of EP_4 and IP receptor localization in neurons in mixed DRG cell cultures and neuron-enriched cultures. Fixed and permeabilized DRG cells were incubated with antibodies against EP_4 or IP receptors (Cy3 secondary antibodies, red; B, F, J, N), and neurons were detected using anti-TUJ-1

antibodies (FITC secondary antibodies, green; A, E, I, M). Cell nuclei were detected by Hoescht 33342 staining (blue). Merged images are shown in (C, G, K, O) and the insets were magnified to demonstrate subcellular localization of receptors (D, H, L, P). A – H: Confocal microscopy images for EP_4 receptors in neurons of mixed DRG cell cultures (A – D) and neuron-enriched cell cultures (E – H). I – P: Confocal microscopy images for IP receptors in neurons of mixed DRG cell cultures (I – L) and neuron-enriched cell cultures (M – P). Note the red ring on the surface of neurons (arrows) and yellow colocalization in the cytoplasm (asterisk). Images are representative of 2 independent experiments. (Q) Blocking peptides was used to confirm the specificity of with antibodies against EP_4 or IP receptors. Representative phase contrast and fluorescence microscopic images of DRG cell cultures stained by antibodies against EP_4 or IP receptors (Cy3 secondary antibodies) with or without corresponding blocking peptide. Scale bars = 25 μm.

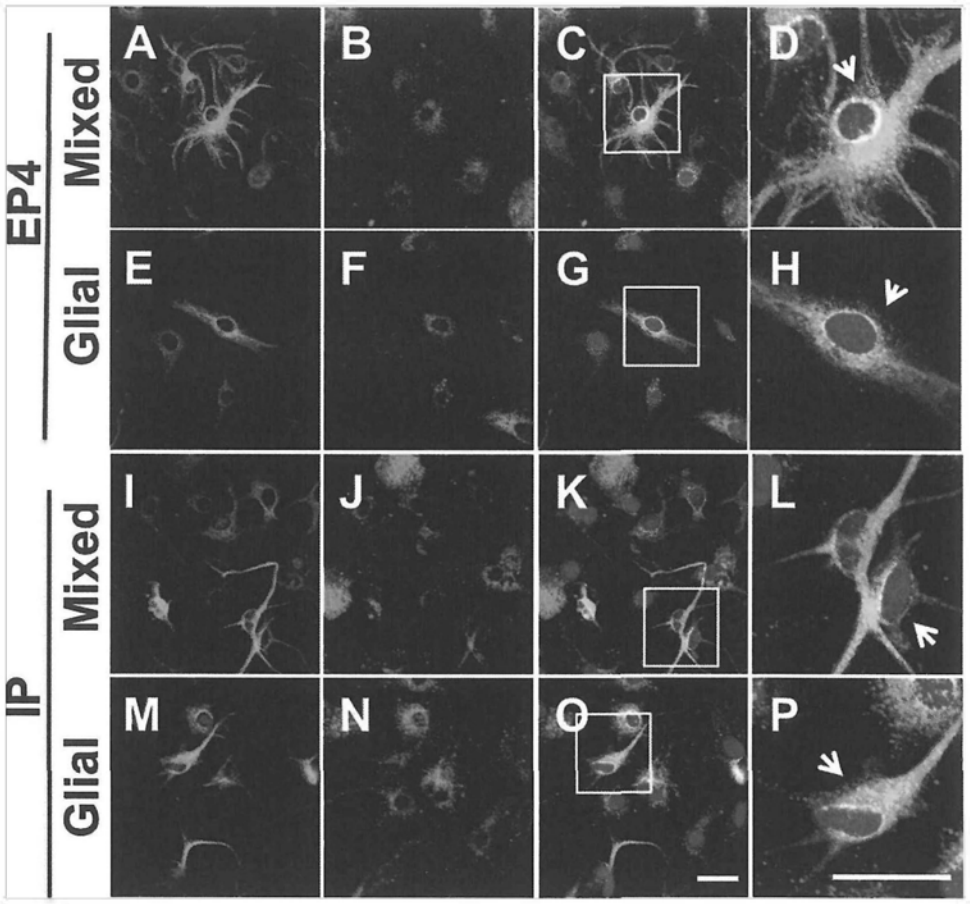

Figure 6.6. Investigation of EP_4 and IP receptors localization in glial cells in mixed DRG cell cultures and purified glial cell cultures. Fixed and permeabilized DRG cells were incubated with antibodies against EP_4 or IP receptors (FITC secondary antibodies, red; B, F, J, N), and glial cells were detected using Cy3-labeled anti-GFAP antibodies (green; A, E, I, M). Cell nuclei were detected by Hoescht 33342 staining (blue). Merged images are shown in C, G, K, O and the insets were magnified to demonstrated subcellular localization of receptors (D, H, L, P). A – H: Confocal microscopy images for EP_4 receptors in glial cells of mixed DRG cell cultures (A – D) and purified glial cell cultures (E – H). I – P: Confocal microscopy images for IP receptors in glial cells of mixed DRG cell cultures (I – L) and purified glial cell cultures (M – P). Note the red dots on the surface of glial cells (arrows) and yellow colocalization in the cytoplasm. Images are representative of 2 independent experiments. Scale bars = 25 μm.

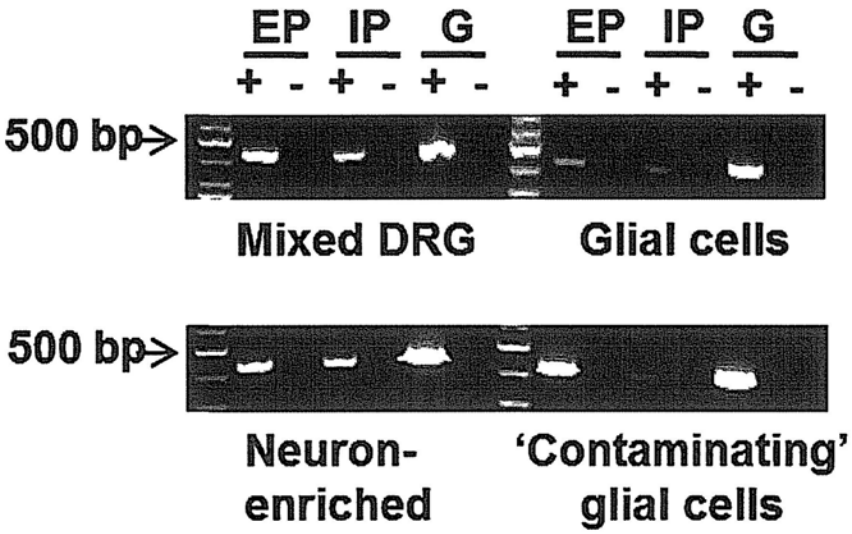

Figure 6.7. Investigation of EP_4 and IP receptor mRNA expression in DRG cell preparations. As shown in upper panel, EP_4 and IP receptor mRNA was detected in both mixed DRG cell cultures and glial cell cultures by the presence of PCR products on an agarose gel. As shown in lower panel, EP_4 and IP receptor mRNA was detected in both neuron-enriched cell cultures and glial cells fractions (representating glial cell numbers expected in the neuron-enriched fractions). Expected product sizes are EP (EP_4) 423 bp, IP 431 bp, and G (GAPDH) 452 bp. Lack of PCR products in the samples without reverse transcriptase (-) indicates a lack of contamination by genomic DNA. Data is representative of three independent experiments.

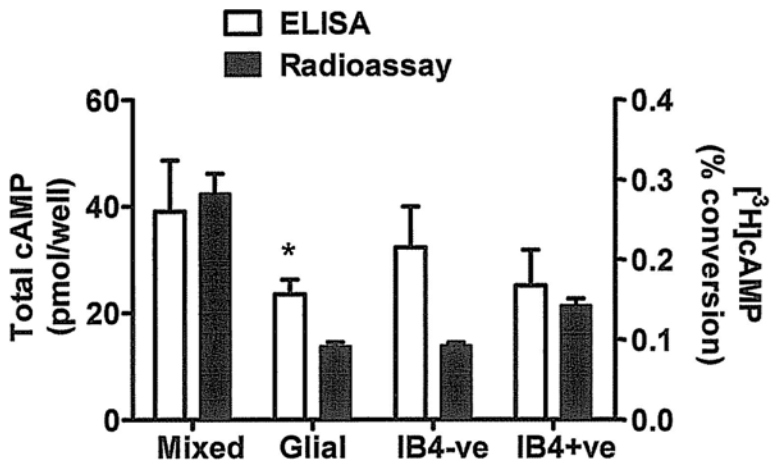

Figure 6.8. Basal adenylyl cyclase activity is lower in purified DRG neuron cultures and glial cell cultures than mixed DRG cell cultures. Adenylyl cyclase activity was determined in unstimulated cultures of mixed DRG cells (Mixed), glial cells (glial), IB4-negative cells (IB4-ve) and IB4-positive cells (IB4+ve) using or [^{3}H]cAMP radioassays. Data are presented as mean ± SEM (n = 3 for ELISA, n = 5 for radioassay). *$p < 0.05$ compared with mixed cell culture; two-way ANOVA with Bonferroni's *post hoc* test.

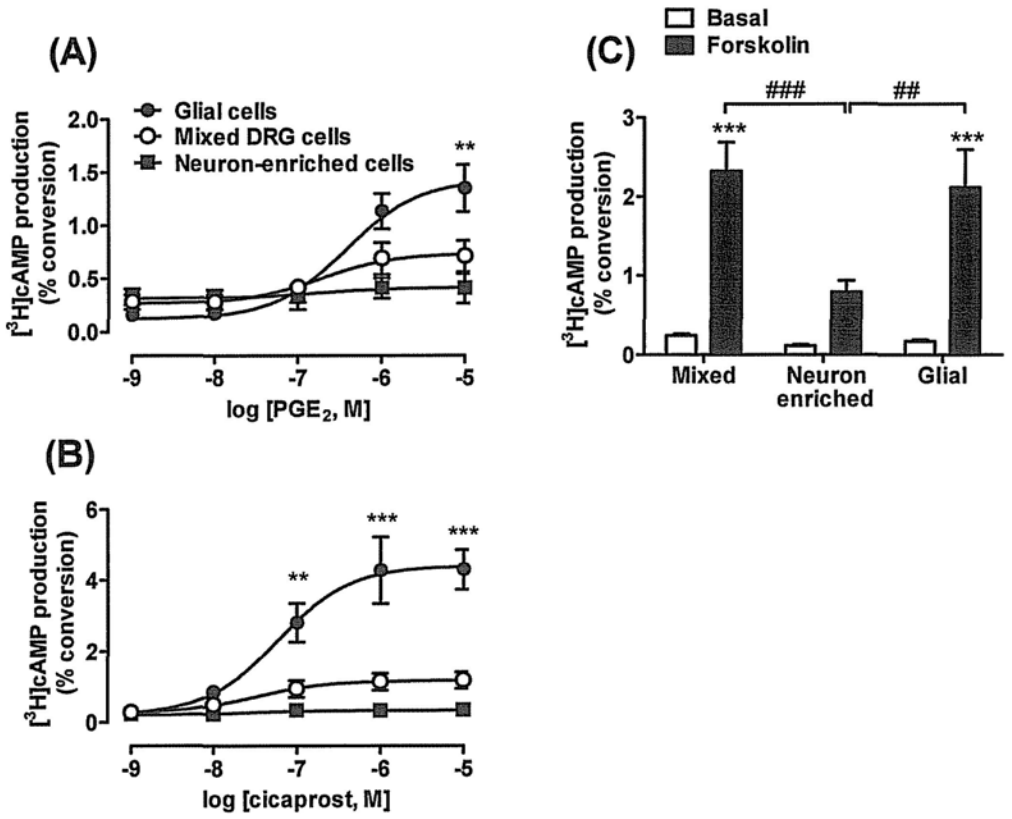

Figure 6.9. A comparison of EP_4 and IP-dependent adenylyl cyclase activity in DRG cell cultures. Mixed DRG cells, neuron-enriched cells and glial cells were incubated with increasing concentrations of the EP receptor agonist PGE_2 (A), or the IP receptor agonist cicaprost (B). C, a comparison of basal and forskolin (1 μM)-induced response in mixed DRG cells, neuron-enriched cells and glial cells. Data are presented as mean ± SEM, from 3 independent experiments. Error bars smaller than the symbol size are not shown. (A, B) ** $p < 0.01$, *** $p < 0.001$ compared with mixed cell cultures; two-way ANOVA with Bonferroni's *post hoc* test. (C) *** $p < 0.001$ compared with basal activities; ## $p < 0.01$, ### $p < 0.001$; two-way ANOVA with Bonferroni's *post hoc* test

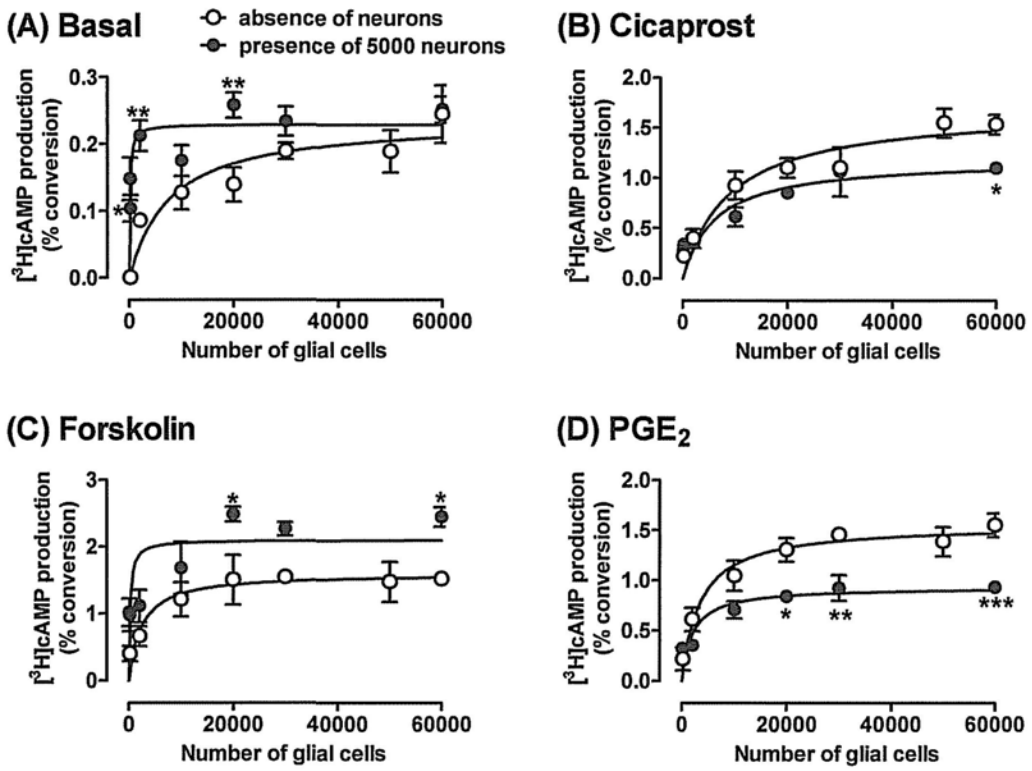

Figure 6.10. Differential effect of DRG neurons on agonist-dependent and agonist-independent adenylyl cyclase activity in glial cells. Increasing numbers of glial cells were plated in the presence or absence of 5000 neurons. After 1 day in culture, [^{3}H]cAMP production was determined in response to assay buffer (A), 40 nM cicaprost (B), 1 μM forskolin (C) or 1 μM PGE_2 (D). Each data point is the mean ± SEM, from 3 independent experiments. Error bars smaller than the symbol size are not shown. *$p < 0.05$, **$p < 0.01$, and ***$p < 0.001$ compared with glial cells alone; two-way ANOVA.

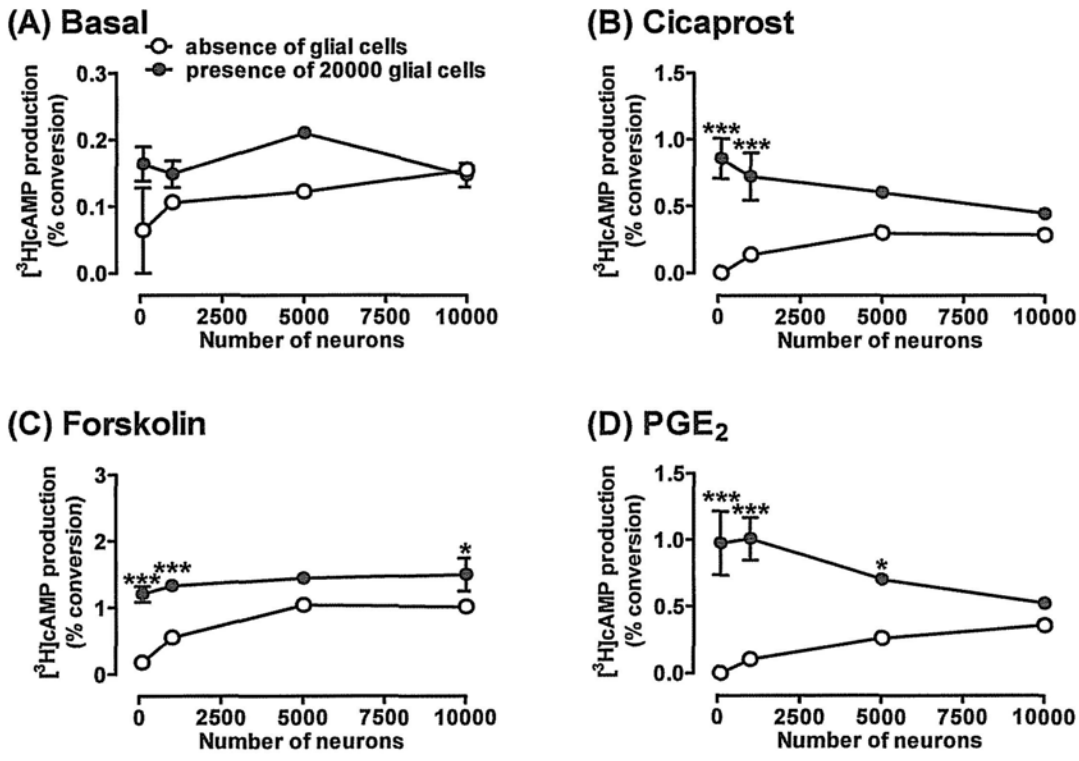

Figure 6.11. Increasing numbers of DRG neurons decrease agonist-dependent, but not agonist-independent, stimulation of adenylyl cyclase activity of glial cells. Increasing numbers of neurons were assayed in the presence or absence of 20000 glial cells. After 1 day in culture, [^{3}H]cAMP production was determined in response to assay buffer (A), 40 nM cicaprost (B), 1 μM forskolin (C) or 1 μM PGE_2 (D). Each data point is the mean ± SEM, from 3 independent experiments. Error bars smaller than the symbol size are not shown. *$p < 0.05$ and ***$p < 0.001$ compared with neurons alone; two-way ANOVA.

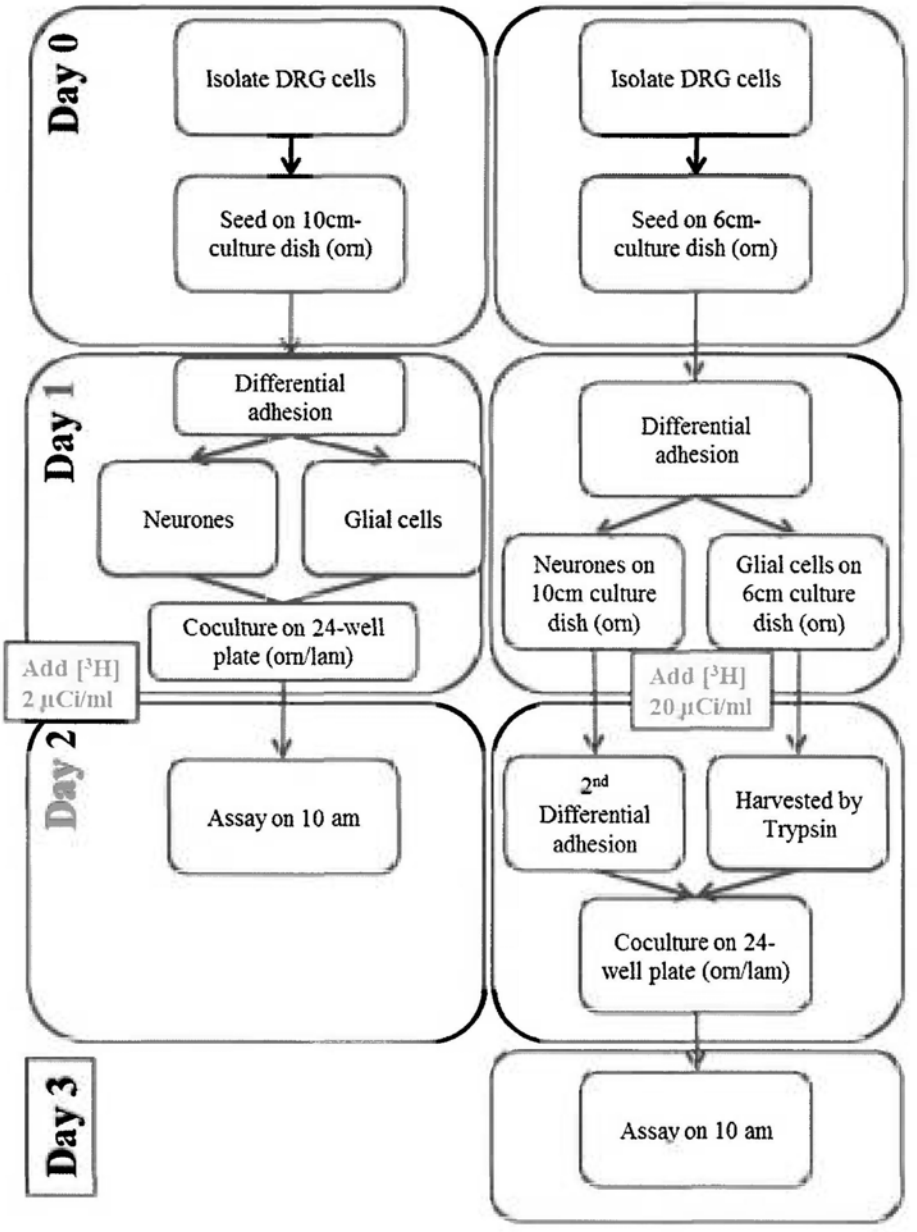

Figure 6.12. Labelling protocol for different cAMP assays. A regular [^{3}H]adenine labelling protocol (left panel) was used to load [^{3}H]adenine to all of the cells (including both neurons and glial cells) in the cultures. In order to study the cAMP production in a specific cell type, an alternative protocol was used to selectively load [^{3}H]adenine to individual cell types (right panel). It is noted that cells need to be incubated with ten times more [^{3}H]adenine for the alternative method. orn = poly-DL-ornithine; lam = laminin.

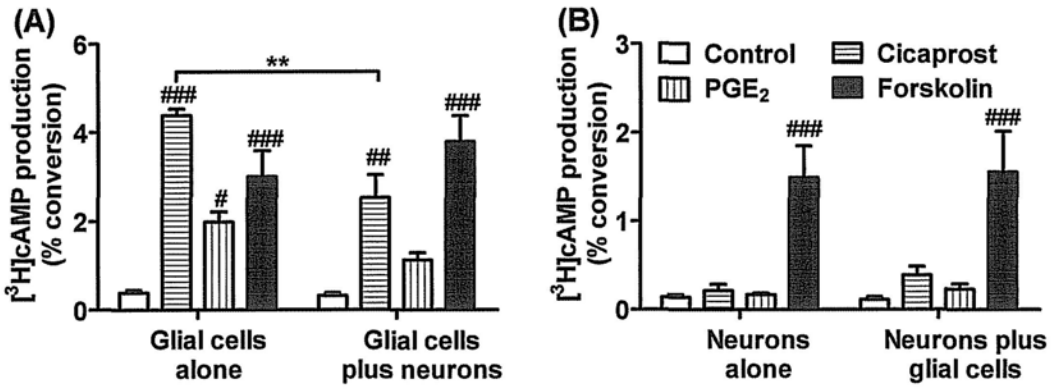

Figure 6.13. DRG neurons inhibit agonist-dependent, but not agonist-independent [^{3}H]cAMP production by [^{3}H]adenine-labeled glial cells. DRG neurons and glial cells were individually labeled with [^{3}H]adenine prior to co-culture with unlabeled glial cells and neurons, respectively. A: [^{3}H]adenine-loaded glial cells (20000) were co-cultured with unlabeled DRG neurons (0 or 10000). B: [^{3}H]adenine-loaded DRG neurons (10000) were co-cultured with unlabeled glial cells (0 or 20000). After 1 day in co-culture, cell-specific [^{3}H]cAMP production was determined in response to assay buffer, 40 nM cicaprost, 1 mM PGE_2 or 1 mM forskolin. Each data point is the mean ± SEM, from 3 independent experiments. $^{**}p < 0.01$ compared with glial cells alone, and $\#\ p < 0.05$, $\#\#\ p < 0.01$ and $\#\#\#\ p < 0.001$ compared with own control group; two-way ANOVA.

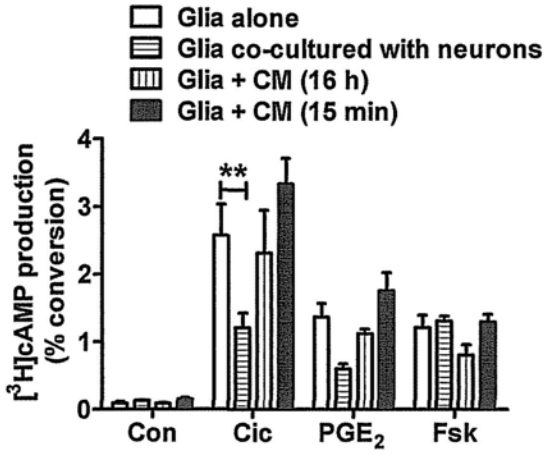

Figure 6.14. No effect of conditioned medium on EP_4 and IP receptor-mediated [^{3}H]cAMP production. (open bars) Glial cells (20000), (horizontal bars) glial cells (20000) co-cultured with neurons (5000), (vertical bars) glial cells (20000) incubated with conditional medium overnight and (filled bars) glial cells (20000) incubated with neuron-conditioned medium for 15 min. Cells were incubated with control solution (assay buffer; Con), cicaprost (40 nM; Cic), PGE_2 (1 μM) or forskolin (1 μM; Fsk). Data are presented as means ± SEM, from 4 independent experiments. $^{**}p < 0.01$; two-way ANOVA.

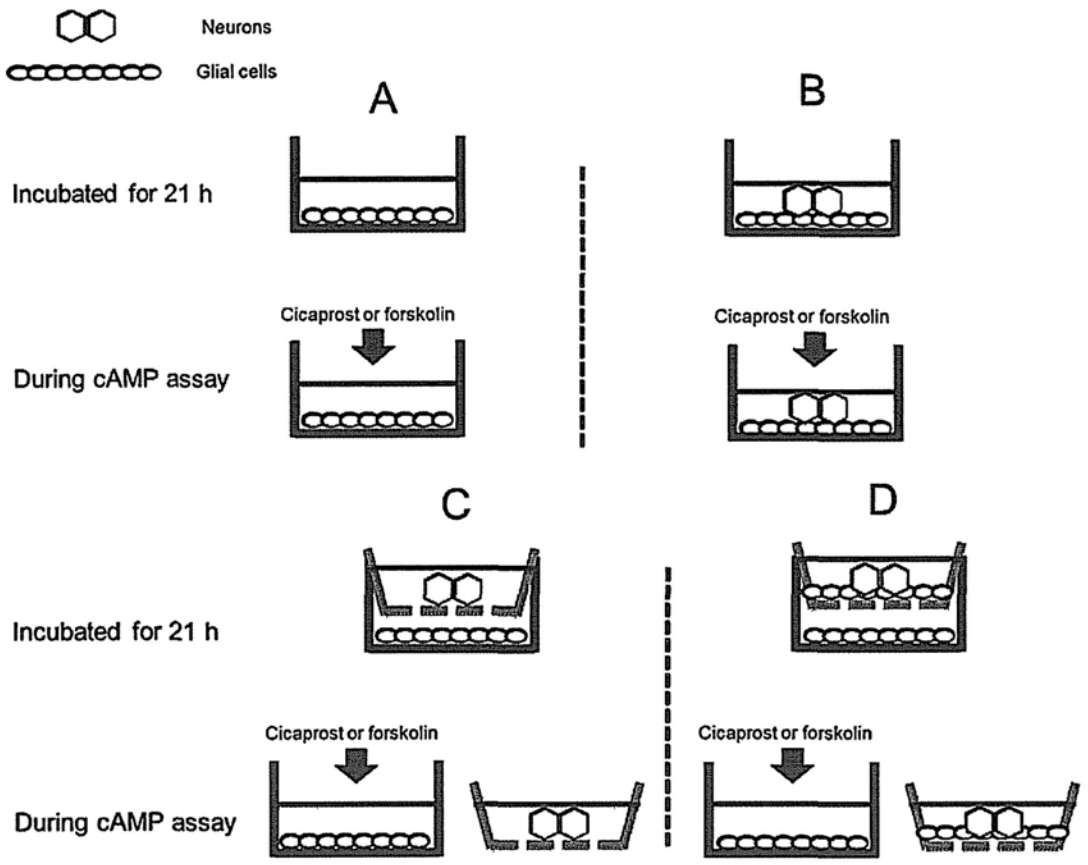

Figure 6.15 Schematic diagram for transwell study. Physical contact between neurons and glial cells are present in typical DRG cell cultures. In order to distinguish the effects of soluble factors and cell-cell contact in our observed neuron-glia interactions, neurons and glial cells were physically separated by a transwell membrane, and soluble factors can freely diffuse across the pores (0.4 μm) on the membrane. (A) Glial cells (20000) were plated on the wells of a 12-well plate. (B) Glial cells (20000) with additional neurons (5000) were plated together in the wells as a positive control for neuron-glia interactions. (C) Glial cells (20000) were plated in the wells, and neurons (5000) were plated on membrane inserts for studying the effect of soluble factors; and (D) Glial cells (20000) were plated in the wells, and both neurons (5000) and glial cells (20000) were plated on membrane inserts for investigating whether the release of soluble factors required physical contact between neurons and glial cells.

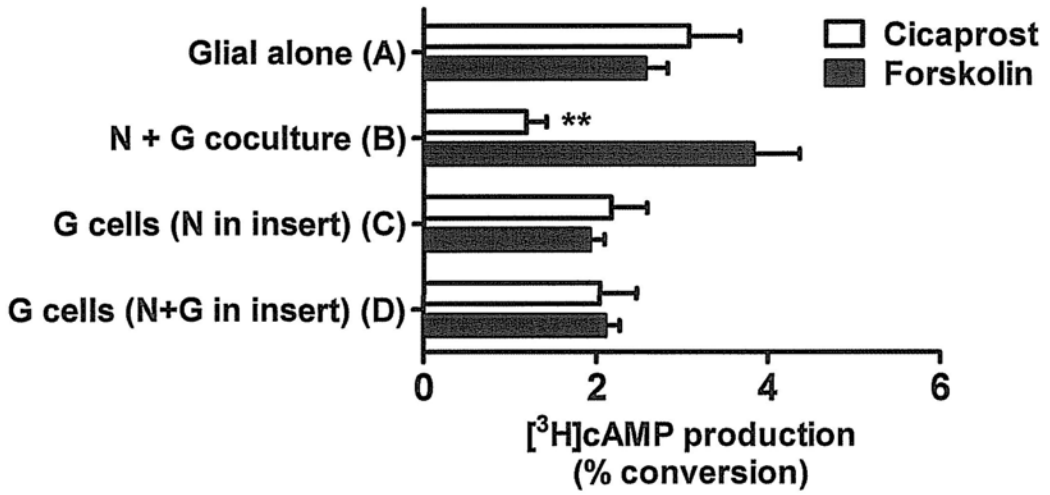

Figure 6.16 Both soluble factors and physical contact is required for neuronal inhibition of adenylyl cyclase activities of glial cells. In order to distinguish the effects of soluble factors and cell-cell contacts in regulating the adenylyl cyclase activities of glial cells, cicaprost- and forskolin-stimulated responses were studied. Glial cells were cultured with or without neurons for 16 h as shown in Fig. 6.15 A-D. Cells were labelled with [^{3}H]adenine 16 h before assay. [^{3}H]cAMP production was determined in response to 40 nM cicaprost or 1 μM forskolin. Each data point is the mean ± SEM, from 3 independent experiments. $^{**}p < 0.01$ compared with glial cells alone; two-way ANOVA.

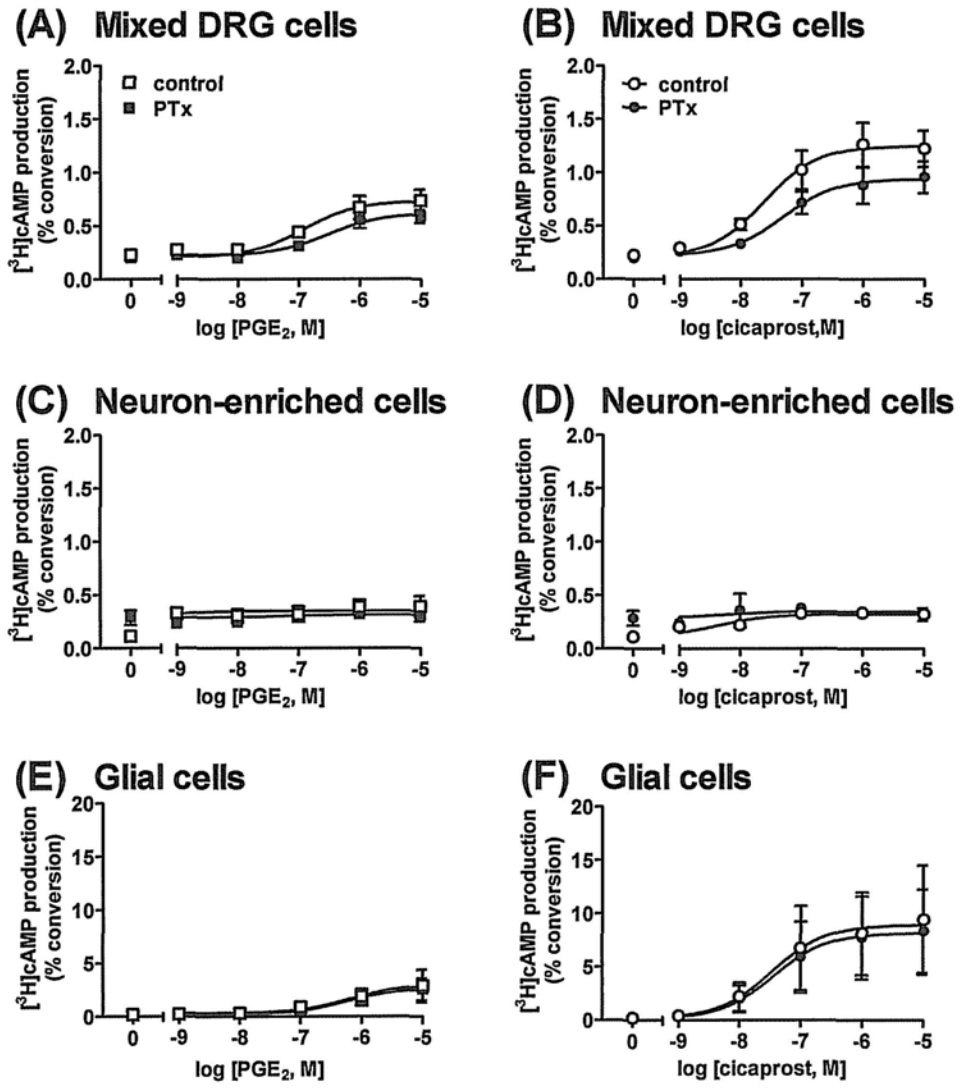

Figure 6.17. Effect of PTx on EP_4 and IP receptor-mediated adenylyl cyclase activity in DRG cell cultures. (A,B) Mixed DRG cells, (C,D) neuron-enriched cells and (E,F) glial cells were incubated with increasing concentrations of PGE_2 (A,C,E), or cicaprost (B,D,F) in the absence (open symbols) or presence (black symbols) of PTx (100 ng/ml). Data are presented as means ± SEM, from 4 independent experiments.

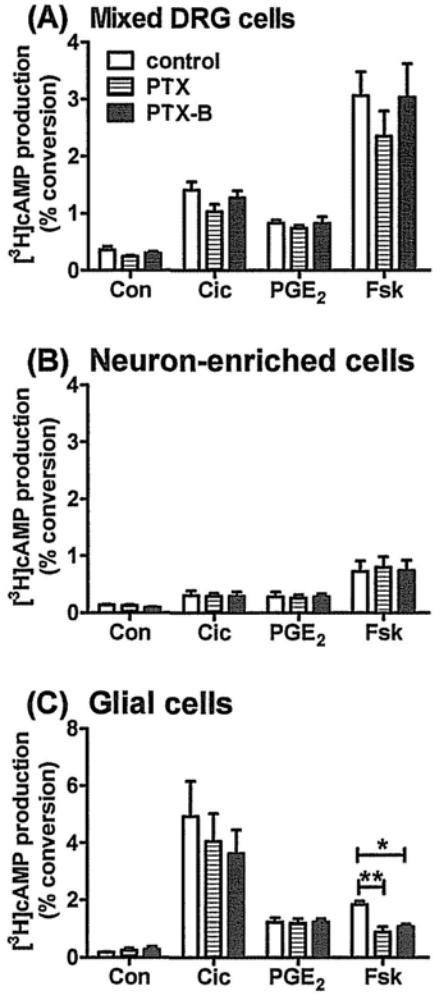

Figure 6.18. Comparative effect of PTx and PTx B-oligomer on EP_4 and IP receptor-mediated [^{3}H]cAMP production. (A) Mixed DRG cells, (B) neuron-enriched cells and (C) glial cells were incubated with control solution (assay buffer; Con), cicaprost (40 nM; Cic), PGE_2 (1 μM) and Forskolin (1 μM; Fsk) either alone (open bars) or following overnight incubation with PTx (100 ng/ml; horizontal bars) or PTx B-oligomer (100 ng/ml; black bars). Data are presented as means ± SEM, from 3 independent experiments. * $p < 0.05$ and ** $p < 0.01$; one-way ANOVA.

Chapter 7

Future studies

From our neurite extension studies, we clearly showed that glial cells are essential for PTx-dependent neurite retraction in large diameter neurons and glial cells constitutively release factor(s) that stimulate neurite retraction in larger diameter neurons. The majority of these glial cells in culture are GFAP-positive and GFAP can be expressed by both SGCs and non-myelinating Schwann cells *in vitro* (Scholz and Woolf 2007). However, at the present time we are unable to distinguish SGCs from Schwann cells using immunocytochemical techniques. There are other proteins unique to SGCs, such as Kir4.1, Cx43 subunit of gap junctions, P2Y4 and soluble GC (Vit 2006). We may be able to find an optimal marker for distinguishing SGCs and to investigate the relative population of SGCs and Schwann cells in DRG cell cultures. Once we can find an optimal marker for identifying SGCs in our culture, SGCs can be isolated by immunoselection strategies, such as immunopanning or MACS with the suitable antibody (Fex Svenningsen *et al.*, 2004; Runyan *et al.*, 2009; Thippeswamy *et al.*, 2005). Briefly, SGCs in the culture can be captured by antibodies against a specific cell surface marker, which are either immobilized on culture plates or linked to magnetic beads. The remaining cell fraction will be enriched in Schwann cells. After that, we aim to generate cultures enriched in SGCs to study their prostanoid-stimulated responses. From this study, we can deduce whether the prostanoid-stimulated response is contributed by SGCs or Schwann cells in the cultures. Moreover, we study contributions by SGCs and Schwann cells on the PTx-dependent neurite retraction by incubating IB4-negative cells with conditioned medium derived from SGC-enriched fraction or Schwann cell-enriched fraction.

Furthermore, we found that glial cells constitutively release factor(s) that stimulate neurite retraction in large diameter neurons, which is counterbalanced by neuroprotective $G_{i/o}$-protein signalling pathway. A full understanding of this neuron-glia interaction requires an investigation of which $G_{i/o}$-protein coupled GPCRs are expressed by which cells. Our objective is to examine the expression of $G_{i/o}$-protein coupled GPCRs by neurons and glial cells and we started with those GPCRs that have already been identified in neurons *in vivo*. To determine the activation of $G_{i/o}$-protein coupled GPCRs, we will look for an inhibition of forskolin-stimulated adenylyl cyclase activity by agonists for μ-opioid receptor (DAMGO), ORL-1 receptor (N/OFQ), CB1 receptor (methanandamine) and CB2 receptor (L-759,656). Moreover, the mRNA expression of these $G_{i/o}$-protein coupled receptors can further be investigated by RT-PCR. As a result, the expression patterns observed among the mixed DRG cell cultures, neuron-enriched cultures and purified glial cell cultures would provide insight for the relative expression of $G_{i/o}$-protein coupled GPCRs by neurons and glial cells. In order to confirm the involvement of $G_{i/o}$-protein GPCRs in our PTx-dependent neurite retraction, DRG cells will be treated with appropriate $G_{i/o}$-protein GPCRs antagonist and will be observed for the neurite retraction response.

Furthermore, RhoA/ROCK, PI3K/Akt, ERK1/2 and ERK5 pathways were reported to be involved in mediating neurite extension and retraction. In order to investigate the downstream effectors of the neuroprotective $G_{i/o}$-protein signalling, untreated or PTx-pretreated DRG cells will be harvested and their expression of phospho-Akt, phospho-ERK1/2 and phospho-ERK5 will be detected by immunocytochemistry. On the other hand, in order to study the effectors for stress-induced neurite retraction response, DRG cells will be harvested at 1 h after stress-induction. In addition, PTx-pretreated DRG cells will be treated with selective

inhibitors for Rho-kinase (Y27632), PI3K (LY294002, Wortmannin), ERK1/2 and ERK5 (U0126) for 15 min and will be observed for inhibition of PTx-dependent neurite retraction in DRG cell cultures. These results would give us insight on which intracellular signalling pathways are involved in multifactorial PTx-dependent neurite retraction.

We reported that prostanoid receptor-mediated [^{3}H]cAMP production was regulated by the cell density of cultured DRG cells in 2001. Moreover, this cell density regulation was specific to certain types of G_s-coupled GPCRs (e.g. EP_4, IP and CGRP receptors, but not β-adrenoceptor) (Rowlands *et al.*, 2001). Activation of CGRP receptor was reported to generate hyperalgesia (Sun *et al.*, 2003); while activation of β-adrenoceptor was reported to have antinociceptive effect and chronic stimulation of β_2-adrenoceptor can suppress neuropathic allodynia (Brochet *et al.*, 1986; Yalcin *et al.*, 2010). From our current studies, we concluded that there was an interaction between isolated cells of dorsal root ganglia (DRG) whereby the neurons regulated adenylyl cyclase activity of associated glial cells in a receptor-dependent manner. We have shown that the presence of neurons inhibited the EP_4 receptor and IP receptor-mediated adenylyl cyclase activity of glial cells. Therefore, in order to further understand this neuron-glia interaction on non-prostanoid G_s-coupled signalling, we will study the CGRP, isoprenaline ($\beta_{1/2}$) and formoterol (β_2)-stimulated [^{3}H]cAMP production. To identify the neuron-glia interaction on G_s-coupled GPCR responses, we will determine agonist-stimulated [^{3}H]cAMP production in mixed DRG cell cultures, neuron-enriched cultures and purified glial cell cultures. From this study, we expect to determine whether this neuron-glia interaction is specific to prostanoid G_s-coupled GPCRs or all receptors associated with a hyperalgesic effect.

Furthermore, we discovered an unexpected inhibitory effect of PTx on adenylyl

cyclase activity of DRG cell cultures. Since we reported a PTx-dependent neurite retraction in DRG cell cultures, it is possible that neurite retraction would reduce the EP_4 and IP receptors expression on the surface of neurites. As the glial cells are the major contributor for the observed [^{3}H]cAMP production in DRG cell cultures, one would expect a reduction of the EP_4 and IP receptor expression on the surface of glial cells (i.e. internalization). In order to study this hypothesis, DRG cells will first be pretreated in complete F14 medium with or without PTx or PTx B-oligomer for 16 h. Then, the medium will be replaced by assay buffer for cAMP assay after washing. After 45 min incubation in 37°C water bath (equivalent to the total incubation period in current cAMP assay, the DRG cells will be fixed and stained for TUJ-1 (neuron marker), GFAP (glial cell marker), EP_4 receptors and IP receptors. Then the localization of EP_4 and IP receptor can be visualized using confocal microscope. Another possible option for the unexpected inhibitory effects is the GPCR desensitization, which can be PKA- or PKC-dependent. Studies on HEK 293 cells transfected with the human IP receptor indicate a PKC-dependent desensitization of IP receptor to iloprost-stimulated cAMP production (Smyth *et al.*, 1996).The rat EP_2 and EP_4 receptors can be phosphorylated by both PKA and PKC (Boie *et al.*, 1997). The potential involvement of PKA or PKC in regulating prostanoid receptors responsiveness can be examined using H89 (PKA inhibitor) or GF 109203X (PKC inhibitor). Briefly, DRG cells will first be pretreated in complete F14 medium with PTx alone or together with PKA/PKC inhibitors for 16 h. Then, the prostanoid stimulated adenylyl cyclase activities can be investigated. For example, if a PKA inhibitor can rescue the PTx-dependent inhibitory effect on adenylyl cyclase activity of DRG cell cultures, it is likely that PTx induces receptor desensitization. These results would give us insights to answer why PTx unexpectedly inhibit the prostanoid receptor-mediated response in mixed DRG cell

cultures.

Another possible explanation for this unexpected inhibitory effect of PTx is that the inhibition of the $G_{i/o}$-protein signalling in DRG neurons may enhance the neuron-glia interaction which inhibits the adenylyl cyclase activities of glial cells. This hypothesis can be tested by coculturing glial cells with either untreated or PTx-pretreated neuron-enriched cells, and measure the PGE_2 (EP_4 receptor), cicaprost (IP receptor) and forskolin (receptor-independent)-stimulated responses. Reduction in agonist-stimulated response in glial cells coculturing with PTx-pretreated neuron-enriched cells would indicate that $G_{i/o}$-protein coupled signalling regulates neuron-glia interaction.

Moreover, receptors that are primarily coupled to $G\alpha_s$ may switch its coupling preference to $G\alpha_i$ after a prolonged stimulation (Halls *et al.*, 2006). We observed an unexpected inhibition of prostanoid receptor-mediated cAMP production in PTx-treated mixed DRG cells. A similar phenomenon has been also found in RXFP1-receptor mediated relaxin signalling (Halls *et al.*, 2006). cAMP accumulation after activation of RXFP1 involves a time-dependent biphasic pathway with an early phase involving coupling to G_s and G_{oB} and a delayed phase coupling to G_{i3}. In the delayed phase, $\beta\gamma$ subunits can activate adenylyl cyclase via PI3K, PKCζ (Halls *et al.*, 2006). As a result, PTx can enhance cAMP accumulation via inhibition of G_{oB} protein, but suppress cAMP accumulation via inhibition of G_{i3}. We aim to evaluate whether this biphasic phenomenon is occurring in prostanoid receptor signalling system. In order to achieve this goal, we can pretreat our mixed DRG cell cultures with PTx or wortmannin and study the time course for cicaprost, PGE_2 and forskolin. If we observe a biphasic regulation of adenylyl cyclase activity after PTx or wortmannin treatment, it would suggest that the prostanoid receptors change their coupling preference to G_{oB} proteins. As a result, it can explain why PTx

can inhibit adenylyl cyclase activities in mixed DRG cell cultures. It is noted that the PTx do not inhibit the adenylyl cyclase activities in glial cell cultures. The absence of PTx effect on purified glial cell cultures suggest that glial cells behave differently in the presence or absence of neurons.

References

Aley KO, Levine JD (1997). Dissociation of tolerance and dependence for opioid peripheral antinociception in rats. *J Neurosci* **17**(10)**:** 3907-3912.

Aley KO, Levine JD (1999). Role of protein kinase A in the maintenance of inflammatory pain. *J Neurosci* **19**(6)**:** 2181-2186.

Aoki E, Semba R, Kashiwamata S (1991). Evidence for the presence of L-arginine in the glial components of the peripheral nervous system. *Brain Res* **559**(1)**:** 159-162.

Arevalo JC, Wu SH (2006). Neurotrophin signaling: many exciting surprises! *Cell Mol Life Sci* **63**(13)**:** 1523-1537.

Ayer LM, Wilson SM, Traves SL, Proud D, Giembycz MA (2008). 4,5-Dihydro-1H-imidazol-2-yl)-[4-(4-isopropoxy-benzyl)-phenyl]-amine (RO1138452) is a selective, pseudo-irreversible orthosteric antagonist at the prostacyclin (IP)-receptor expressed by human airway epithelial cells: IP-receptor-mediated inhibition of CXCL9 and CXCL10 release. *J Pharmacol Exp Ther* **324**(2)**:** 815-826.

Balsinde J, Dennis EA (1997). Function and inhibition of intracellular calcium-independent phospholipase A2. *J Biol Chem* **272**(26)**:** 16069-16072.

Bandtlow CE (2003). Regeneration in the central nervous system. *Exp Gerontol* **38**(1-2)**:** 79-86.

Barber R, Ray KP, Butcher RW (1980). Turnover of adenosine 3',5'-monophosphate in WI-38 cultured fibroblasts. *Biochemistry* **19**(12)**:** 2560-2567.

Basbaum AI, Bautista DM, Scherrer G, Julius D (2009). Cellular and molecular mechanisms of pain. *Cell* **139**(2)**:** 267-284.

Benarroch EE (2010). Central neuron-glia interactions and neuropathic pain: overview of recent concepts and clinical implications. *Neurology* **75**(3)**:** 273-278.

Bennett DL, Michael GJ, Ramachandran N, Munson JB, Averill S, Yan Q, *et al.* (1998). A distinct subgroup of small DRG cells express GDNF receptor components and GDNF is protective for these neurons after nerve injury. *J Neurosci* **18**: 3059-3072.

Bhave G, Zhu W, Wang H, Brasier DJ, Oxford GS, Gereau RW (2002). cAMP-dependent protein kinase regulates desensitization of the capsaicin receptor (VR1) by direct phosphorylation. *Neuron* **35**(4): 721-731.

Bingham S, Beswick PJ, Blum DE, Gray NM, Chessell IP (2006). The role of the cylooxygenase pathway in nociception and pain. *Semin Cell Dev Biol* **17**(5): 544-554.

Bley KR, Bhattacharya A, Daniels DV, Gever J, Jahangir A, O'Yang C, *et al.* (2006). RO1138452 and RO3244794: characterization of structurally distinct, potent and selective IP (prostacyclin) receptor antagonists. *Br J Pharmacol* **147**(3): 335-345.

Bley KR, Hunter JC, Eglen RM, Smith JA (1998). The role of IP prostanoid receptors in inflammatory pain. *Trends Pharmacol Sci* **19**(4): 141-147.

Boie Y, Stocco R, Sawyer N, Slipetz DM, Ungrin MD, Neuschafer-Rube F, *et al.* (1997). Molecular cloning and characterization of the four rat prostaglandin E2 prostanoid receptor subtypes. *Eur J Pharmacol* **340**(2-3): 227-241.

Borisoff JF, Chan CC, Hiebert GW, Oschipok L, Robertson GS, Zamboni R, *et al.* (2003). Suppression of Rho-kinase activity promotes axonal growth on inhibitory CNS substrates. *Mol Cell Neurosci* **22**(3): 405-416.

Brochet D, Mico JA, Martin P, Simon P (1986). Antinociceptive activity of beta-adrenoceptor agonists in the hot plate test in mice. *Psychopharmacology* **88**(4): 527-528.

Burgess GM, Perkins MN, Rang HP, Campbell EA, Brown MC, McIntyre P, *et al.* (2000). Bradyzide, a potent non-peptide B(2) bradykinin receptor antagonist with long-lasting oral activity in animal models of inflammatory hyperalgesia. *Br J Pharmacol* **129**(1): 77-86.

Buschmann T, Martin-Villalba A, Kocsis JD, Waxman SG, Zimmermann M,

Herdegen T (1998). Expression of Jun, Fos, and ATF-2 proteins in axotomized explanted and cultured adult rat dorsal root ganglia. *Neuroscience* **84**(1)**:** 163-176.

Cafferty WB, Gardiner NJ, Gavazzi I, Powell J, McMahon SB, Heath JK, *et al.* (2001). Leukemia inhibitory factor determines the growth status of injured adult sensory neurons. *J Neurosci* **21**(18)**:** 7161-7170.

Cai D, Shen Y, De Bellard M, Tang S, Filbin MT (1999). Prior exposure to neurotrophins blocks inhibition of axonal regeneration by MAG and myelin via a cAMP-dependent mechanism. *Neuron* **22**(1)**:** 89-101.

Campana WM (2007). Schwann cells: activated peripheral glia and their role in neuropathic pain. *Brain, behavior, and immunity* **21**(5)**:** 522-527.

Campana WM, Li X, Shubayev VI, Angert M, Cai K, Myers RR (2006). Erythropoietin reduces Schwann cell TNF-alpha, Wallerian degeneration and pain-related behaviors after peripheral nerve injury. *Eur J Neurosci* **23**(3)**:** 617-626.

Canning DR, Hoke A, Malemud CJ, Silver J (1996). A potent inhibitor of neurite outgrowth that predominates in the extracellular matrix of reactive astrocytes. *Int J Dev Neurosci* **14**(3)**:** 153-175.

Cao J, Shayibuzhati M, Tajima T, Kitazawa T, Taneike T (2002). In vitro pharmacological characterization of the prostanoid receptor population in the non-pregnant porcine myometrium. *Eur J Pharmacol* **442**(1-2)**:** 115-123.

Caspary T, Anderson KV (2003). Patterning cell types in the dorsal spinal cord: what the mouse mutants say. *Nature reviews* **4**(4)**:** 289-297.

Castro C, Kuffler DP (2006). Membrane-bound CSPG mediates growth cone outgrowth and substrate specificity by Schwann cell contact with the DRG neuron cell body and not via growth cone contact. *Exp Neurol* **200**(1)**:** 19-25.

Chapman RA, Miller DJ (1974). Structure-activity relations for caffeine: a comparative study of the inotropic effects of the methylxanthines, imidazoles and related compounds on the frog's heart. *J Physiol* **242**(3)**:** 615-634.

Chen MS, Huber AB, van der Haar ME, Frank M, Schnell L, Spillmann AA, *et al.*

(2000). Nogo-A is a myelin-associated neurite outgrowth inhibitor and an antigen for monoclonal antibody IN-1. *Nature* **403**(6768): 434-439.

Chen Y, Zhang X, Wang C, Li G, Gu Y, Huang LY (2008). Activation of P2X7 receptors in glial satellite cells reduces pain through downregulation of P2X3 receptors in nociceptive neurons. *Proc Natl Acad Sci USA* **105**(43): 16773-16778.

Chopra B, Giblett S, Little JG, Donaldson LF, Tate S, Evans RJ, *et al.* (2000). Cyclooxygenase-1 is a marker for a subpopulation of putative nociceptive neurons in rat dorsal root ganglia. *Eur J Neurosci* **12**(3): 911-920.

Clarke GA, Moss DJ (1997). GP55 inhibits both cell adhesion and growth of neurons, but not non-neuronal cells, via a G-protein-coupled receptor. *Eur J Neurosci* **9**(2): 334-341.

Cunha FQ, Poole S, Lorenzetti BB, Ferreira SH (1992). The pivotal role of tumour necrosis factor alpha in the development of inflammatory hyperalgesia. *Br J Pharmacol* **107**(3): 660-664.

da Silva JS, Dotti CG (2002). Breaking the neuronal sphere: regulation of the actin cytoskeleton in neuritogenesis. *Nature reviews* **3**(9): 694-704.

Daly JW, Jacobson KA, Ukena D (1987). Adenosine receptors: development of selective agonists and antagonists. *Prog Clin Biol Res* **230:** 41-63.

David S, Lacroix S (2003). Molecular approaches to spinal cord repair. *Annu Rev Neurosci* **26:** 411-440.

de Rooij J, Zwartkruis FJ, Verheijen MH, Cool RH, Nijman SM, Wittinghofer A, *et al.* (1998). Epac is a Rap1 guanine-nucleotide-exchange factor directly activated by cyclic AMP. *Nature* **396**(6710): 474-477.

Dennis EA (1994). Diversity of group types, regulation, and function of phospholipase A2. *J Biol Chem* **269**(18): 13057-13060.

Doi Y, Minami T, Nishizawa M, Mabuchi T, Mori H, Ito S (2002). Central nociceptive role of prostacyclin (IP) receptor induced by peripheral inflammation. *Neuroreport* **13**(1): 93-96.

Dublin P, Hanani M (2007). SGCs in sensory ganglia: their possible contribution to inflammatory pain. *Brain, behavior, and immunity* **21**(5): 592-598.

Dubovy P, Jancalek R, Klusakova I, Svizenska I, Pejchalova K (2006). Intra- and extraneuronal changes of immunofluorescence staining for TNF-alpha and TNFR1 in the dorsal root ganglia of rat peripheral neuropathic pain models. *Cell Mol Neurobiol* **26**(7-8): 1205-1217.

England S, Bevan S, Docherty RJ (1996). PGE2 modulates the tetrodotoxin-resistant sodium current in neonatal rat dorsal root ganglion neurones via the cyclic AMP-protein kinase A cascade. *J Physiol* **495 (Pt 2):** 429-440.

Fang X, Djouhri L, McMullan S, Berry C, Waxman SG, Okuse K, *et al.* (2006). Intense isolectin-B4 binding in rat dorsal root ganglion neurons distinguishes C-fiber nociceptors with broad action potentials and high Nav1.9 expression. *J Neurosci* **26**(27): 7281-7292.

Ferreira SH, Lorenzetti BB (1996). Intrathecal administration of prostaglandin E_2 causes sensitization of the primary afferent neuron via the spinal release of glutamate. *Inflamm Res* **45**(10): 499-502.

Ferreira SH, Nakamura M, de Abreu Castro MS (1978). The hyperalgesic effects of prostacyclin and prostaglandin E_2. *Prostaglandins* **16**(1): 31-37.

Fex Svenningsen A, Colman DR, Pedraza L (2004). Satellite cells of dorsal root ganglia are multipotential glial precursors. *Neuron glia biology* **1**(1): 85-93.

Fields RD, Stevens-Graham B (2002). New insights into neuron-glia communication. *Science (New York, N.Y* **298**(5593): 556-562.

Fitzgerald EM, Okuse K, Wood JN, Dolphin AC, Moss SJ (1999). cAMP-dependent phosphorylation of the tetrodotoxin-resistant voltage-dependent sodium channel SNS. *J Physiol* **516 (Pt 2):** 433-446.

Franklin SL, Davies AM, Wyatt S (2009). Macrophage stimulating protein is a neurotrophic factor for a sub-population of adult nociceptive sensory neurons. *Mol Cell Neurosci* **41**(2): 175-185.

Fujino H, Regan JW (2006). EP_4 prostanoid receptor coupling to a pertussis toxin-sensitive inhibitory G protein. *Mol Pharmacol* **69**(1): 5-10.

Gainetdinov RR, Premont RT, Bohn LM, Lefkowitz RJ, Caron MG (2004). Desensitization of G protein-coupled receptors and neuronal functions. *Annu Rev Neurosci* **27:** 107-144.

Gao Y, Deng K, Hou J, Bryson JB, Barco A, Nikulina E, *et al.* (2004). Activated CREB is sufficient to overcome inhibitors in myelin and promote spinal axon regeneration in vivo. *Neuron* **44**(4): 609-621.

Gavazzi I, Kumar RD, McMahon SB, Cohen J (1999). Growth responses of different subpopulations of adult sensory neurons to neurotrophic factors in vitro. *Eur J Neurosci* **11**(10): 3405-3414.

Gerke MB, Plenderleith MB (2001). Binding sites for the plant lectin Bandeiraea simplicifolia I-isolectin B(4) are expressed by nociceptive primary sensory neurones. *Brain Res* **911**(1): 101-104.

Gold MS, Dastmalchi S, Levine JD (1996). Co-expression of nociceptor properties in dorsal root ganglion neurons from the adult rat in vitro. *Neuroscience* **71**(1): 265-275.

Grados-Munro EM, Fournier AE (2003). Myelin-associated inhibitors of axon regeneration. *J Neurosci Res* **74**(4): 479-485.

Guo A, Vulchanova L, Wang J, Li X, Elde R (1999). Immunocytochemical localization of the vanilloid receptor 1 (VR1): relationship to neuropeptides, the P2X3 purinoceptor and IB4 binding sites. *Eur J Neurosci* **11**(3): 946-958.

Guseva D, Chelyshev Y (2006). The plasticity of the DRG neurons belonging to different subpopulations after dorsal rhizotomy. *Cell Mol Neurobiol* **26**(7-8): 1225-1234.

Halls ML, Bathgate RA, Summers RJ (2006). Relaxin family peptide receptors RXFP1 and RXFP2 modulate cAMP signaling by distinct mechanisms. *Mol Pharmacol* **70**(1): 214-226.

Hanani M (2005). SGCs in sensory ganglia: from form to function. *Brain Res Brain Res Rev* **48**(3): 457-476.

Hannila SS, Filbin MT (2008). The role of cyclic AMP signaling in promoting axonal regeneration after spinal cord injury. *Exp Neurol* **209**(2): 321-332.

Hatae T, Wada M, Yokoyama C, Shimonishi M, Tanabe T (2001). Prostacyclin-dependent apoptosis mediated by PPAR delta. *J Biol Chem* **276**(49): 46260-46267.

Hatten ME (1987). Neuronal inhibition of astroglial cell proliferation is membrane mediated. *J Cell Biol* **104**(5): 1353-1360.

Hayat S, Thomas A, Afshar F, Sonigra R, Wigley CB (2003). Manipulation of olfactory ensheathing cell signaling mechanisms: effects on their support for neurite regrowth from adult CNS neurons in coculture. *Glia* **44**(3): 232-241.

He JC, Neves SR, Jordan JD, Iyengar R (2006). Role of the Go/i signaling network in the regulation of neurite outgrowth. *Can J Physiol Pharmacol* **84**(7): 687-694.

Heblich F, England S, Docherty RJ (2001). Indirect actions of bradykinin on neonatal rat dorsal root ganglion neurones: a role for non-neuronal cells as nociceptors. *J Physiol* **536**(Pt 1): 111-121.

Hingtgen CM, Waite KJ, Vasko MR (1995). Prostaglandins facilitate peptide release from rat sensory neurons by activating the adenosine 3',5'-cyclic monophosphate transduction cascade. *J Neurosci* **15**(7 Pt 2): 5411-5419.

Hoke A, Redett R, Hameed H, Jari R, Zhou C, Li ZB, *et al.* (2006). Schwann cells express motor and sensory phenotypes that regulate axon regeneration. *J Neurosci* **26**(38): 9646-9655.

Huang LY, Neher E (1996). Ca(2+)-dependent exocytosis in the somata of dorsal root ganglion neurons. *Neuron* **17**(1): 135-145.

Hucho TB, Dina OA, Levine JD (2005). Epac mediates a cAMP-to-PKC signaling in inflammatory pain: an isolectin B4(+) neuron-specific mechanism. *J Neurosci*

25(26): 6119-6126.

Igarashi M, Strittmatter SM, Vartanian T, Fishman MC (1993). Mediation by G proteins of signals that cause collapse of growth cones. *Science (New York, N.Y* **259**(5091): 77-79.

Iwanaga T, Takahashi Y, Fujita T (1989). Immunohistochemistry of neuron-specific and glia-specific proteins. *Arch Histol Cytol* **52 Suppl:** 13-24.

Jasmin L, Vit JP, Bhargava A, Ohara PT (2010). Can SGCs be therapeutic targets for pain control? *Neuron Glia Biol* **6**(1): 63-71.

Jones RL, Wise H, Clark R, Whiting RL, Bley KR (2006). Investigation of the prostacyclin (IP) receptor antagonist RO1138452 on isolated blood vessel and platelet preparations. *Br J Pharmacol* **149**(1): 110-120.

Jordan JD, He JC, Eungdamrong NJ, Gomes I, Ali W, Nguyen T, *et al.* (2005). Cannabinoid receptor-induced neurite outgrowth is mediated by Rap1 activation through $G\alpha_{o/i}$-triggered proteasomal degradation of Rap1GAPII. *J Biol Chem* **280**(12): 11413-11421.

Julius D, Basbaum AI (2001). Molecular mechanisms of nociception. *Nature* **413**(6852): 203-210.

Kabashima K, Saji T, Murata T, Nagamachi M, Matsuoka T, Segi E, *et al.* (2002). The prostaglandin receptor EP_4 suppresses colitis, mucosal damage and CD4 cell activation in the gut. *J Clin Invest* **109**(7): 883-893.

Kam Y, Chow KB, Wise H (2001). Factors affecting prostacyclin receptor agonist efficacy in different cell types. *Cell Signal* **13**(11): 841-847.

Kashiba H, Uchida Y, Senba E (2001). Difference in binding by isolectin B4 to trkA and c-ret mRNA-expressing neurons in rat sensory ganglia. *Brain Res Mol Brain Res* **95**(1-2): 18-26.

Kaslow HR, Burns DL (1992). Pertussis toxin and target eukaryotic cells: binding, entry, and activation. *FASEB J* **6**(9): 2684-2690.

Khasar SG, Ouseph AK, Chou B, Ho T, Green PG, Levine JD (1995). Is there more than one prostaglandin E receptor subtype mediating hyperalgesia in the rat hindpaw? *Neuroscience* **64**(4): 1161-1165.

Kidd BL, Urban LA (2001). Mechanisms of inflammatory pain. *Br J Anaesth* **87**(1): 3-11.

Kimpinski K, Mearow K (2001). Neurite growth promotion by nerve growth factor and insulin-like growth factor-1 in cultured adult sensory neurons: role of phosphoinositide 3-kinase and mitogen activated protein kinase. *J Neurosci Res* **63**(6): 486-499.

Kindt RM, Lander AD (1995). Pertussis toxin specifically inhibits growth cone guidance by a mechanism independent of direct G protein inactivation. *Neuron* **15**(1): 79-88.

Kingham PJ, Cuzner ML, Pocock JM (1999). Apoptotic pathways mobilized in microglia and neurones as a consequence of chromogranin A-induced microglial activation. *J Neurochem* **73**(2): 538-547.

Kobayashi T, Narumiya S (2002). Prostanoids in health and disease; lessons from receptor-knockout mice. *Adv Exp Med Biol* **507**: 593-597.

Kopp UC, Cicha MZ, Nakamura K, Nusing RM, Smith LA, Hokfelt T (2004). Activation of EP_4 receptors contributes to prostaglandin E_2-mediated stimulation of renal sensory nerves. *Am J Physiol Renal Physiol* **287**(6): F1269-1282.

Korhonen JM, Said FA, Wong AJ, Kaplan DR (1999). Gab1 mediates neurite outgrowth, DNA synthesis, and survival in PC12 cells. *J Biol Chem* **274**(52): 37307-37314.

Leclere PG, Norman E, Groutsi F, Coffin R, Mayer U, Pizzey J, *et al.* (2007). Impaired axonal regeneration by isolectin B4-binding dorsal root ganglion neurons in vitro. *J Neurosci* **27**(5): 1190-1199.

Li X, Gonias SL, Campana WM (2005). Schwann cells express erythropoietin receptor and represent a major target for Epo in peripheral nerve injury. *Glia* **51**(4): 254-265.

Lin CR, Amaya F, Barrett L, Wang H, Takada J, Samad TA, *et al.* (2006). Prostaglandin E_2 receptor EP_4 contributes to inflammatory pain hypersensitivity. *J Pharmacol Exp Ther* **319**(3)**:** 1096-1103.

Lindsay RM (1988). Nerve growth factors (NGF, BDNF) enhance axonal regeneration but are not required for survival of adult sensory neurons. *J Neurosci* **8**(7)**:** 2394-2405.

Liu Y, Ma Q (2010). Generation of somatic sensory neuron diversity and implications on sensory coding. *Curr Opin Neurobiol*. Epub ahead of print

Lonze BE, Ginty DD (2002). Function and regulation of CREB family transcription factors in the nervous system. *Neuron* **35**(4)**:** 605-623.

Lopshire JC, Nicol GD (1998). The cAMP transduction cascade mediates the prostaglandin E_2 enhancement of the capsaicin-elicited current in rat sensory neurons: whole-cell and single-channel studies. *J Neurosci* **18**(16)**:** 6081-6092.

Lotto B, Upton L, Price DJ, Gaspar P (1999). Serotonin receptor activation enhances neurite outgrowth of thalamic neurones in rodents. *Neurosci Lett* **269**(2)**:** 87-90.

Lu X, Richardson PM (1991). Inflammation near the nerve cell body enhances axonal regeneration. *J Neurosci* **11**(4)**:** 972-978.

Lu X, Richardson PM (1993). Responses of macrophages in rat dorsal root ganglia following peripheral nerve injury. *J Neurocytol* **22**(5)**:** 334-341.

Lustig M, Zanazzi G, Sakurai T, Blanco C, Levinson SR, Lambert S, et al. (2001). Nr-CAM and neurofascin interactions regulate ankyrin G and sodium channel clustering at the node of Ranvier. Curr Biol 11(23): 1864-1869.

Ma W, Chabot JG, Vercauteren F, Quirion R (2010). Injured nerve-derived $COX2/PGE_2$ contributes to the maintenance of neuropathic pain in aged rats. *Neurobiol Aging*. **31**(7): 1227-1237

Ma W, Eisenach JC (2002). Morphological and pharmacological evidence for the role of peripheral prostaglandins in the pathogenesis of neuropathic pain. *Eur J*

Neurosci **15**(6): 1037-1047.

Maihofner C, Tegeder I, Euchenhofer C, deWitt D, Brune K, Bang R, *et al.* (2000). Localization and regulation of cyclo-oxygenase-1 and -2 and neuronal nitric oxide synthase in mouse spinal cord. *Neuroscience* **101**(4): 1093-1108.

Malmberg AB, Brandon EP, Idzerda RL, Liu H, McKnight GS, Basbaum AI (1997). Diminished inflammation and nociceptive pain with preservation of neuropathic pain in mice with a targeted mutation of the type I regulatory subunit of cAMP-dependent protein kinase. *J Neurosci* **17**(19): 7462-7470.

Marmigere F, Ernfors P (2007). Specification and connectivity of neuronal subtypes in the sensory lineage. *Nature reviews* **8**(2): 114-127.

Matsumura K, Watanabe Y, Onoe H, Watanabe Y (1995). Prostacyclin receptor in the brain and central terminals of the primary sensory neurons: an autoradiographic study using a stable prostacyclin analogue [3H]iloprost. *Neuroscience* **65**(2): 493-503.

Meyer G, Feldman EL (2002). Signaling mechanisms that regulate actin-based motility processes in the nervous system. *J Neurochem* **83**(3): 490-503.

Milligan ED, Watkins LR (2009). Pathological and protective roles of glia in chronic pain. *Nature reviews* **10**(1): 23-36.

Mills J, Digicaylioglu M, Legg AT, Young CE, Young SS, Barr AM, *et al.* (2003). Role of integrin-linked kinase in nerve growth factor-stimulated neurite outgrowth. *J Neurosci* **23**(5): 1638-1648.

Minami T, Nishihara I, Uda R, Ito S, Hyodo M, Hayaishi O (1994). Characterization of EP-receptor subtypes involved in allodynia and hyperalgesia induced by intrathecal administration of prostaglandin E_2 to mice. *Br J Pharmacol* **112**(3): 735-740.

Mingorance A, Fontana X, Soriano E, Del Rio JA (2005). Overexpression of myelin-associated glycoprotein after axotomy of the perforant pathway. *Mol Cell Neurosci* **29**(3): 471-483.

Mitchison T, Kirschner M (1988). Cytoskeletal dynamics and nerve growth. *Neuron* **1**(9): 761-772.

Molliver DC, Wright DE, Leitner ML, Parsadanian AS, Doster K, Wen D, *et al.* (1997). IB4-binding DRG neurons switch from NGF to GDNF dependence in early postnatal life. *Neuron* **19**(4): 849-861.

Moriyama T, Higashi T, Togashi K, Iida T, Segi E, Sugimoto Y, *et al.* (2005). Sensitization of TRPV1 by EP1 and IP reveals peripheral nociceptive mechanism of prostaglandins. *Mol Pain* **1**: 3.

Muja N, Nelson JK, DeVries GH (2007). Schwann cells express IP prostanoid receptors coupled to an elevation in intracellular cyclic AMP. *J Neurosci Res* **85**(6): 1159-1169.

Murray AJ, Shewan DA (2008). Epac mediates cyclic AMP-dependent axon growth, guidance and regeneration. *Mol Cell Neurosci* **38**(4): 578-588.

Murray AJ, Tucker SJ, Shewan DA (2009). cAMP-dependent axon guidance is distinctly regulated by Epac and protein kinase A. *J Neurosci* **29**(49): 15434-15444.

Murwani R, Armati P (1998). Peripheral nerve fibroblasts as a source of IL-6, TNFalpha and IL-1 and their modulation by IFNgamma. *J Neurol Sci* **161**(2): 99-109.

Namba T, Sugimoto Y, Negishi M, Irie A, Ushikubi F, Kakizuka A, *et al.* (1993). Alternative splicing of C-terminal tail of prostaglandin E receptor subtype EP_3 determines G-protein specificity. *Nature* **365**(6442): 166-170.

Narumiya S, Sugimoto Y, Ushikubi F (1999). Prostanoid receptors: structures, properties, and functions. *Physiol Rev* **79**(4): 1193-1226.

Neumann S, Woolf CJ (1999). Regeneration of dorsal column fibers into and beyond the lesion site following adult spinal cord injury. *Neuron* **23**(1): 83-91.

Ng KY, Wong YH, Wise H (2010). The role of glial cells in influencing neurite extension by dorsal root ganglion cells. *Neuron glia biology* **6**(1): 19-29.

Nicolson TA, Foster AF, Bevan S, Richards CD (2007). Prostaglandin E_2 sensitizes primary sensory neurons to histamine. *Neuroscience* **150**(1)**:** 22-30.

Niederost B, Oertle T, Fritsche J, McKinney RA, Bandtlow CE (2002). Nogo-A and myelin-associated glycoprotein mediate neurite growth inhibition by antagonistic regulation of RhoA and Rac1. *J Neurosci* **22**(23)**:** 10368-10376.

Ohara PT, Vit JP, Bhargava A, Jasmin L (2008). Evidence for a role of connexin 43 in trigeminal pain using RNA interference in vivo. *J Neurophysiol* **100**(6)**:** 3064-3073.

Ohara PT, Vit JP, Bhargava A, Romero M, Sundberg C, Charles AC, *et al.* (2009). Gliopathic pain: when SGCs go bad. *Neuroscientist* **15**(5)**:** 450-463.

Oida H, Namba T, Sugimoto Y, Ushikubi F, Ohishi H, Ichikawa A, *et al.* (1995). In situ hybridization studies of prostacyclin receptor mRNA expression in various mouse organs. *Br J Pharmacol* **116**(7)**:** 2828-2837.

Opree A, Kress M (2000). Involvement of the proinflammatory cytokines tumor necrosis factor-alpha, IL-1 beta, and IL-6 but not IL-8 in the development of heat hyperalgesia: effects on heat-evoked calcitonin gene-related peptide release from rat skin. *J Neurosci* **20**(16)**:** 6289-6293.

Oshita K, Inoue A, Tang HB, Nakata Y, Kawamoto M, Yuge O (2005). CB(1) cannabinoid receptor stimulation modulates transient receptor potential vanilloid receptor 1 activities in calcium influx and substance P Release in cultured rat dorsal root ganglion cells. *J Pharmacol Sci* **97**(3)**:** 377-385.

Pang L, Sawada T, Decker SJ, Saltiel AR (1995). Inhibition of MAP kinase kinase blocks the differentiation of PC-12 cells induced by nerve growth factor. *J Biol Chem* **270**(23)**:** 13585-13588.

Pannese E (2002). Perikaryal surface specializations of neurons in sensory ganglia. *Int Rev Cytol* **220:** 1-34.

Parrinello S, Noon LA, Harrisingh MC, Digby PW, Rosenberg LH, Cremona CA, *et al.* (2008). NF1 loss disrupts Schwann cell-axonal interactions: a novel role for semaphorin 4F. *Genes & development* **22**(23)**:** 3335-3348.

Pitchford S, Levine JD (1991). Prostaglandins sensitize nociceptors in cell culture. *Neurosci Lett* **132**(1)**:** 105-108.

Price TJ, Flores CM (2007). Critical evaluation of the colocalization between calcitonin gene-related peptide, substance P, transient receptor potential vanilloid subfamily type 1 immunoreactivities, and isolectin B4 binding in primary afferent neurons of the rat and mouse. *J Pain* **8**(3)**:** 263-272.

Priestley JV, Michael GJ, Averill S, Liu M, Willmott N (2002). Regulation of nociceptive neurons by nerve growth factor and glial cell line derived neurotrophic factor. *Can J Physiol Pharmacol* **80**(5)**:** 495-505.

Qiu J, Cai D, Dai H, McAtee M, Hoffman PN, Bregman BS, *et al.* (2002). Spinal axon regeneration induced by elevation of cyclic AMP. *Neuron* **34**(6)**:** 895-903.

Raye WS, Tochon-Danguy N, Pouton CW, Haynes JM (2007). Heterogeneous population of dopaminergic neurons derived from mouse embryonic stem cells: preliminary phenotyping based on receptor expression and function. *Eur J Neurosci* **25**(7)**:** 1961-1970.

Reinoso BS, Undie AS, Levitt P (1996). Dopamine receptors mediate differential morphological effects on cerebral cortical neurons in vitro. *J Neurosci Res* **43**(4)**:** 439-453.

Rosch S, Ramer R, Brune K, Hinz B (2005). Prostaglandin E_2 induces cyclooxygenase-2 expression in human non-pigmented ciliary epithelial cells through activation of p38 and p42/44 mitogen-activated protein kinases. *Biochem Biophys Res Commun* **338**(2)**:** 1171-1178.

Rowlands DK, Kao C, Wise H (2001). Regulation of prostacyclin and prostaglandin E(2) receptor mediated responses in adult rat dorsal root ganglion cells, in vitro. *Br J Pharmacol* **133**(1)**:** 13-22.

Runyan SA, Phelps PE (2009). Mouse olfactory ensheathing glia enhance axon outgrowth on a myelin substrate in vitro. *Exp Neurol* **216**(1)**:** 95-104.

Sachs D, Villarreal C, Cunha F, Parada C, Ferreira S (2009). The role of PKA and

PKCepsilon pathways in prostaglandin E_2-mediated hypernociception. *Br J Pharmacol* **156**(5): 826-834.

Safieh-Garabedian B, Poole S, Allchorne A, Winter J, Woolf CJ (1995). Contribution of interleukin-1 beta to the inflammation-induced increase in nerve growth factor levels and inflammatory hyperalgesia. *Br J Pharmacol* **115**(7): 1265-1275.

Salomon Y (1991). Cellular responsiveness to hormones and neurotransmitters: conversion of [3H]adenine to [3H]cAMP in cell monolayers, cell suspensions, and tissue slices. *Methods Enzymol* **195:** 22-28.

Salzer JL, Bunge RP, Glaser L (1980). Studies of Schwann cell proliferation. III. Evidence for the surface localization of the neurite mitogen. *J Cell Biol* **84**(3): 767-778.

Samad TA, Sapirstein A, Woolf CJ (2002). Prostanoids and pain: unraveling mechanisms and revealing therapeutic targets. *Trends Mol Med* **8**(8): 390-396.

Schoenen J, Delree P, Leprince P, Moonen G (1989). Neurotransmitter phenotype plasticity in cultured dissociated adult rat dorsal root ganglia: an immunocytochemical study. *J Neurosci Res* **22**(4): 473-487.

Scholz J, Woolf CJ (2007). The neuropathic pain triad: neurons, immune cells and glia. *Nat Neurosci* **10**(11): 1361-1368.

Schreyer DJ, Skene JH (1993). Injury-associated induction of GAP-43 expression displays axon branch specificity in rat dorsal root ganglion neurons. *J Neurobiol* **24**(7): 959-970.

Schultz J, Daly JW (1973). Cyclic adenosine 3',5'-monophosphate in guinea pig cerebral cortical slices. II. The role of phosphodiesterase activity in the regulation of levels of cyclic adenosine 3',5'-monophosphate. *J Biol Chem* **248**(3): 853-859.

Shamash S, Reichert F, Rotshenker S (2002). The cytokine network of Wallerian degeneration: tumor necrosis factor-alpha, interleukin-1alpha, and interleukin-1beta. *J Neurosci* **22**(8): 3052-3060.

Shen YJ, DeBellard ME, Salzer JL, Roder J, Filbin MT (1998). Myelin-associated glycoprotein in myelin and expressed by Schwann cells inhibits axonal regeneration and branching. *Mol Cell Neurosci* **12**(1-2): 79-91.

Shibuya I, Setiadji SV, Ibrahim N, Harayama N, Maruyama T, Ueta Y, *et al.* (2002). Involvement of postsynaptic EP_4 and presynaptic EP_3 receptors in actions of prostaglandin E_2 in rat supraoptic neurones. *J Neuroendocrinol* **14**(1): 64-72.

Smith JA, Davis CL, Burgess GM (2000). Prostaglandin E_2-induced sensitization of bradykinin-evoked responses in rat dorsal root ganglion neurons is mediated by cAMP-dependent protein kinase A. *Eur J Neurosci* **12**(9): 3250-3258.

Smyth EM, Nestor PV, FitzGerald GA (1996). Agonist-dependent phosphorylation of an epitope-tagged human prostacyclin receptor. *J Biol Chem* **271**(52): 33698-33704.

Snider WD, McMahon SB (1998). Tackling pain at the source: new ideas about nociceptors. *Neuron* **20**(4): 629-632.

Sommer C, Kress M (2004). Recent findings on how proinflammatory cytokines cause pain: peripheral mechanisms in inflammatory and neuropathic hyperalgesia. *Neurosci Lett* **361**(1-3): 184-187.

Southall MD, Vasko MR (2001). Prostaglandin receptor subtypes, EP_{3C} and EP_4, mediate the prostaglandin E_2-induced cAMP production and sensitization of sensory neurons. *J Biol Chem* **276**(19): 16083-16091.

Strittmatter SM, Fishman MC, Zhu XP (1994). Activated mutants of the α subunit of G_o promote an increased number of neurites per cell. *J Neurosci* **14**(4): 2327-2338.

Stucky CL, Lewin GR (1999). Isolectin B_4-positive and -negative nociceptors are functionally distinct. *J Neurosci* **19**(15): 6497-6505.

Stucky CL, Rossi J, Airaksinen MS, Lewin GR (2002). GFR α2/neurturin signalling regulates noxious heat transduction in isolectin B4-binding mouse sensory neurons. *J Physiol* **545**(Pt 1): 43-50.

Stucky CL, Thayer SA, Seybold VS (1996). Prostaglandin E_2 increases the

proportion of neonatal rat dorsal root ganglion neurons that respond to bradykinin. *Neuroscience* **74**(4)**:** 1111-1123.

Suadicani SO, Cherkas PS, Zuckerman J, Smith DN, Spray DC, Hanani M (2009). Bidirectional calcium signaling between SGCs and neurons in cultured mouse trigeminal ganglia. *Neuron Glia Biol***:** 1-9.

Sugimoto Y, Narumiya S, Ichikawa A (2000). Distribution and function of prostanoid receptors: studies from knockout mice. *Prog Lipid Res* **39**(4)**:** 289-314.

Sugimoto Y, Shigemoto R, Namba T, Negishi M, Mizuno N, Narumiya S, *et al.* (1994). Distribution of the messenger RNA for the prostaglandin E receptor subtype EP3 in the mouse nervous system. *Neuroscience* **62**(3)**:** 919-928.

Sun RQ, Lawand NB, Willis WD (2003). The role of calcitonin gene-related peptide (CGRP) in the generation and maintenance of mechanical allodynia and hyperalgesia in rats after intradermal injection of capsaicin. *Pain* **104**(1-2)**:** 201-208.

Sung B, Lim G, Mao J (2003). Altered expression and uptake activity of spinal glutamate transporters after nerve injury contribute to the pathogenesis of neuropathic pain in rats. *J Neurosci* **23**(7)**:** 2899-2910.

Suzawa T, Miyaura C, Inada M, Maruyama T, Sugimoto Y, Ushikubi F, *et al.* (2000). The role of prostaglandin E receptor subtypes (EP_1, EP_2, EP_3, and EP_4) in bone resorption: an analysis using specific agonists for the respective EPs. *Endocrinology* **141**(4)**:** 1554-1559.

Swarzenski BC, O'Malley KL, Todd RD (1996). PTX-sensitive regulation of neurite outgrowth by the dopamine D3 receptor. *Neuroreport* **7**(2)**:** 573-576.

Taiwo YO, Bjerknes LK, Goetzl EJ, Levine JD (1989). Mediation of primary afferent peripheral hyperalgesia by the cAMP second messenger system. *Neuroscience* **32**(3)**:** 577-580.

Taiwo YO, Levine JD (1991). Further confirmation of the role of adenyl cyclase and of cAMP-dependent protein kinase in primary afferent hyperalgesia. *Neuroscience* **44**(1)**:** 131-135.

Takeda M, Tanimoto T, Kadoi J, Nasu M, Takahashi M, Kitagawa J, *et al.* (2007). Enhanced excitability of nociceptive trigeminal ganglion neurons by satellite glial cytokine following peripheral inflammation. *Pain* **129**(1-2)**:** 155-166.

Tamura M, Nogimori K, Murai S, Yajima M, Ito K, Katada T, *et al.* (1982). Subunit structure of islet-activating protein, pertussis toxin, in conformity with the A-B model. *Biochemistry* **21**(22)**:** 5516-5522.

Tanaka T, Minami M, Nakagawa T, Satoh M (2004). Enhanced production of monocyte chemoattractant protein-1 in the dorsal root ganglia in a rat model of neuropathic pain: possible involvement in the development of neuropathic pain. *Neurosci Res* **48**(4)**:** 463-469.

Tang HB, Li YS, Nakata Y (2007). The release of substance P from cultured dorsal root ganglion neurons requires the non-neuronal cells around these neurons. *J Pharmacol Sci* **105**(3)**:** 264-271.

Thippeswamy T, McKay JS, Morris R, Quinn J, Wong LF, Murphy D (2005). Glial-mediated neuroprotection: evidence for the protective role of the NO-cGMP pathway via neuron-glial communication in the peripheral nervous system. *Glia* **49**(2)**:** 197-210.

Thippeswamy T, Morris R (2002). The roles of nitric oxide in dorsal root ganglion neurons. *Ann N Y Acad Sci* **962:** 103-110.

Tilley SL, Coffman TM, Koller BH (2001). Mixed messages: modulation of inflammation and immune responses by prostaglandins and thromboxanes. *J Clin Invest* **108**(1)**:** 15-23.

Togashi H, Sakisaka T, Takai Y (2009). Cell adhesion molecules in the central nervous system. *Cell adhesion & migration* **3**(1)**:** 29-35.

Tucker BA, Rahimtula M, Mearow KM (2005a). Integrin activation and neurotrophin signaling cooperate to enhance neurite outgrowth in sensory neurons. *J Comp Neurol* **486**(3)**:** 267-280.

Tucker BA, Rahimtula M, Mearow KM (2006). Laminin and growth factor receptor activation stimulates differential growth responses in subpopulations of adult DRG

neurons. *Eur J Neurosci* **24**(3)**:** 676-690.

Tucker BA, Rahimtula M, Mearow KM (2005b). A procedure for selecting and culturing subpopulations of neurons from rat dorsal root ganglia using magnetic beads. *Brain Res Brain Res Protoc* **16**(1-3)**:** 50-57.

Vit JP, Jasmin L, Bhargava A, Ohara PT (2006). SGCs in the trigeminal ganglion as a determinant of orofacial neuropathic pain. *Neuron Glia Biol* **2**(4)**:** 247-257.

Vit JP, Ohara PT, Bhargava A, Kelley K, Jasmin L (2008). Silencing the Kir4.1 potassium channel subunit in SGCs of the rat trigeminal ganglion results in pain-like behavior in the absence of nerve injury. *J Neurosci* **28**(16)**:** 4161-4171.

Vossler MR, Yao H, York RD, Pan MG, Rim CS, Stork PJ (1997). cAMP activates MAP kinase and Elk-1 through a B-Raf- and Rap1-dependent pathway. *Cell* **89**(1)**:** 73-82.

Vulchanova L, Riedl MS, Shuster SJ, Stone LS, Hargreaves KM, Buell G, *et al.* (1998). P2X3 is expressed by DRG neurons that terminate in inner lamina II. *Eur J Neurosci* **10**(11)**:** 3470-3478.

Waetzig V, Herdegen T (2005). MEKK1 controls neurite regrowth after experimental injury by balancing ERK1/2 and JNK2 signaling. *Mol Cell Neurosci* **30**(1)**:** 67-78.

Wagner R, Myers RR (1996). Endoneurial injection of TNF-alpha produces neuropathic pain behaviors. *Neuroreport* **7**(18)**:** 2897-2901.

Wang C, Li GW, Huang LY (2007). Prostaglandin E_2 potentiation of P2X3 receptor mediated currents in dorsal root ganglion neurons. *Mol Pain* **3:** 22.

Weick M, Cherkas PS, Hartig W, Pannicke T, Uckermann O, Bringmann A, *et al.* (2003). P2 receptors in SGCs in trigeminal ganglia of mice. *Neuroscience* **120**(4)**:** 969-977.

Wewetzer K, Lausch M, Christ B (1999). Macrowell cultures identify a subpopulation of neonatal rat dorsal root ganglionic neurons displaying nerve growth factor independent survival. *Neurosci Lett* **276**(1)**:** 9-12.

White DM, Walker S, Brenneman DE, Gozes I (2000). CREB contributes to the increased neurite outgrowth of sensory neurons induced by vasoactive intestinal polypeptide and activity-dependent neurotrophic factor. *Brain Res* **868**(1): 31-38.

Wise H (2006). Lack of interaction between prostaglandin E_2 receptor subtypes in regulating adenylyl cyclase activity in cultured rat dorsal root ganglion cells. *Eur J Pharmacol* **535**(1-3): 69-77.

Wong WS, Rosoff PM (1996). Pharmacology of pertussis toxin B-oligomer. *Can J Physiol Pharmacol* **74**(5): 559-564.

Woolf CJ (2004). Pain: moving from symptom control toward mechanism-specific pharmacologic management. *Ann Intern Med* **140**(6): 441-451.

Woolf CJ, Ma Q (2007). Nociceptors--noxious stimulus detectors. *Neuron* **55**(3): 353-364.

Woolf CJ, Salter MW (2000). Neuronal plasticity: increasing the gain in pain. *Science (New York, N.Y* **288**(5472): 1765-1769.

Wu D, Zhang Y, Bo X, Huang W, Xiao F, Zhang X, *et al.* (2007). Actions of neuropoietic cytokines and cyclic AMP in regenerative conditioning of rat primary sensory neurons. *Exp Neurol* **204**(1): 66-76.

Wu J, Yang X, Zhang YF, Zhou SF, Zhang R, Dong XQ, *et al.* (2009). Angiotensin II upregulates Toll-like receptor 4 and enhances lipopolysaccharide-induced CD40 expression in rat peritoneal mesothelial cells. *Inflamm Res* **58**(8): 473-482.

Yalcin I, Tessier LH, Petit-Demouliere N, Waltisperger E, Hein L, Freund-Mercier MJ, *et al.* (2010). Chronic treatment with agonists of β_2-adrenergic receptors in neuropathic pain. *Exp Neurol* **221**(1): 115-121.

Yamashita T, Tohyama M (2003). The p75 receptor acts as a displacement factor that releases Rho from Rho-GDI. *Nat Neurosci* **6**(5): 461-467.

Yamashita T, Tucker KL, Barde YA (1999). Neurotrophin binding to the p75 receptor modulates Rho activity and axonal outgrowth. *Neuron* **24**(3): 585-593.

Zeilhofer HU (2007). Prostanoids in nociception and pain. *Biochem Pharmacol* **73**(2): 165-174.

Zhang X, Chen Y, Wang C, Huang LY (2007). Neuronal somatic ATP release triggers neuron-satellite glial cell communication in dorsal root ganglia. *Proc Natl Acad Sci USA* **104**(23): 9864-9869.

Zheng JH, Walters ET, Song XJ (2007). Dissociation of dorsal root ganglion neurons induces hyperexcitability that is maintained by increased responsiveness to cAMP and cGMP. *J Neurophysiol* **97**(1): 15-25.

Zhou FQ, Zhou J, Dedhar S, Wu YH, Snider WD (2004). NGF-induced axon growth is mediated by localized inactivation of GSK-3β and functions of the microtubule plus end binding protein APC. *Neuron* **42**(6): 897-912.